

# Nuclear Reactions for Weak Interactions

Horst Lenske

Institut für Theoretische Physik, JLU Giessen

and

NUMEN Collaboration

# Agenda

**Lecture 1:** Basic Concepts of Quantum-Mechanical Scattering Theory

**Lecture 2:** Nuclear Reaction Theory in a Nutshell

**Lecture 3:** Theory of Nuclear Direct Reactions

**Lecture 4:** Optical Potentials and Elastic Scattering

**Lecture 5:** Perturbative Approach to Non-Elastic Reactions

**Lecture 6:** Single Charge Exchange (SCE) Reactions

**Lecture 7:** Light Ion SCE Reactions and beta-Decay

**Lecture 8:** The Gamow-Teller Quenching Mystery

**Lecture 9:** Nuclear Matrix Elements for Astrophysics

**Lecture 10:** Heavy Ion SCE Reactions

**Lecture 11:** Heavy Ion SCE Reactions at Relativistic Energies

**Lecture 12:** Double Charge Exchange (DCE) Reactions

# Readings

- **Textbooks:**

- M. L. Goldberger and K. M. Watson, *Collision Theory* (Wiley, New York, 1964); Dover reprint (2004).
- N. Austern, *Direct Nuclear Reaction Theories* (Wiley, New York, 1970).
- G. R. Satchler, *Direct Nuclear Reactions* (Oxford University Press, Oxford, 1983).
- H. Feshbach, *Theoretical Nuclear Physics: Nuclear Reactions* (Wiley, New York, 1992).

- **Research Articles:**

- H. Lenske, *Theory and applications of nuclear direct reactions*, Int.Jour.Mod.Phys. E30 (2021) 2130010
- F. Cappuzzello, H. Lenske et al., **Shedding light on nuclear aspects of neutrinoless double beta decay by heavy-ion double charge exchange reactions**, *Prog.Part.Nucl.Phys.* 128 (2023) 103999
- H. Lenske, F. Cappuzzello et al., **Heavy ion charge exchange reactions as probes for nuclear  $\beta$ -decay**, *Prog.Part.Nucl.Phys.* 109 (2019) 103716
- H. Lenske, M. Dhar et al., *Baryons and Baryon Resonances in Nuclear Matter*, *Prog.Part.Nucl.Phys.* 98 (2018) 119;

# Lecture 1:

# Basic Concepts and Characteristics of Nuclear Reaction

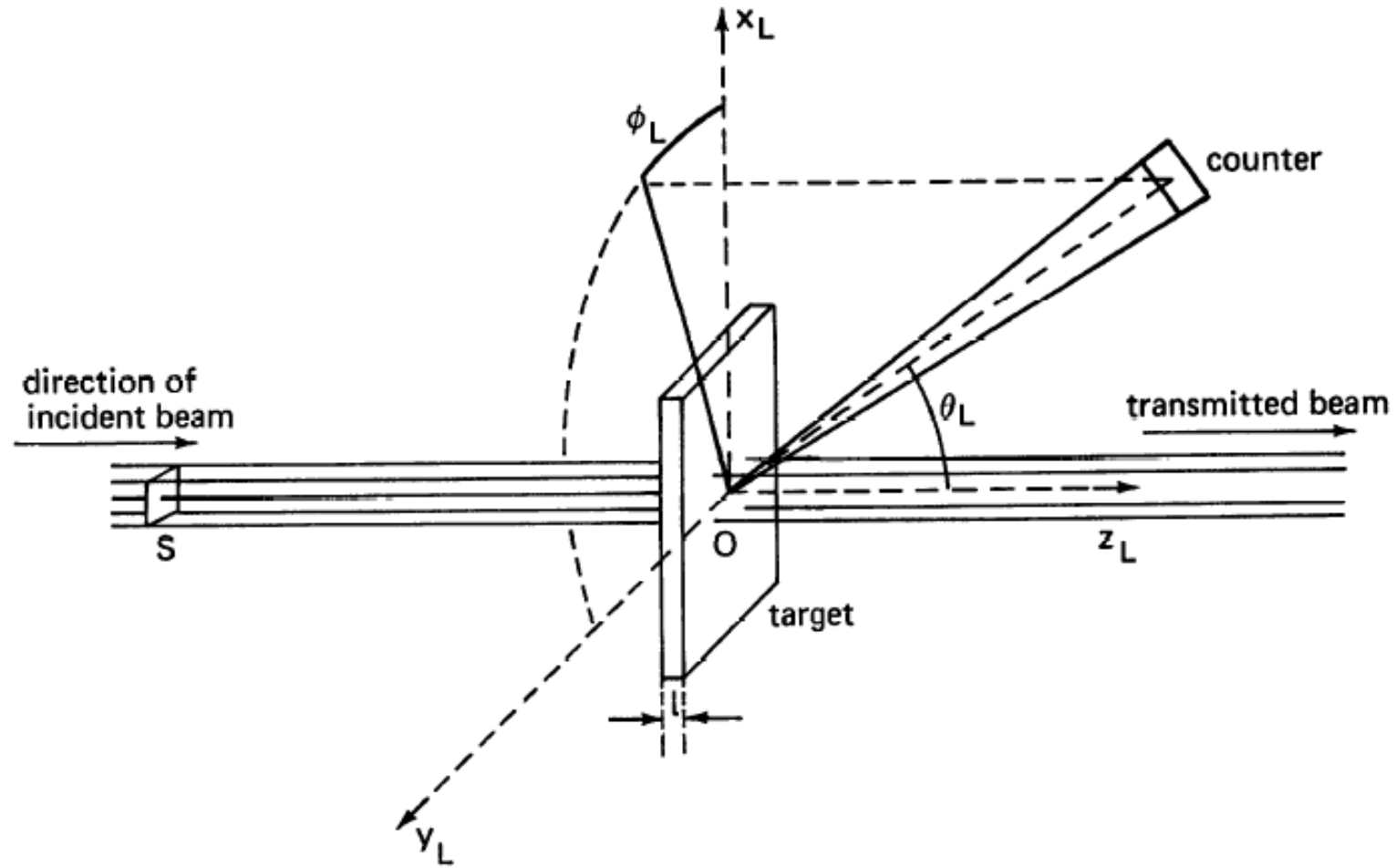


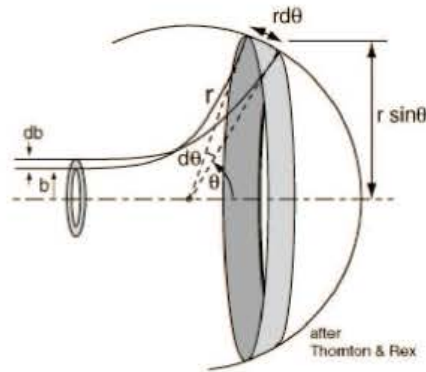
Fig. 1.2. Illustration of various quantities used in the definition of cross sections.

# Recap of Classical Scattering Theory:

- In classical mechanics, for a central potential,  $V(r)$ , the angle of scattering is determined by **impact parameter**  $b(\theta)$ .
- The number of particles scattered per unit time between  $\theta$  and  $\theta + d\theta$  is equal to the number incident particles per unit time between  $b$  and  $b + db$ .
- Therefore, for incident flux  $j_I$ , the number of particles scattered into the solid angle  $d\Omega = 2\pi \sin\theta d\theta$  per unit time is given by

$$N d\Omega = 2\pi \sin\theta d\theta N = 2\pi b db j_I$$

$$\text{i.e. } \frac{d\sigma(\theta)}{d\Omega} \equiv \frac{N}{j_I} = \frac{b}{\sin\theta} \left| \frac{db}{d\theta} \right|$$



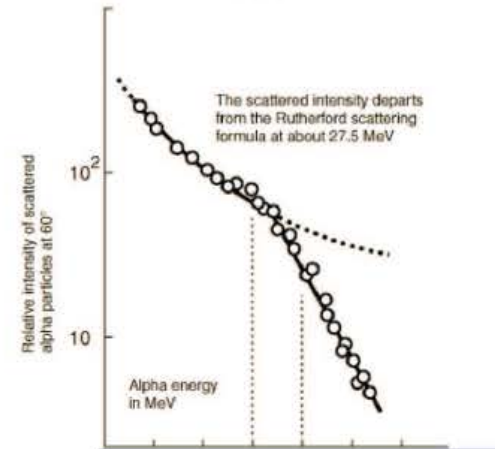
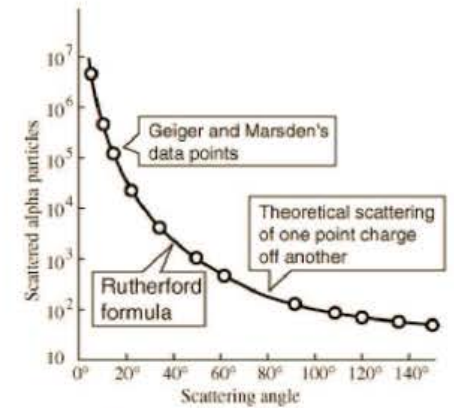
- For **classical Coulomb scattering**,

$$V(r) = \frac{\kappa}{r}$$

particle follows hyperbolic trajectory.

- In this case, a straightforward calculation obtains the **Rutherford formula**:

$$\frac{d\sigma}{d\Omega} = \frac{b}{\sin\theta} \left| \frac{db}{d\theta} \right| = \frac{\kappa^2}{16E^2} \frac{1}{\sin^4\theta/2}$$



# Quantum Mechanical Scattering

Scattering is a time-dependent process as expressed by the Schrödinger equation

$$i\hbar \frac{\partial}{\partial t} \Psi(\mathbf{r}, t) = H(\mathbf{r}, \mathbf{p}) \Psi(\mathbf{r}, t)$$

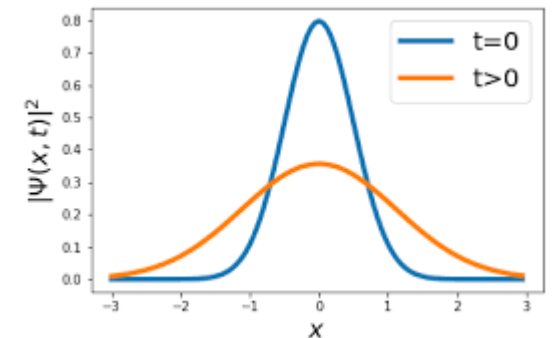
The formal solution is

$$\Psi(\mathbf{r}, t) = e^{-iH(\mathbf{r}, \mathbf{p})(t-t_0)} \Psi(\mathbf{r}, t_0)$$

...propagating the initial state  $\Psi(\mathbf{r}, t_0)$  from  $t_0 \rightarrow t$ .

Free motion of a point particle ( $t_0=0$ ):

$$\Psi_0(\vec{\mathbf{r}}) = \mathbf{A}(\gamma) \int \frac{\mathbf{d}^3 \mathbf{k}}{(2\pi)^{3/2}} e^{i\vec{\mathbf{k}} \cdot \vec{\mathbf{r}} - \frac{1}{2}\gamma^2 \mathbf{k}^2} ; \langle \Psi_0 | \Psi_0 \rangle = 1$$



# Nucleus-Nucleus Scattering

$$H(\vec{r}, \vec{p}) \rightarrow H_{cm}(\vec{q}, \xi) + \frac{\vec{P}^2}{2M}$$

Relative motion in the center-of-mass system:

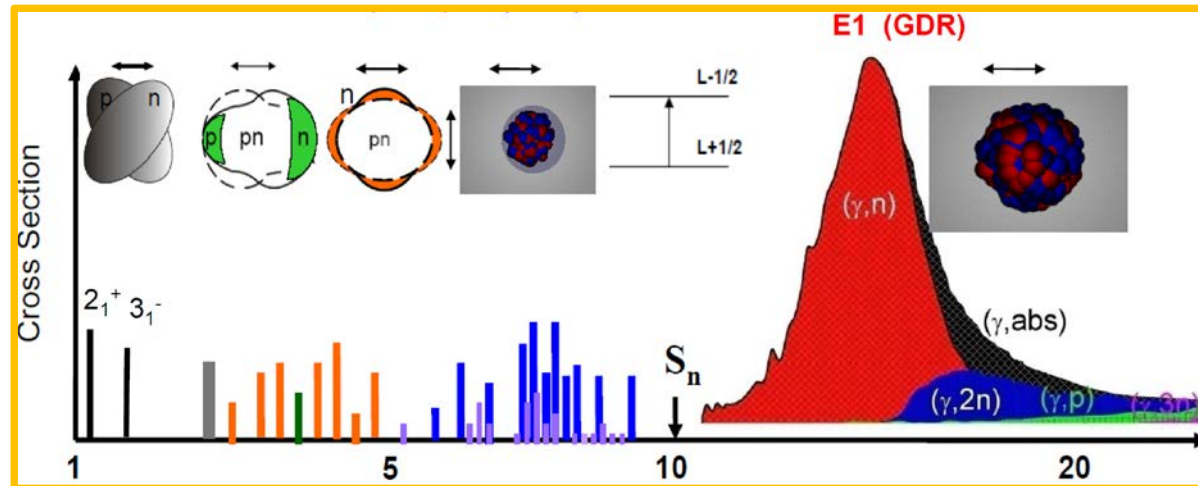
$$H_{cm}(\vec{q}, \xi) = K_{PT}(\vec{q}) + V_{PT}(\vec{r}, \xi_P, \xi_T) + H_P(\xi_P) + H_T(\xi_T)$$

$$\text{Eigenstates: } \Phi(t, \vec{x}, \xi_P, \xi_T) = e^{-i\omega_c t} \psi_c(\vec{r}, \vec{k}) |c\rangle ; |c\rangle = [P_n \otimes T_m]$$

## Nuclear Eigenstates

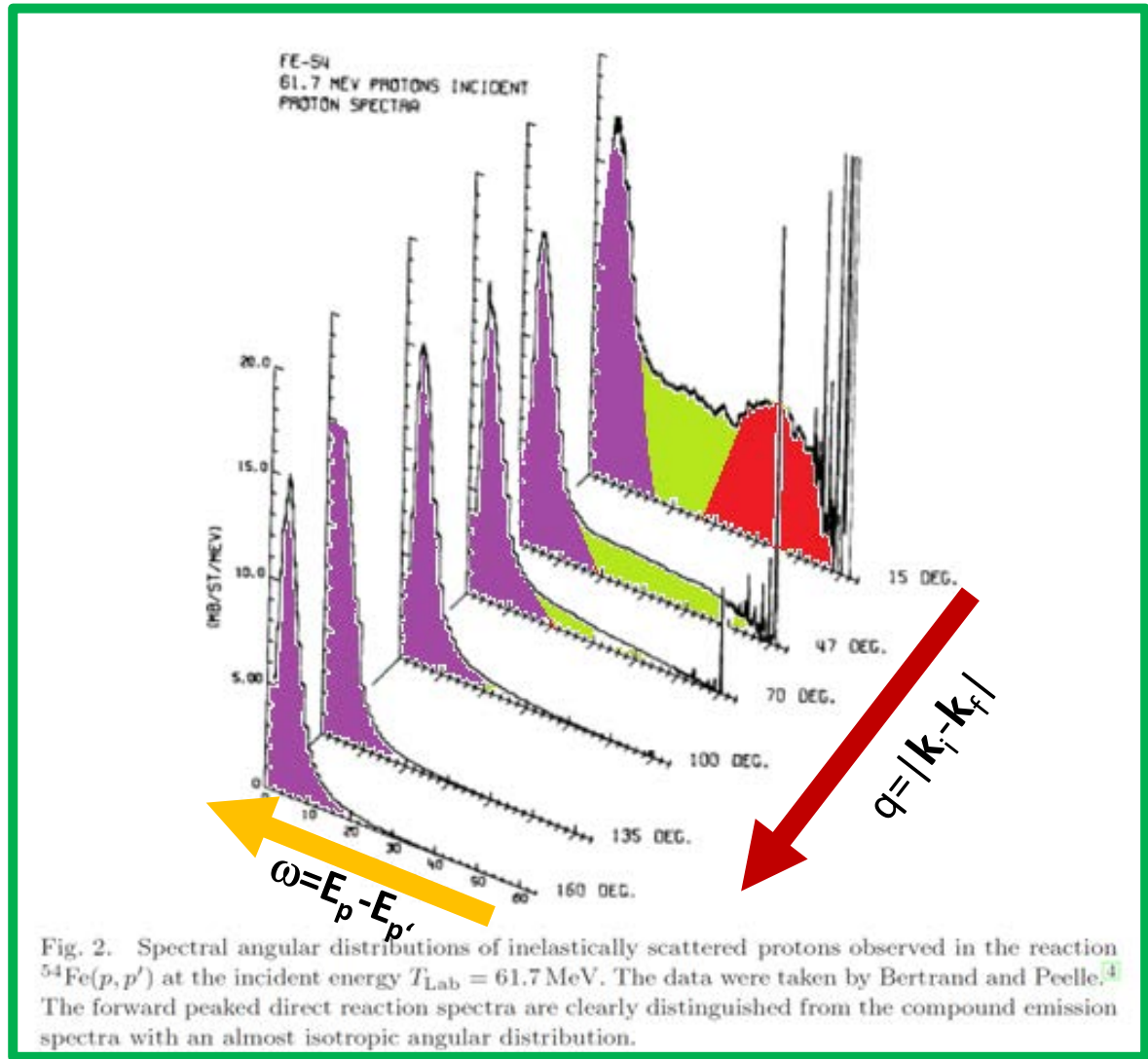
$$(H_A - E_{A_n}) |A_n\rangle = 0 ; A=P,T ; n = 0 \dots \infty$$

**In nuclear reactions two objects of a highly complex intrinsic structure are interacting!**



# A Real Physics Example: Inelastic Scattering of a proton beam on a $^{54}\text{Fe}$ target at $T_{\text{lab}}=61.7$ MeV

**Rule of Thumb:**  
Complexity of spectra increases with  $\omega, q$  and for small impact parameters  $b \approx \ell/k$



Nuclear Cross sections are depending on energy ( $\omega$ ) transfer and momentum ( $q$ ) transfer covering

- Discret Spectra
- Giant resonances
- Pre-Equilibrium States
- Thermalized Compound States

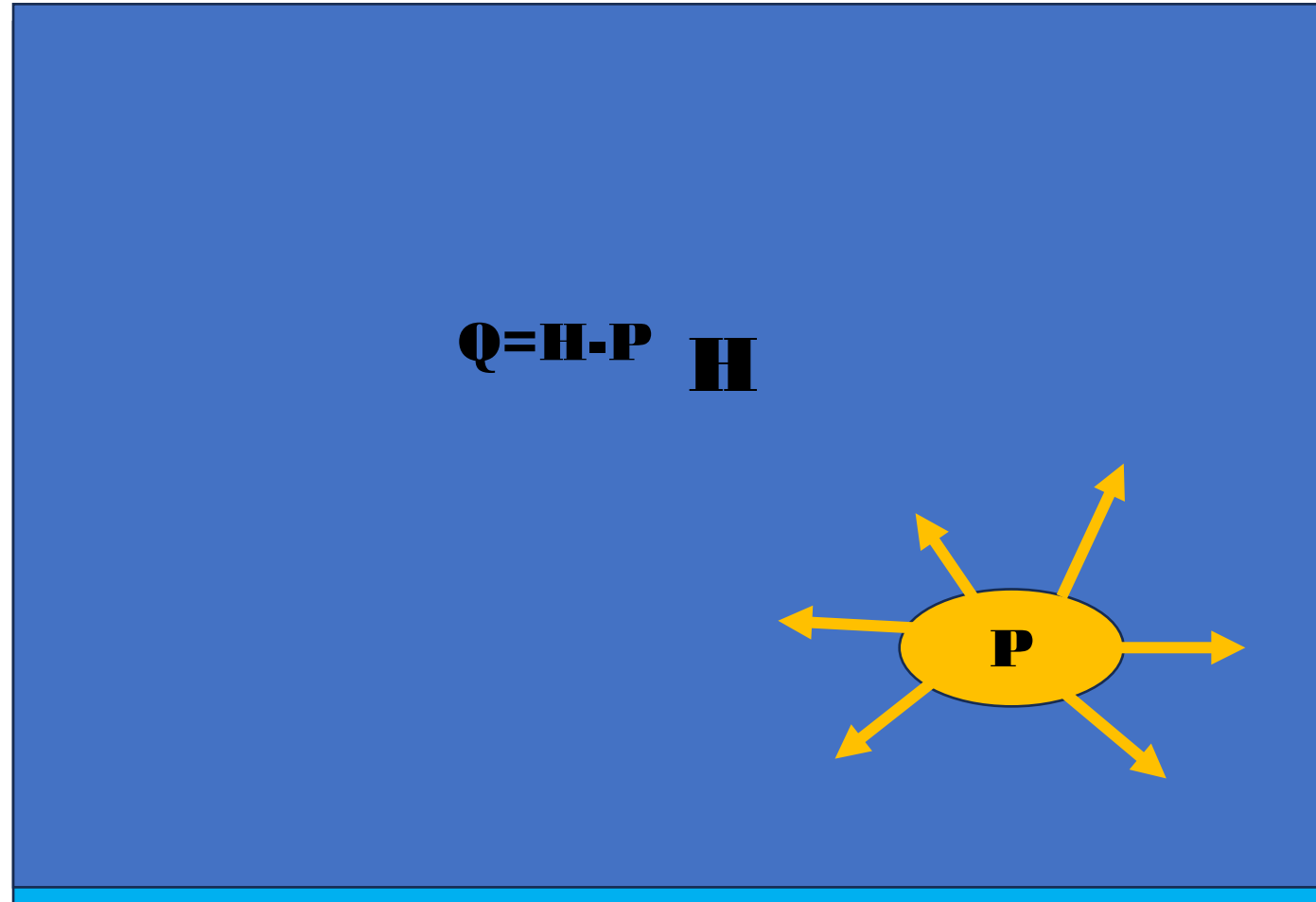
# Lecture 2:

## Nuclear Reaction Theory in a Nutshell

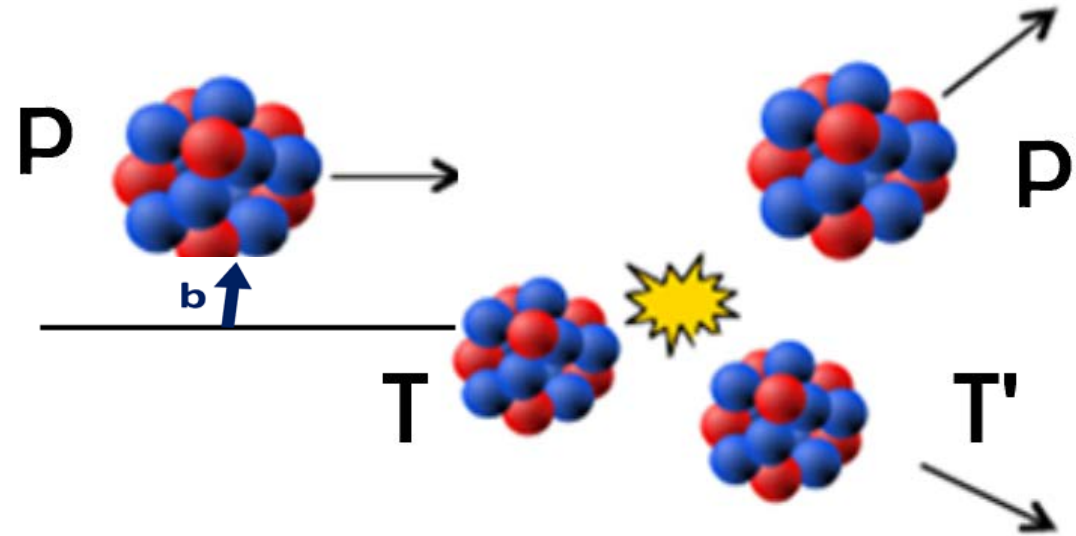
...for Stationary  
Scattering States:

$$\Phi(\vec{r}, t, \xi) = e^{-iEt} \Psi(\vec{r}, \xi) :$$
$$(\mathbf{H}(\vec{r}, \vec{q}, \xi) - E) \Psi(\vec{r}, \xi) = 0$$

# Division of the Hilbert-Space $\mathbf{H}=\mathbf{P}+\mathbf{Q}$ into a Model Space $\mathbf{P}$ and the Complementary Space $\mathbf{Q}$



**Nuclear Reactions as Spectroscopic Tools:  
Peripheral Reactions ↔ Direct Reactions**  
Elastic & Inelastic scattering, transfer reactions, charge exchange reactions...



**Our P-Space Choice**

**Direct Reactions ↔ Grazing Reactions with Impact Parameters**

$$b \sim R_T \sim r_0 A^{1/3}$$

$$(r_0 \approx 1.12 \text{ fm})$$

# Feshbach Projection

$$(H - E)\Psi = 0$$

- Orthogonal Projectors P and Q with  $P+Q=1$  and  $PQ=QP=0$
- Hamiltonian  $H = (P+Q)H(P+Q) = H_{PP} + H_{QQ} + H_{QP} + H_{PQ}$
- Wavefunction  $\Psi = (P+Q)\Psi = \Psi_P + \Psi_Q$

$$(H_{PP} - E)\Psi_P + H_{PQ}\Psi_Q = 0$$

$$(H_{QQ} - E)\Psi_Q + H_{QP}\Psi_P = 0 \rightarrow \Psi_Q = \frac{1}{E - H_{QQ} + i\eta} H_{QP}\Psi_P$$

- Effective Wave Equation in P-space ( $H=K+V$ ):

$$(K_{PP} + V_{PP} + \Sigma_{PP}(E) - E)\Psi_P = 0$$

- Self-energy in P-space  $\rightarrow$  non-Hermitian, energy dependent effective interaction:

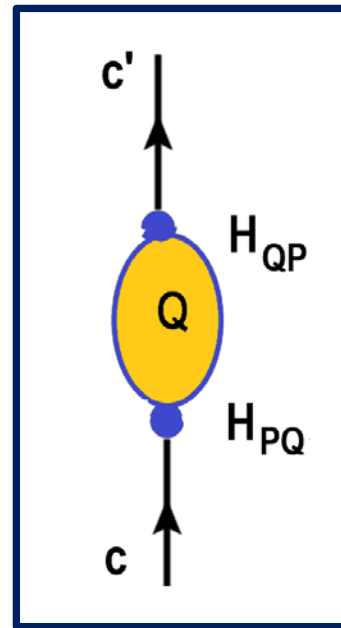
$$\Sigma_{PP}(E) = H_{PQ} \frac{1}{E - H_{QQ} + i\varepsilon} H_{QP}$$

# Structure of the Self-Energy Operator

$$\Sigma_{PP}(E) = H_{PQ} \frac{P}{E - H_{QQ}} H_{QP} - i\pi H_{PQ} \delta(E - H_{QQ}) H_{QP}$$

„Off-shell“

„On-shell“



$$c, c' \in P$$

# Lecture 3:

# Nuclear Direct Reaction Theory

## Channel States, Channel Configurations, and Relative Motion

Expand the channel states  $\Psi_c$  into nuclear configurations and wave functions of relative motion:

$$\Psi_c(\vec{r}, \vec{k}_c) = \psi_c(\vec{r}, \vec{k}_c) |c\rangle \quad ; \quad |c\rangle = \left[ \Phi_P^{(c)} \otimes \Phi_T^{(c)} \right]_{L_c S_c J_c \dots} \quad ; \quad \langle c | c' \rangle = \delta_{cc'}$$

- Projection onto the nuclear states  $c$
- Integration over the intrinsic nuclear coordinates  $\xi = \{r, \sigma, \tau \dots\}$

Non-hermitian, non-local **Self-Energy** connecting P-space channel states  $c$  and  $c'$ :

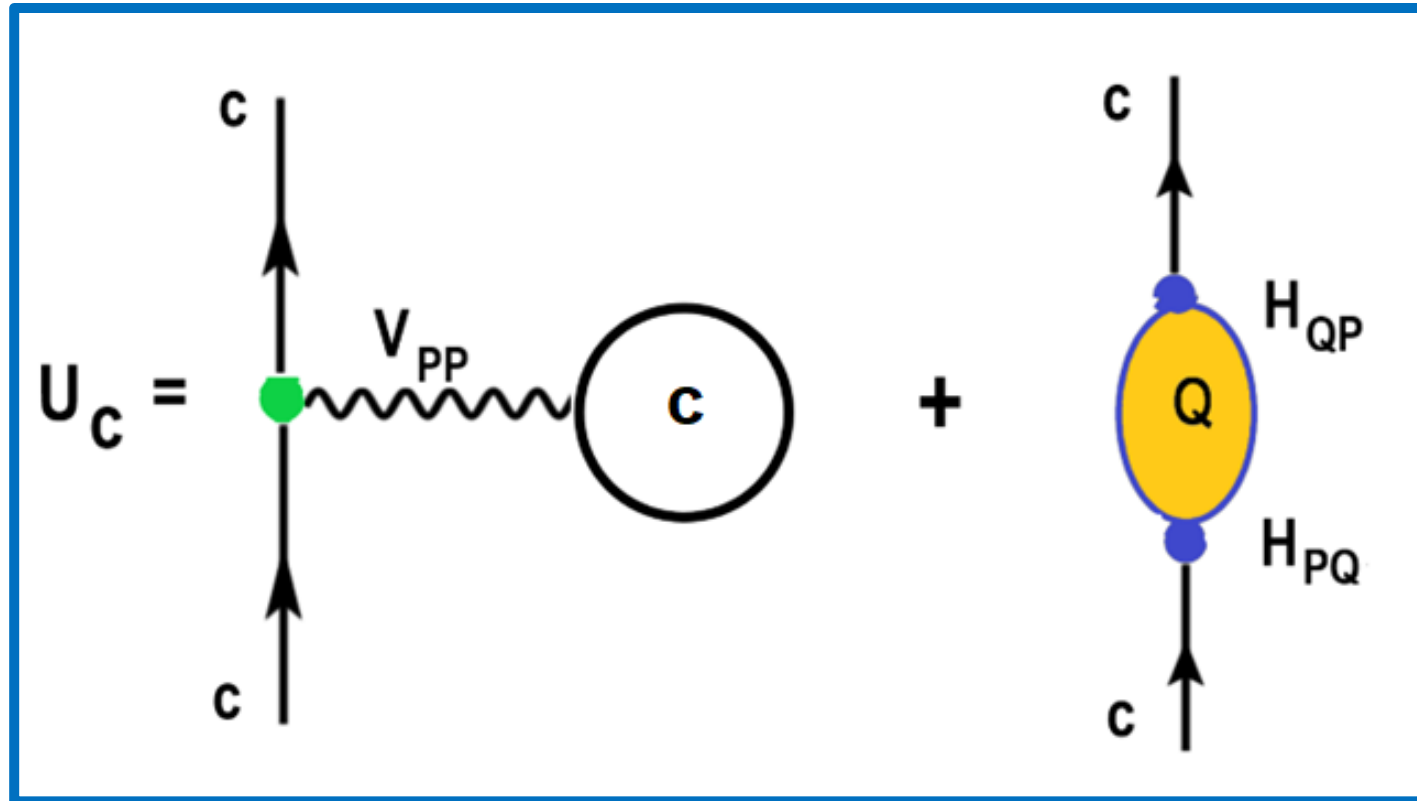
$$\Sigma_{cc'}(\vec{r}, \vec{r}' | E) = \sum_{n \in Q} \int \frac{d^3 k_n}{(2\pi)^3} \langle c | H_{PQ} | \Psi_n \rangle(\vec{r}) \left[ \frac{P}{E - \omega_n(k_n)} - i\pi \delta(E - \omega_n(k_n)) \right] \langle \Psi_n | H_{QP} | c' \rangle(\vec{r}')$$

Effective **Channel Potentials** in P-space for  $c=c'$

$$U_c(\vec{r} | E) \approx \langle c | V_{PP} | c \rangle(\vec{r}) + \Sigma_{cc}(\vec{r} | E)$$

# The Channel Potential

$$U_c(\vec{r} | E) \approx \langle c | V_{PP} | c \rangle(\vec{r}) + \Sigma_{cc}(\vec{r} | E)$$



**Non-local (momentum dependent) dispersive self-energy**

# The Reaction Network in P-Space

Coupled Channels (CC) Problem in P-space:

$$\left( K_c + U_c(\vec{r} | E) - \varepsilon_c \right) \psi_c(\vec{r}, \vec{k}_c) + \sum_{c' \neq c} F_{cc'}(\vec{r} | E) \psi_{c'}(\vec{r}, \vec{k}_{c'}) = 0$$
$$F_{cc'}(\vec{r} | E) = \langle c | V_{PP} | c' \rangle(\vec{r}) + \Sigma_{cc'}(\vec{r} | E)$$

...to be solved under the asymptotic boundary condition:

$$\Psi_c \rightarrow e^{i\vec{k}_i \cdot \vec{r}_i} |a_i A_i\rangle \delta_{ic} + f_{ic}(\Omega_c) \frac{e^{ik_c r_c}}{r_c} |a_c A_c\rangle$$

...by expansion into (several hundred) partial waves and solved for a given incident channel  $c=i$  with plane **and** outgoing waves while for  $c \neq i$  **only** outgoing spherical waves occur

## Example: Elastic Scattering as 1-Channel Problem

Partial Wave expansion and wave equation

$$\Psi_{\mathbf{c}}^{(+)}(\vec{r}, \vec{k}_{\mathbf{c}}) = \frac{4\pi}{k_{\mathbf{c}} r} \sum_{\ell m} Y_{\ell m}^*(\hat{\mathbf{k}}) Y_{\ell m}(\hat{\mathbf{r}}) u_{\ell}(r, k_{\mathbf{c}}) \longrightarrow \left( \frac{d^2}{dr^2} - \frac{\ell(\ell+1)}{r^2} - \frac{2m_{\mathbf{c}}}{\hbar^2} U_{\mathbf{c}}(r | \mathbf{E}) + k_{\mathbf{c}}^2(\mathbf{E}) \right) u_{\ell}(r, k_{\mathbf{c}}) = 0$$

...matching at  $r \gg R(U_{\mathbf{c}})$ :

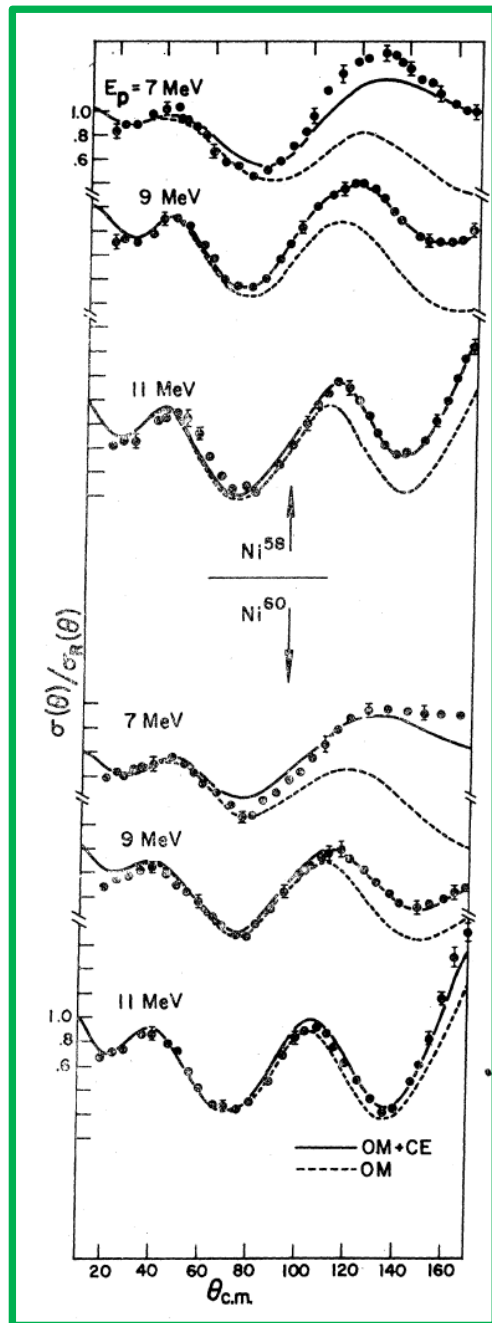
$$A_{\ell} u_{\ell}(r, k_{\mathbf{c}}) \rightarrow F_{\ell}(r, k_{\mathbf{c}}) + C_{\ell}(k_{\mathbf{c}} | U_{\mathbf{c}}) H_{\ell}^{(+)}(r, k_{\mathbf{c}})$$

Partial wave and total scattering amplitudes

$$C_{\ell}(k_{\mathbf{c}} | U_{\mathbf{c}}) = \frac{1}{2i} (\eta_{\ell} e^{2i\delta_{\ell}} - 1) \quad ; \quad 0 < \eta_{\ell} \leq 1$$

$$\mathbf{f}_{\mathbf{c}}^{(\text{elas})}(\vartheta) = \frac{1}{k_{\mathbf{c}}} \sum_{\ell} (2\ell + 1) P_{\ell}(\cos \vartheta) C_{\ell}(k_{\mathbf{c}} | U_{\mathbf{c}})$$

$$d\sigma_{\mathbf{c}}^{(\text{elas})} \sim \left| \mathbf{f}_{\mathbf{c}}^{(\text{elas})}(\vartheta) \right|^2 d\Omega$$



Nucleon-Nucleus Optical-Model Parameters,  $A > 40$ ,  $E < 50$  MeV\*

F. D. BECCHETTI, JR., AND G. W. GREENLEES

- Pioneering work of Becchetti and Greenless in 1969
- Systematic Study on Low-Energy proton-nucleus scattering
- $U_c$  parametrized in terms of optical potentials of simple functional form
- Wood-Saxon form factors

# Lecture 4

## Optical Model Potentials and Elastic Scattering

# Channel Potential and Optical Model Potential

$$U_c(\vec{r} | E) \approx \langle c | V_{PP} | c \rangle + \Sigma_{cc}(\vec{r} | E)$$

Introduce OMP as an AUXILIARY Potential

$$U_c^{opt}(\vec{r} | E) \equiv V_c(\vec{r} | E) - iW_c(\vec{r} | E)$$

$$V_c(\vec{r} | E) \leftrightarrow \text{Re}(\langle c | V_{PP} | c \rangle + \Sigma_{cc}(\vec{r} | E)) ; W_c(\vec{r} | E) \leftrightarrow -\text{Im}(\langle c | V_{PP} | c \rangle + \Sigma_{cc}(\vec{r} | E))$$

...imposed to reproduce as good as possible the scattering amplitude:

$$f_c(U_c, \mathcal{G}) = \langle \vec{k}_c | U_c | \psi_c^{(+)} \rangle = \langle \vec{k}_c | U_c \pm U_c^{opt} | \psi_c^{(+)} \rangle \approx f_c^{opt}(U_c^{opt}, k_c) + \Delta(U_c, U_c^{opt}) \quad (|\vec{k}_c\rangle \mapsto e^{i\vec{k}_c \cdot \vec{r}})$$

$$f_c^{opt}(U_c^{opt}, k_c) = \langle \vec{k}_c | U_c^{opt} | \chi_c^{(+)} \rangle ; \Delta(U_c, U_c^{opt}) = \langle \vec{k}_c | U_c - U_c^{opt} | \chi_c^{(+)} \rangle$$

$U^{opt}$  and the related distorted waves  $\chi^{(+)}$  describe  $\psi^{(+)}$  strictly spoken only in the asymptotic region but accounts globally for strong absorption at short distances.

# Phenomenological Optical Potentials

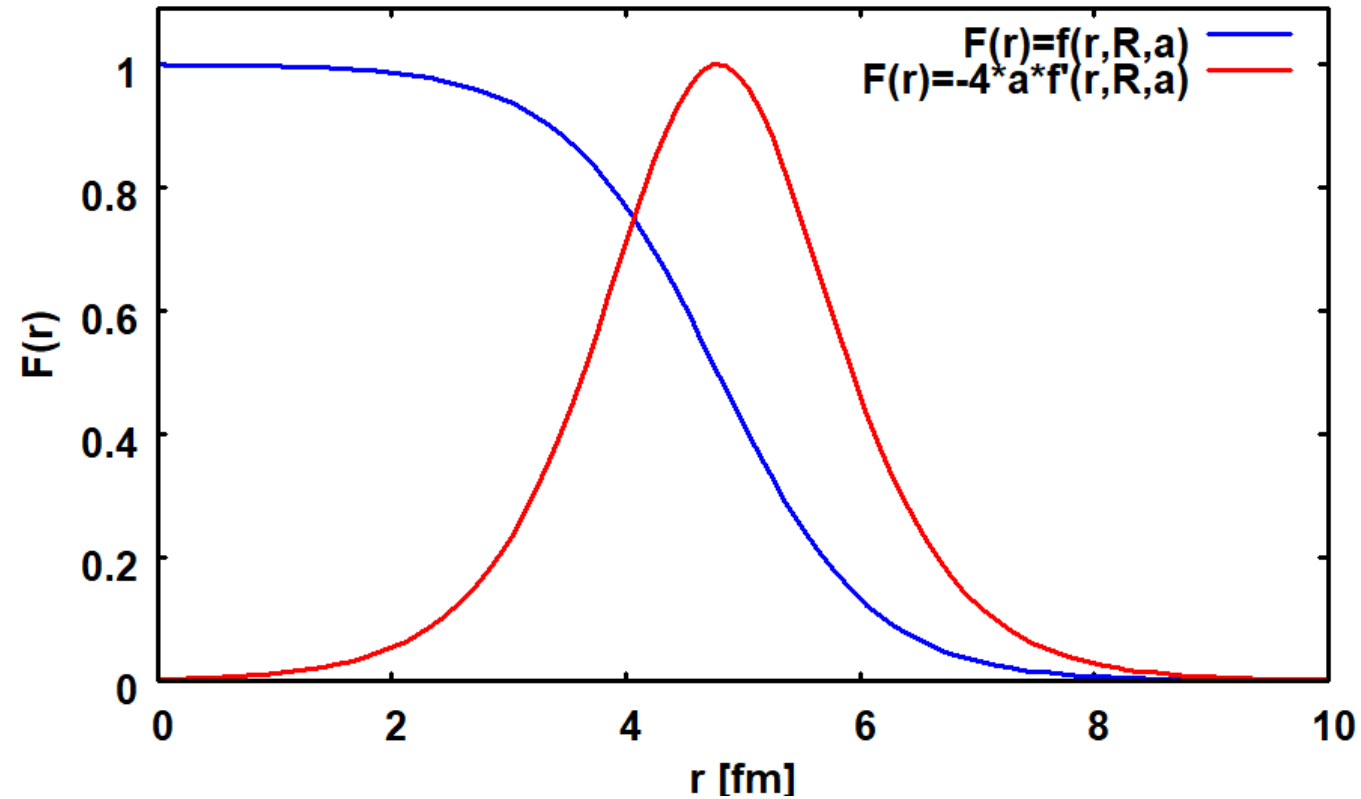
The general form for light (and heavy) ions is:

$$U(r) = V_c(r) - Vf_v(r, R_v, a_v) - i \left[ W_{\text{vol}} f_w(r, R_w, a_w) - 4a_w W_{\text{surf}} \frac{d}{dr} f_w(r, R_w, a_w) \right] \\ + V_{LS} \left[ \frac{\hbar}{m_\pi c} \right]^2 (l \cdot s) \frac{1}{r} \frac{d}{dr} f_{LS}(r, R_{LS}, a_{LS})$$

Form factors of Wood-Saxon (or Fermi) shape:

$$f(r, R, a) = \frac{1}{1 + e^{\frac{r-R}{a}}} \quad ; \quad \frac{d}{dr} f(r, R, a) = -\frac{1}{a} e^{\frac{r-R}{a}} f^2(r, R, a)$$

### Wood-Saxon Form Factor and Derivative



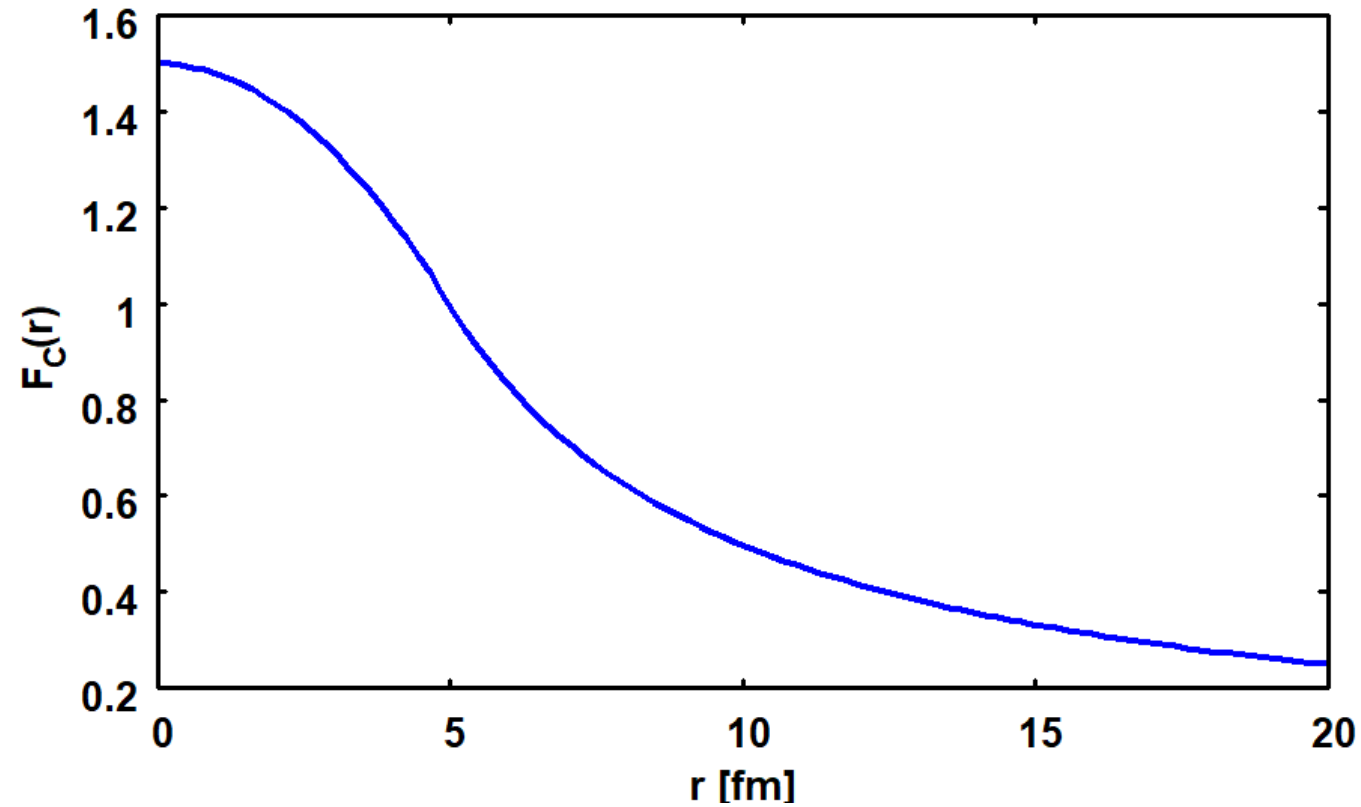
**A=56**  
 **$r_0 = 1.25$  fm ;  $a = 0.65$  fm**  
 **$R(A) = 4.78$  fm**

**Light Ions :  $R(A) = r_0 A^{1/3}$  ;  $r_0 \sim 1.25$  fm ;  $a \sim 0.6 \dots 0.7$  fm**

**Heavy Ions  $A > 10$ :  $R(A_P, A_T) = r_0 (A_P^{1/3} + A_T^{1/3})$  ;  $r_0 \sim 1$  fm**

**...plus Coulomb-Potential  $U_c(r, R_c)$ !**

## Form Factor of the Coulomb-Potential



**A=56, Z=26 (<sup>56</sup>Fe)**

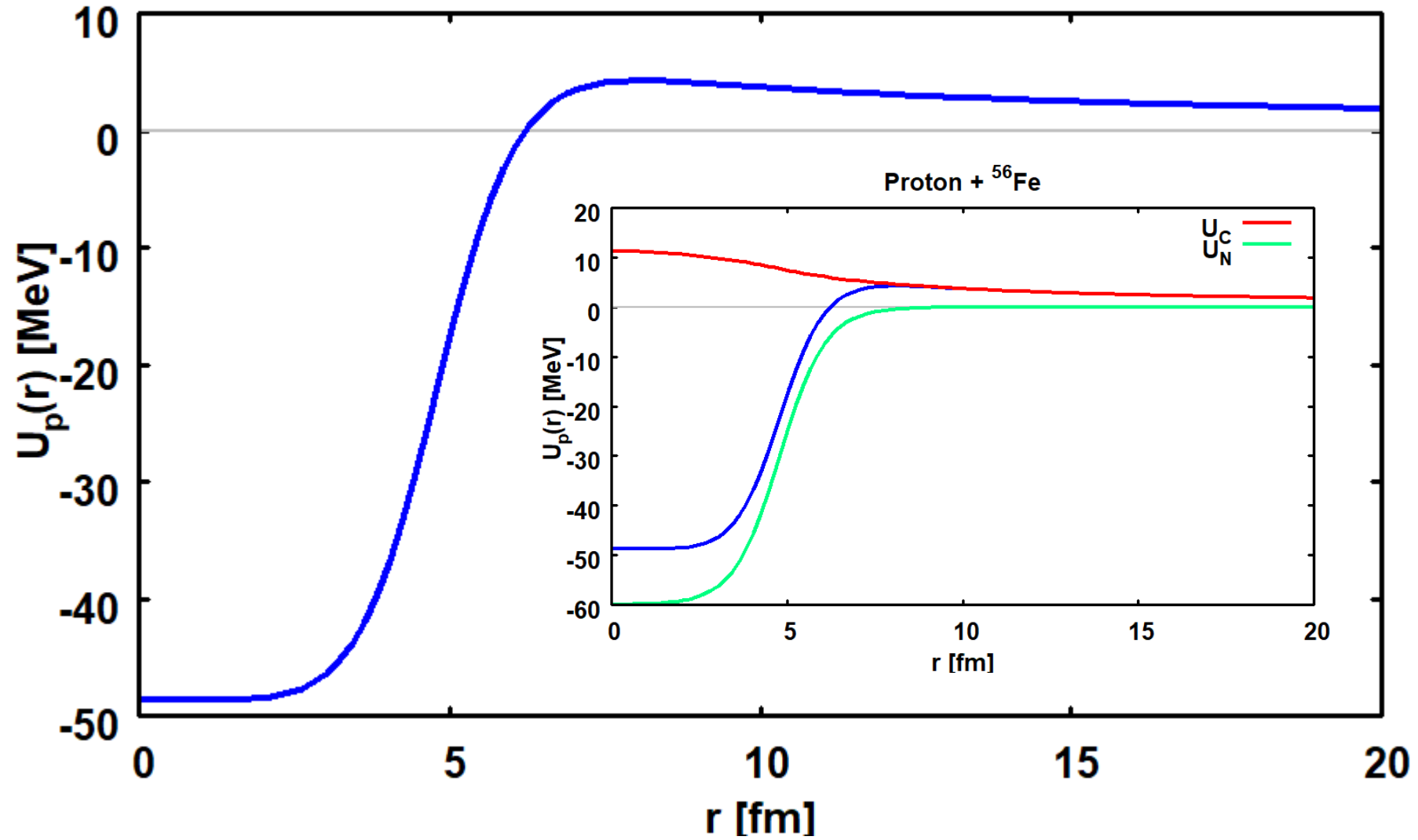
**r<sub>0C</sub>=1.3 fm**

**R<sub>C</sub>(A)=4.97 fm**

$$U_C(r, R_C, Z) = \frac{Z}{R_C} \alpha_f \hbar c F_C(r, R_C) \quad (\alpha_f \hbar \approx 1.44 \text{ MeVfm})$$

$$F_C(r, R_C) = \frac{1}{2} \left( 3 - \left( \frac{r}{R_C} \right)^2 \right) \Theta(R_C - r) + \frac{R_C}{r} \Theta(r - R_C) \quad \left( R_C(A) = r_{0C} A^{\frac{1}{3}} \right)$$

# Proton + $^{56}\text{Fe}$



## OMP, Distorted Waves, and Elastic Scattering

$$\left( K_c + U_c^{opt}(\mathbf{r}_c | E) - E \right) \chi_c^{(\pm)}(\vec{r}_c, \vec{k}_c) = 0$$
$$\chi_c^{(+)}(\vec{r}_c, \vec{k}_c) \rightarrow e^{i\vec{k}_c \cdot \vec{r}_c} + f_c(U_c^{opt}, \mathcal{G}) \frac{e^{ik_c r_c}}{r} ; \chi_c^{(-)\dagger}(\vec{r}_c, \vec{k}_c) = \chi_c^{(+)}(\vec{r}_c, -\vec{k}_c)$$

Scattering amplitude and elastic angular distribution

$$f_c(U_c^{opt}, \mathcal{G}) = \langle \vec{k}_c | U_c^{opt} | \chi_c^{(+)} \rangle ; d\sigma_c^{elas}(U_c^{opt}, \mathcal{G}) \approx |f_c(U_c^{opt}, \mathcal{G})|^2 d\Omega$$

Empirical approach:

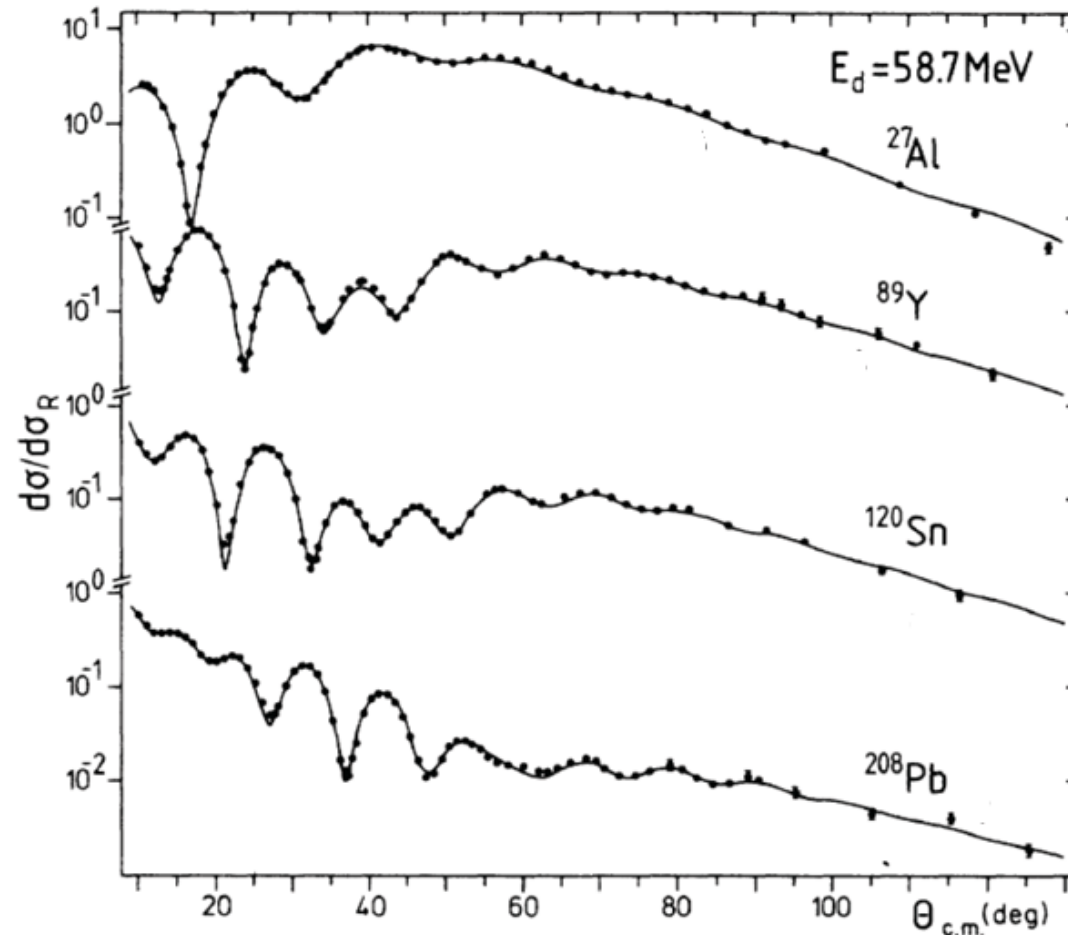
parametrize  $U$  by a convenient functional form and fix the model parameters by  $\chi^2$ -fit to data

$$\chi^2(U_c) = \sum_n \frac{1}{w_n} \left( d\sigma_c^{elast}(U_c^{opt}, \mathcal{G}_n) - d\sigma_c^{exp}(\mathcal{G}_n) \right)^2$$

$$d\sigma_c^{exp}(\mathcal{G}_n) \hat{=} d\sigma_c^{exp}(U_c, \mathcal{G}_n)$$

# High-Precision Phenomenological OMP-Fit to Elastic d+A Data (Hinterberger et al., Phys. Rev. C38:1153 (1988))

$$d\sigma_c^{(\text{elas})} \sim |f_c^{(\text{elas})}(\vartheta)|^2 d\Omega$$

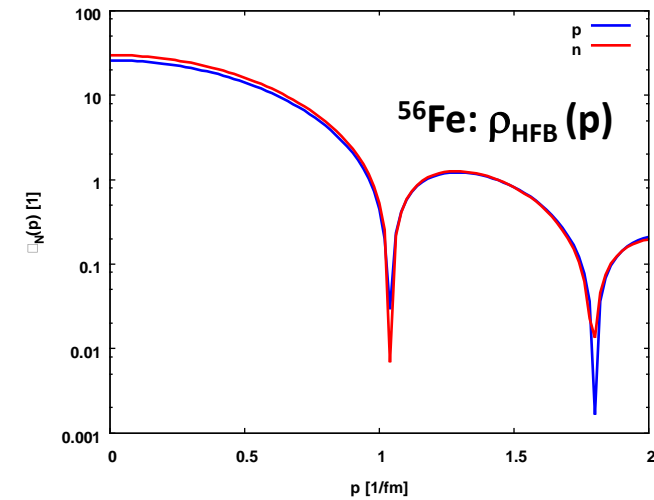
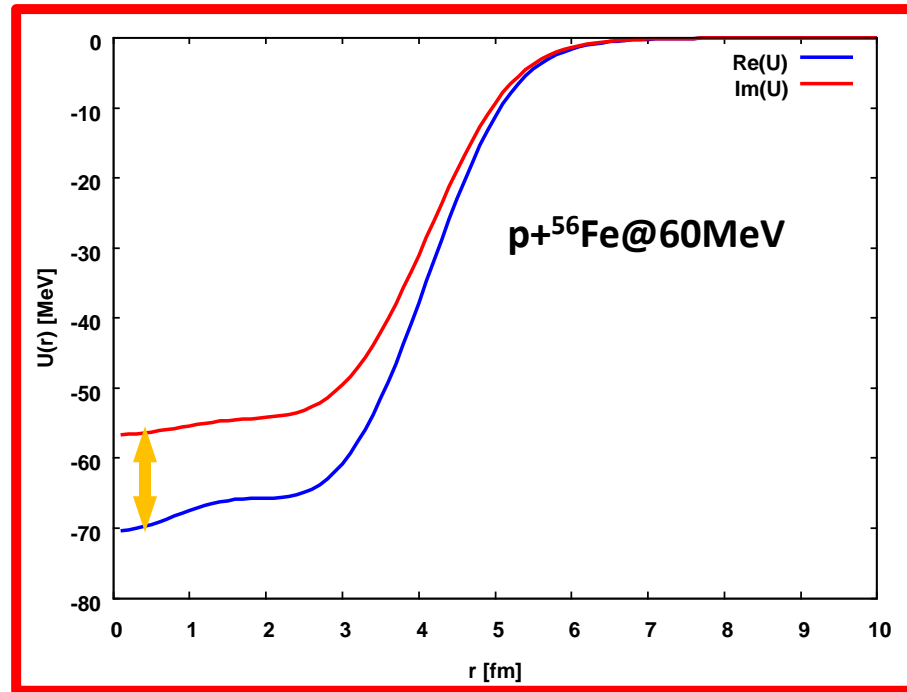
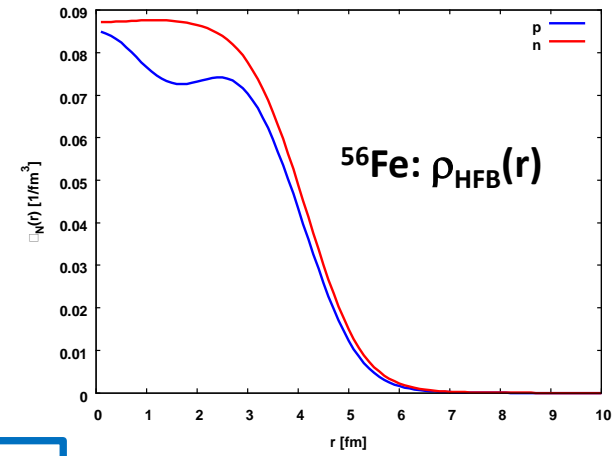


See also: H. Lenske, Int. Journ. Mod. Phys.E Vol. 30 (2021) 2130010

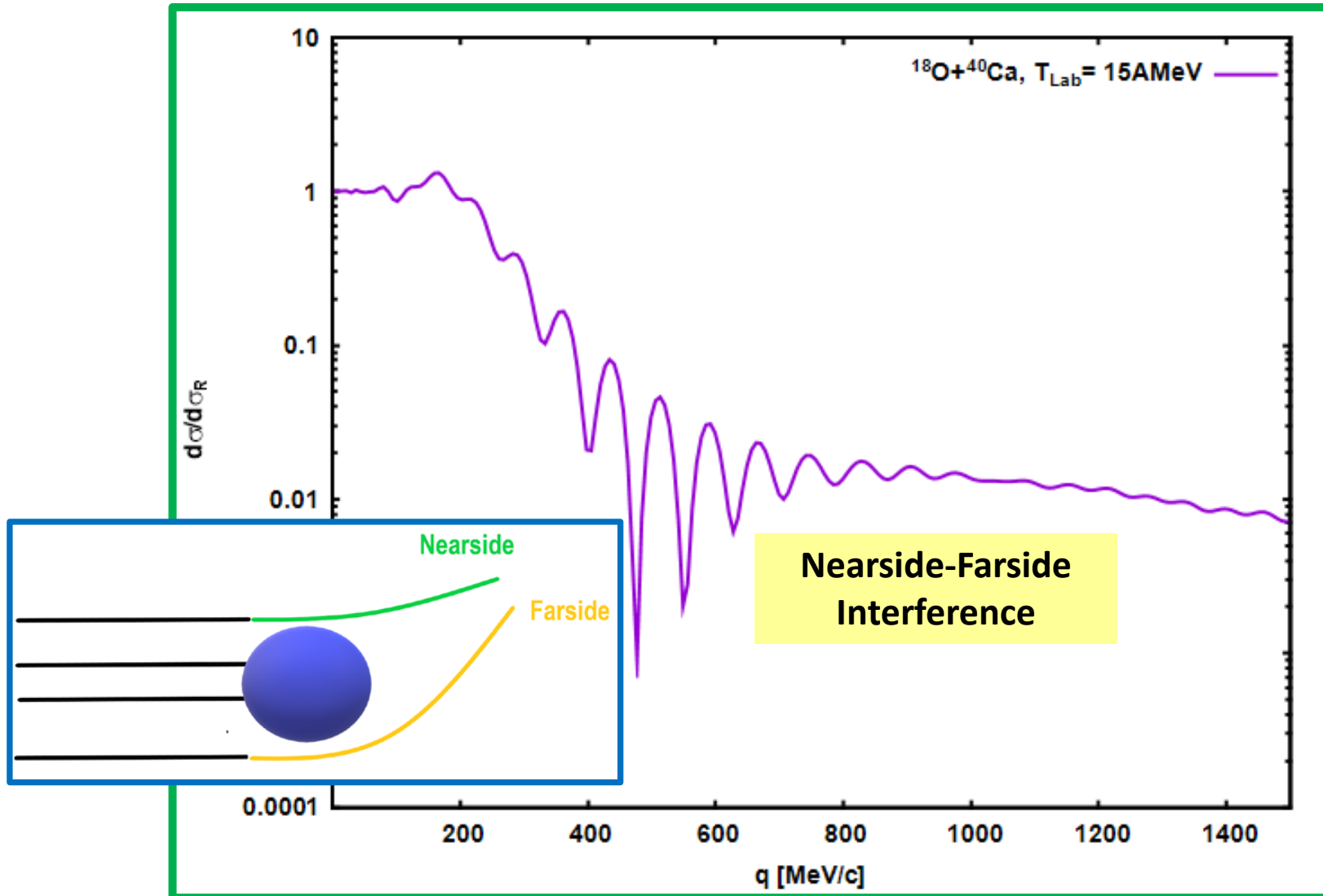
# Microscopic Folding Optical Potentials

- Proton and neutron ground state densities of target (and projectile) - **HFB**
- Projectile-target interaction  $\rightarrow$  **NN T-Matrix in momentum representation**
- Folding of densities and interactions  $\rightarrow$  Potential depending on  $r$

$$U_{\text{fold}}(\mathbf{r}, \mathbf{E}) = \int \frac{d^3\mathbf{p}}{(2\pi)^3} e^{i\mathbf{p}\cdot\mathbf{r}} \left( T_{00}(\mathbf{p} | \mathbf{E}) (\rho_n(\mathbf{p}) + \rho_p(\mathbf{p})) \pm T_{01}(\mathbf{p} | \mathbf{E}) (\rho_n(\mathbf{p}) - \rho_p(\mathbf{p})) + V_C(\mathbf{p}) \rho_C(\mathbf{p}) \right)$$



# $^{18}\text{O} + ^{40}\text{Ca}$ Elastic Scattering Microscopic Double-Folding OMP



# Optical Potentials from Effective Field Theory and Bayesian Optimization

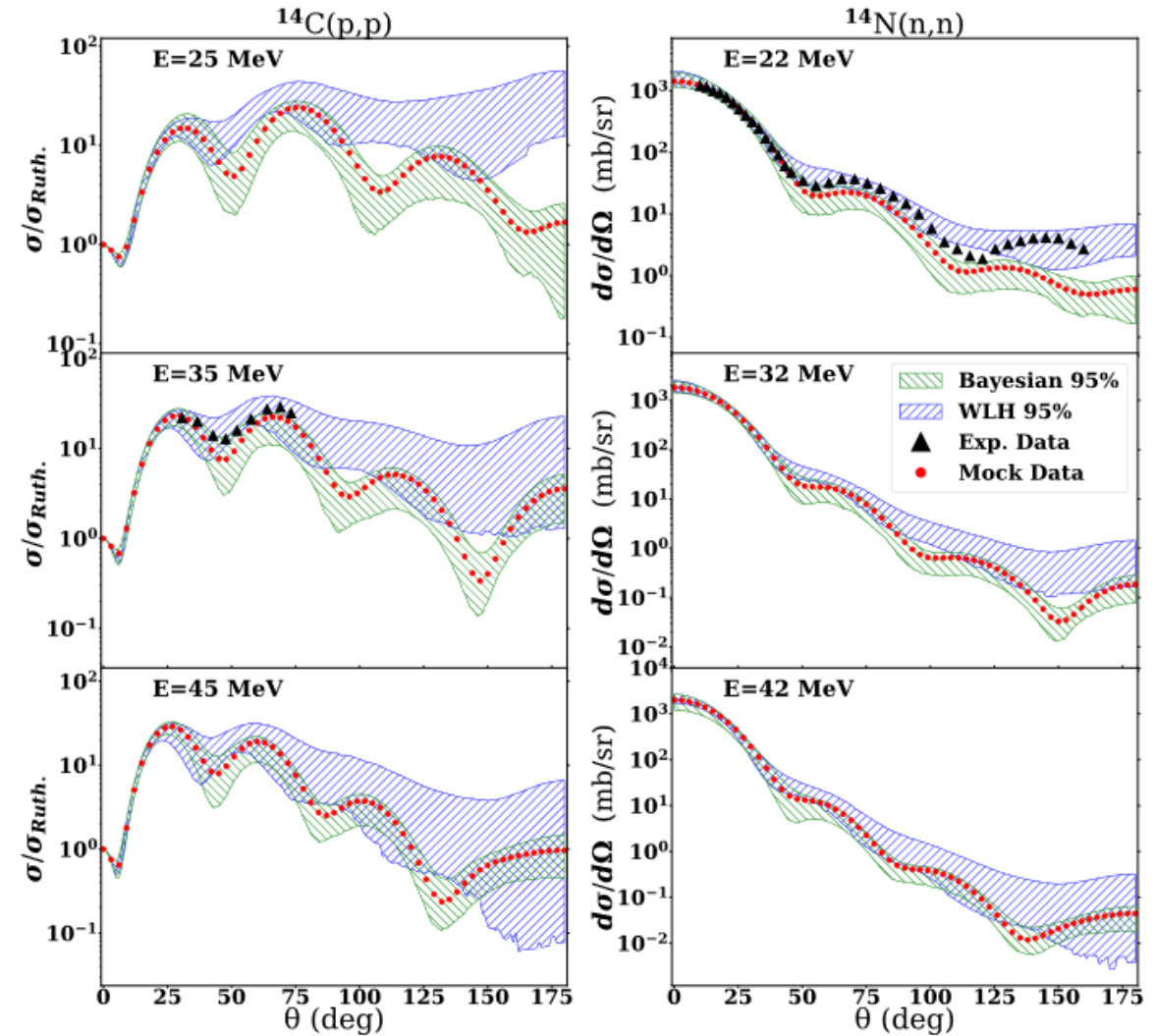
## The Whitehead-Lee-Holt (WLH) Method:

- Use  $\chi$ EFT and many-body perturbation theory
- Derive  $\Sigma_{cc}(\rho|E)$  in infinite matter
- Determine  $U_{cA}(r|E)$  in LDA:  $\Sigma_{cc}(r|E) \equiv \Sigma_{cc}(\rho_A(r)|E)$
- For numerical work, reparametrize  $U_{cA}(r|E)$  in

Wood-Saxon form:

$$\begin{aligned}
 U(r, E) = & -U_V f(r; r_V, a_V) - iU_W f(r; r_W, a_W) \\
 & + i4a_S U_S \frac{d}{dr} f(r; r_S, a_S) \\
 & + U_{SO} \frac{1}{m_\pi^2} \frac{1}{r} \frac{d}{dr} f(r; r_{SO}, a_{SO}) \vec{\ell} \cdot \vec{\sigma},
 \end{aligned}$$

- *A posteriori* Bayesian optimization by fit to data
- Extend the fit to (p,n) charge exchange data and elastic scattering in the incident and exit channel



T.R. Whitehead et al., PHYS. REV. C 105, 054611 (2022)

# Nuclear Reactions for Weak Interactions Part 2

Horst Lenske

Institut für Theoretische Physik, JLU Giessen

and

NUMEN Collaboration

# Agenda

**Lecture 1:** Basic Concepts of Quantum-Mechanical Scattering Theory

**Lecture 2:** Nuclear Reaction Theory in a Nutshell

**Lecture 3:** Theory of Nuclear Direct Reactions

**Lecture 4:** Optical Potentials and Elastic Scattering

**We are here:**

**Lecture 5:** Perturbative Approach to Non-Elastic Reactions

**Lecture 6:** Single Charge Exchange (SCE) Reactions

**Lecture 7:** Light Ion SCE Reactions and beta-Decay

**Lecture 8:** The Gamow-Teller Quenching Mystery

**Lecture 9:** Nuclear Matrix Elements for Astrophysics

**Lecture 10:** Heavy Ion SCE Reactions

**Lecture 11:** Heavy Ion SCE Reactions at Relativistic Energies

**Lecture 12:** Double Charge Exchange (DCE) Reactions

**Lecture 5:**  
**Perturbative Approach to Non-Elastic Reactions**  
**The Distorted Wave Born Approximation**  
**(DWBA)**

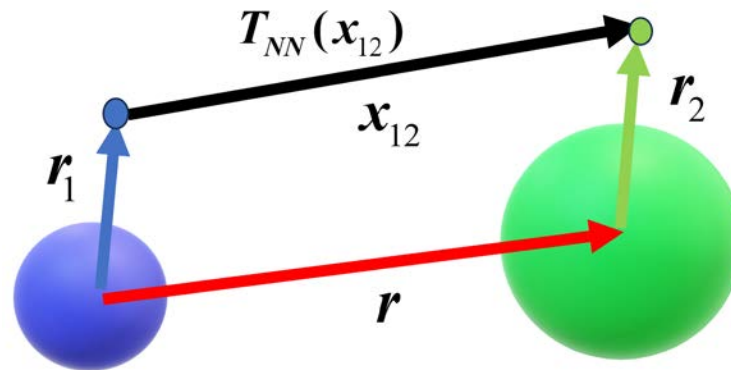
## The Weak Coupling Limit: Distorted Wave Born Approximation (DWBA)

$$\begin{aligned} \left( K_c + U_c^{opt}(\vec{r} | E) - \varepsilon_c \right) \chi_{ci}^{(+)}(\vec{r}, \vec{k}_c) + F_{ci}(\vec{r} | E) \chi_i^{(+)}(\vec{r}, \vec{k}_i) &= \mathbf{0} \\ \chi_{ci}^{(+)}(\vec{r}, \vec{k}_c) &\approx \int d^3r' G_c^{(+)}(\vec{r}, \vec{r}' | \varepsilon_c) F_{ci}(\vec{r}' | E) \chi_i^{(+)}(\vec{r}', \vec{k}_i) \\ \mathbf{f}_{c'i}(\vec{k}_c, \vec{k}_i) &\approx \mathbf{f}_{c'i}^{(DWBA)}(\vec{k}_c, \vec{k}_i) = \left\langle \chi_c^{(-)} \left| F_{ci} \right| \chi_i^{(+)} \right\rangle \end{aligned}$$

Decomposition of the reaction form factor  $F_{cc'}$  into multipole components  $F_{(LS)JM}$

$$\frac{d\sigma_{ci}}{d\Omega} \approx \sum_{LS, JM} \left| \left\langle \chi_c^{(-)} \left| F_{(LS)JM}(\vec{r}) \right| \chi_i^{(+)} \right\rangle \right|^2 = \sum_{\ell=0,1,2\dots} A_{\ell}^{(cc')} (k_c, k_i) P_{\ell}(\cos \mathcal{G})$$

# The Reaction Form Factor



$$\vec{x}_{12} = \vec{r}_2 - \vec{r}_1 + \vec{r}$$

$$\mathbf{T}_{\text{NN}}(\vec{x}_{12}) = \int \frac{d^3\mathbf{p}}{(2\pi)^3} e^{i\mathbf{p}\cdot\vec{x}_{12}} \mathbf{T}_{\text{NN}}(\vec{\mathbf{p}}) = \int \frac{d^3\mathbf{p}}{(2\pi)^3} e^{i\mathbf{p}\cdot(\vec{r}_2 - \vec{r}_1 + \vec{r})} \sum_{\mu=S,T,Tn} v_{\mu}(p^2) [\mathbf{O}_{\mu}(1) \otimes \mathbf{O}_{\mu}(2)]$$

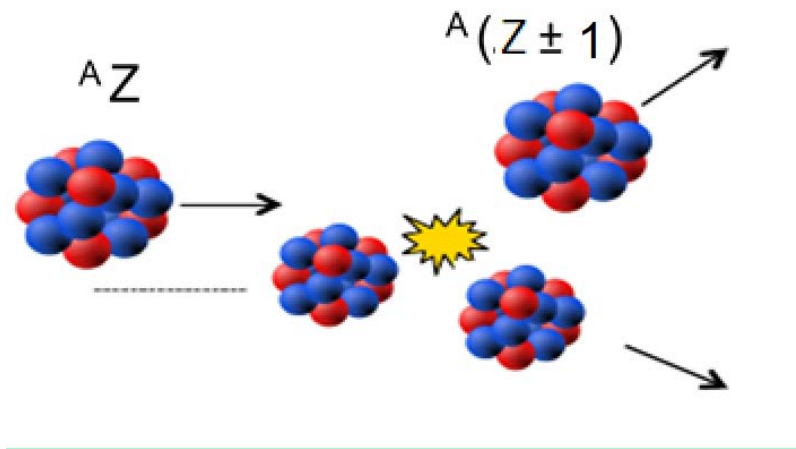
**Reaction Form Factor** describing the nuclear transitions in  $\alpha=a+A \rightarrow \beta=b+B$

$$\mathbf{F}_{\alpha\beta}(\vec{\mathbf{r}}) = \langle \mathbf{aA} | \mathbf{T}_{\text{NN}}(\vec{x}_{12}) | \mathbf{bB} \rangle = \int \frac{d^3\mathbf{p}}{(2\pi)^3} e^{i\mathbf{p}\cdot\vec{\mathbf{r}}} \sum_{\mu=S,T,Tn} v_{\mu}(p^2) \left[ \langle \mathbf{a} | e^{-i\mathbf{p}\cdot\vec{r}_1} \mathbf{O}_{\mu}(1) | \mathbf{b} \rangle \otimes \langle \mathbf{A} | e^{i\mathbf{p}\cdot\vec{r}_2} \mathbf{O}_{\mu}(2) | \mathbf{B} \rangle \right]$$

OBTD

OBTD

# Lecture 6: Single Charge Exchange Reactions



# Nuclear Single Charge Exchange Reaction by Isovector Meson Exchange

$${}^a_z a + {}^A_Z A \rightarrow {}^a_{z\pm 1} b + {}^A_{Z\mp 1} B,$$

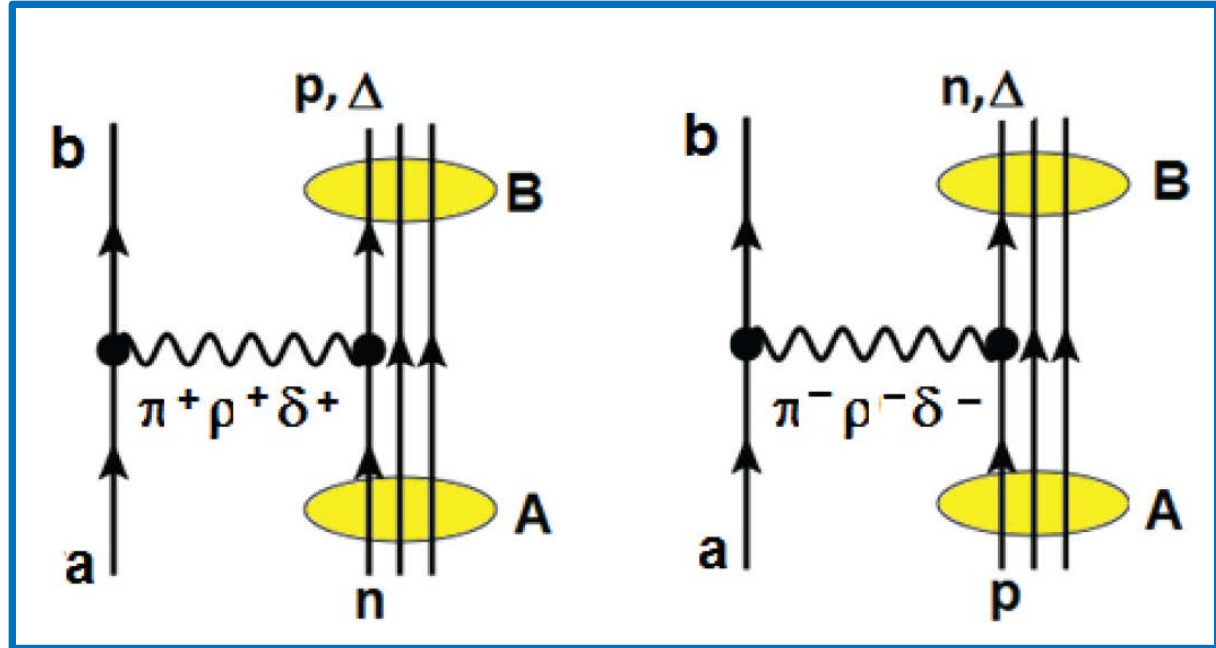
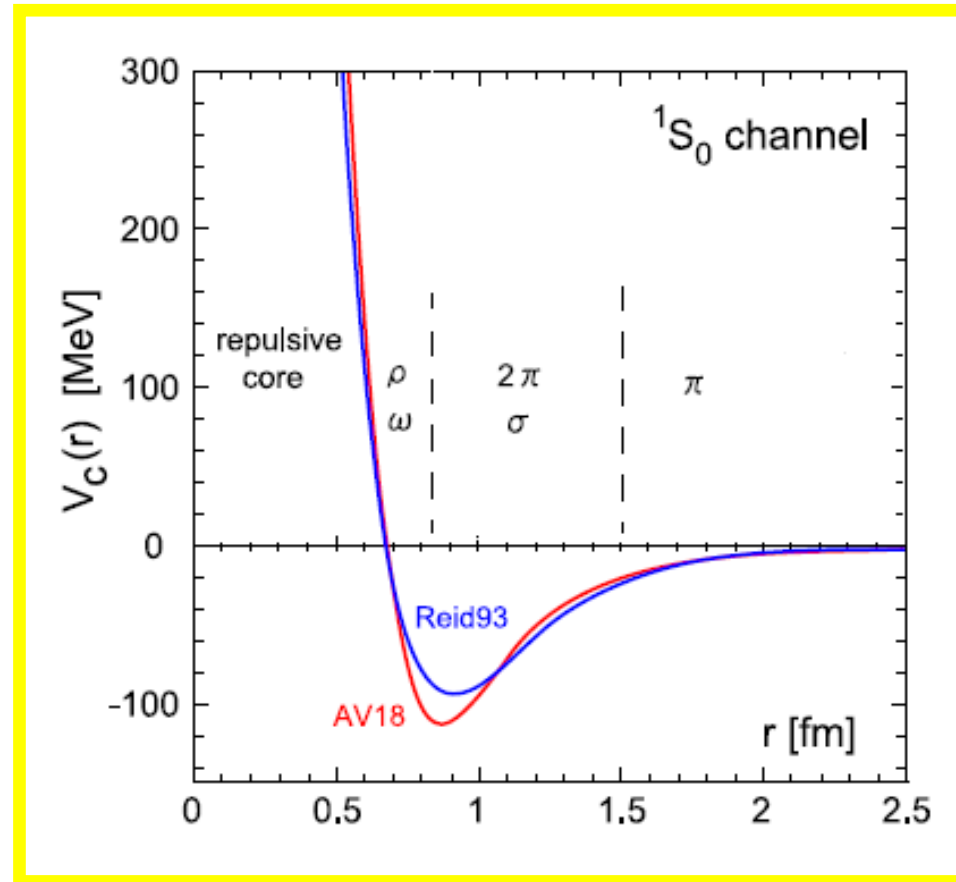


FIG. 1. Graphical representation of a single-charge exchange heavy-ion reaction by hadronic interactions corresponding to  $\nu\beta$  processes. Both  $(n, p)$ -type (left) and  $(p, n)$ -type (right) reactions, as seen in the  $A \rightarrow B$  transition in target system, are displayed, indicating also the exchanged meson.

# NN OBE-Interaction at Tree-Level



**Singularity requires complete summation of the Scattering Series:**

$$T_{NN} = V_{NN} + \int V_{NN} G_{NN} T_{NN} = \frac{1}{1 + \int V_{NN} G_{NN}} V_{NN}$$

# Operator Structure of the Fierz-Transformed (Anti-Symmetrized) NN T-Matrix

$$T_{NN} = V_{NN} + \int V_{NN} G_{NN} T_{NN}$$

$$T_{NN}(\mathbf{p}) = \sum_{S=0,1, T=0,1} \{ V_{ST}^{(C)}(p^2) [\boldsymbol{\sigma}_a \cdot \boldsymbol{\sigma}_A]^S + \delta_{S1} V_T^{(Tn)}(p^2) S_{12}(\mathbf{p}) [\boldsymbol{\tau}_a \cdot \boldsymbol{\tau}_A]^T \}.$$

## Rank-2 Spin-Tensor Interaction

$$S_{12}(\mathbf{p}) = \frac{1}{p^2} (3\boldsymbol{\sigma}_a \cdot \mathbf{p} \boldsymbol{\sigma}_A \cdot \mathbf{p} - \boldsymbol{\sigma}_a \cdot \boldsymbol{\sigma}_A p^2) = \sqrt{\frac{24\pi}{5}} \sum_M Y_{2M}^*(\hat{\mathbf{p}}) S_{2M}; \quad S_{2M} = [\boldsymbol{\sigma}_1 \otimes \boldsymbol{\sigma}_2]_{2M}$$

$$T_{NN}(\mathbf{p}) = \sum_{S,T} \left\{ V_{ST}^{(C)}(p^2) O_{ST}(1) O_{ST}(2) + \delta_{S1} V_T^{(Tn)}(p^2) \sqrt{\frac{24\pi}{5}} Y_2^*(\hat{\mathbf{p}}) \cdot [O_{ST}(1) \otimes O_{ST}(2)]_2 \right\}$$

$$O_{ST}(i) = (\boldsymbol{\sigma}_i)^S (\boldsymbol{\tau}_i)^T$$

## SCE Form Factors, Reaction Kernel and Amplitudes, Cross Section

$$\mathcal{R}_{ST}(\mathbf{p}, \mathbf{r}) = \frac{1}{4\pi} e^{i\mathbf{p}\cdot\mathbf{r}} O_{ST}, \quad F_{ST}^{(XY)}(\mathbf{p}) = \langle J_Y M_Y | \mathcal{R}_{ST}(\mathbf{p}, \mathbf{r}_X) | J_X M_X \rangle.$$

$$K_{\alpha\beta}^{(ST)}(\mathbf{p}) = (4\pi)^2 \left\{ V_{ST}^{(C)}(p^2) F_{ST}^{(ab)\dagger}(\mathbf{p}) \cdot F_{ST}^{(AB)}(\mathbf{p}) + \delta_{S1} \sqrt{\frac{24\pi}{5}} V_{ST}^{(Tn)}(p^2) Y_2^*(\hat{\mathbf{p}}) \cdot [F_{ST}^{(ab)\dagger}(\mathbf{p}) \otimes F_{ST}^{(AB)}(\mathbf{p})]_2 \right\},$$

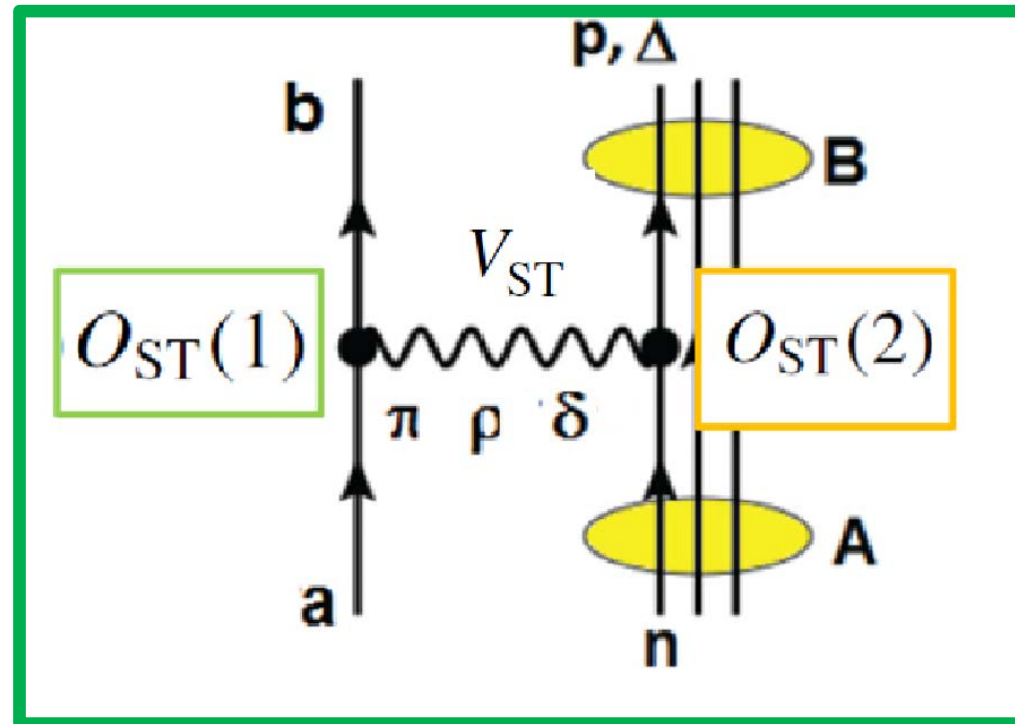
$$M_{\alpha\beta}(\mathbf{k}_\alpha, \mathbf{k}_\beta) = \int \frac{d^3 p}{(2\pi)^3} \langle \chi_\beta^{(-)} | e^{-i\mathbf{p}\cdot\mathbf{r}} \sum_{ST} K_{\alpha\beta}^{(ST)}(\mathbf{p}) | \chi_\alpha^{(+)} \rangle \quad N_{\alpha\beta}(\mathbf{k}_\alpha, \mathbf{k}_\beta, \mathbf{p}) = \frac{1}{(2\pi)^3} \langle \chi_\beta^{(-)} | e^{-i\mathbf{p}\cdot\mathbf{r}} | \chi_\alpha^{(+)} \rangle,$$

$$M_{\alpha\beta}(\mathbf{k}_\alpha, \mathbf{k}_\beta) = \int d^3 p \mathcal{U}_{\alpha\beta}(\mathbf{p}) N_{\alpha\beta}(\mathbf{k}_\alpha, \mathbf{k}_\beta, \mathbf{p}),$$

$$d^2\sigma_{\alpha\beta} = \frac{m_\alpha m_\beta}{(2\pi \hbar^2)^2} \frac{k_\beta}{k_\alpha} \frac{1}{(2J_a + 1)(2J_A + 1)} \sum_{M_a, M_A \in \alpha; M_b, M_B \in \beta} |M_{\alpha\beta}(\mathbf{k}_\alpha, \mathbf{k}_\beta)|^2 d\Omega.$$

# Vertex Structure of Mesonic Single Charge Exchange

...for (p,n), (<sup>3</sup>He,<sup>3</sup>H)...(<sup>12</sup>C,<sup>12</sup>N)...(<sup>48</sup>Ti,<sup>48</sup>Sc)...(<sup>124</sup>Sn,<sup>124</sup>Sb) reactions on any target and at any energy!

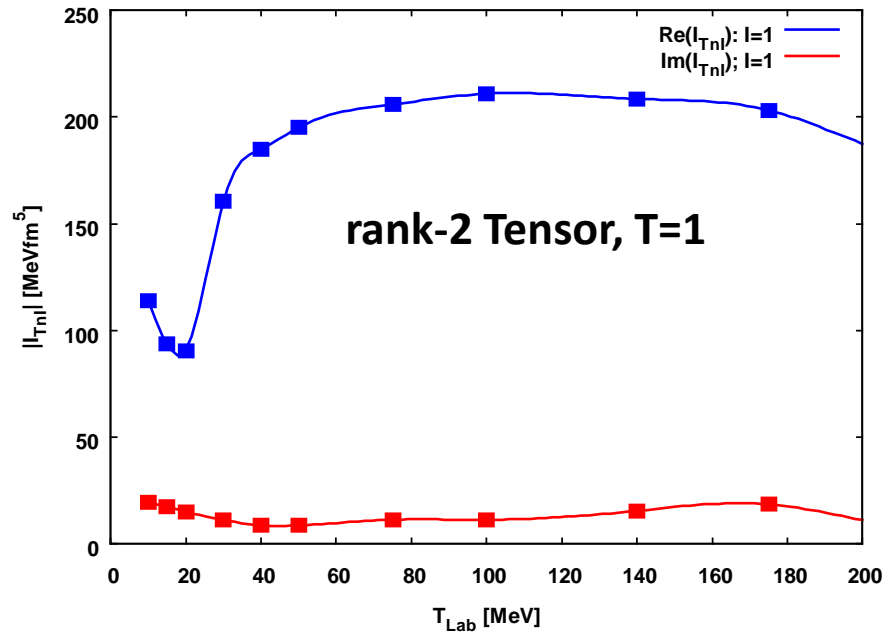
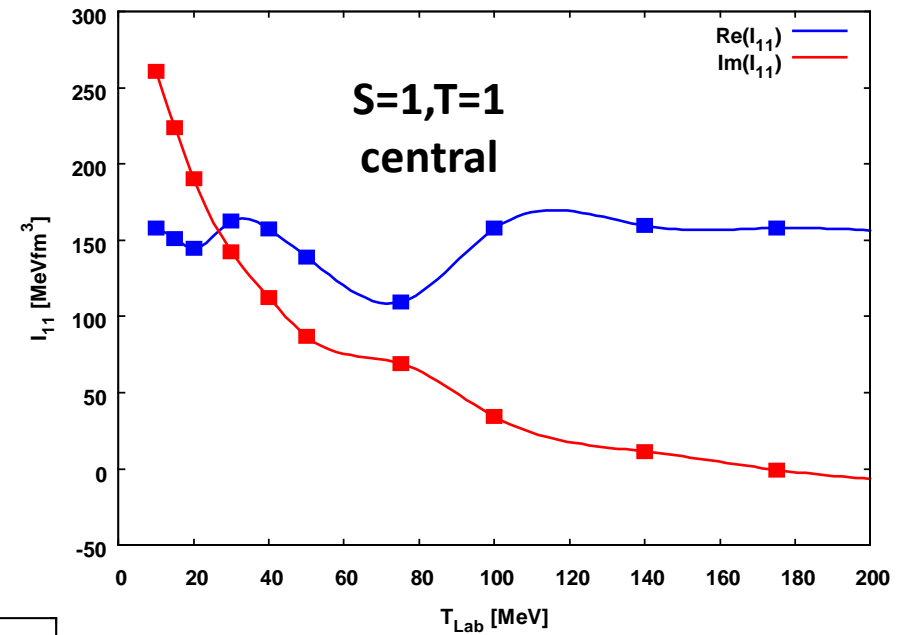
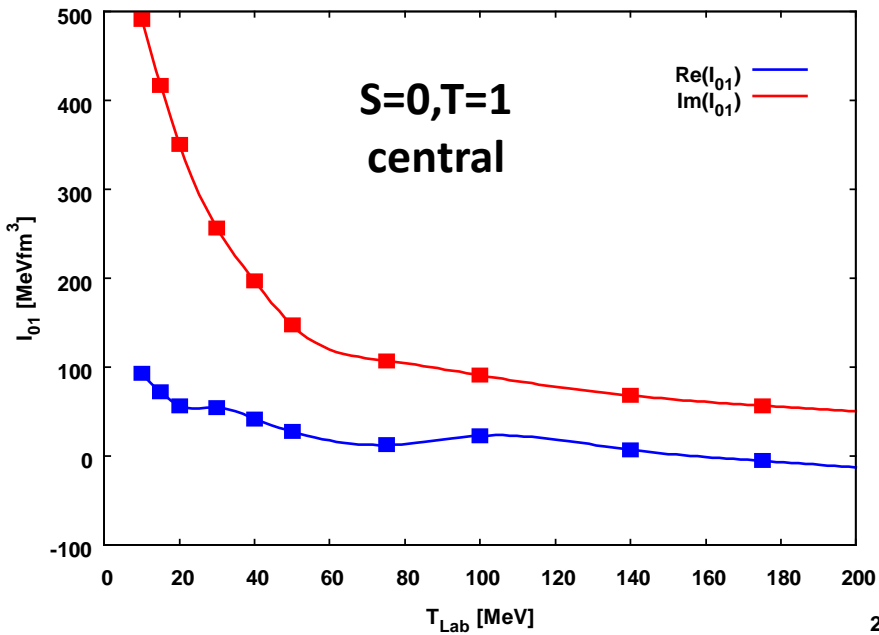


$$O_{ST}(i) = (\sigma_i)^S (\tau_i)^T$$

# Energy Dependence of Isovector NN-Interaction Strengths

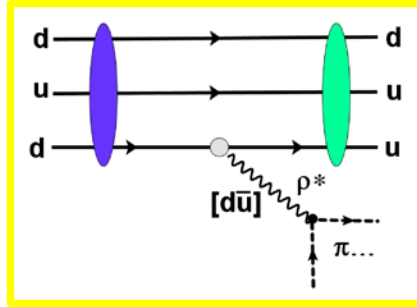
$$I_{ST}(T_{lab}) = V_{ST}(p=0 | T_{lab})$$

$$I_{ST}(T_{lab}) \approx g_{eff}^2(T_{lab})/m_{eff}^2$$

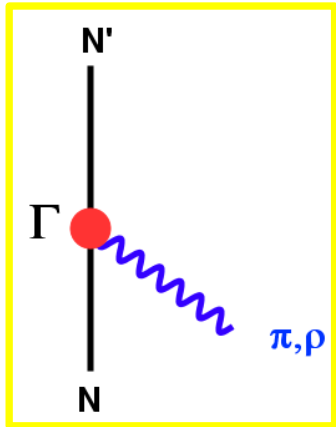
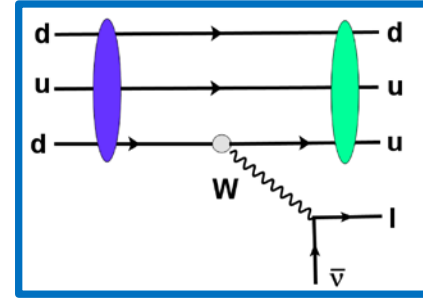


# NN Strong Interaction and Weak Interaction Vertices

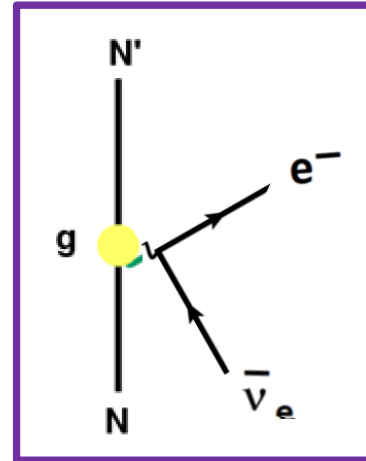
## Strong Interaction



## Weak Interaction



$$\begin{aligned}
 \pi \ \& \ \delta : \Gamma_{01} (q^2) \tau_{\pm} & \Leftrightarrow & \ g_F (q^2) \tau_{\pm} & \text{"Fermi"} \\
 \pi \ \& \ \rho : \Gamma_{11} (q^2) \sigma_1 \tau_{\pm} & \Leftrightarrow & \ g_A (q^2) \sigma \tau_{\pm} & \text{"Gamow-Teller"} \\
 \rho : \Gamma_{T1} (q^2) \sigma \times q \tau_{\pm} & \Leftrightarrow & \ g_M (q^2) \sigma \times q \tau_{\pm} & \text{"weak magnetic"} \\
 & & & & + \dots
 \end{aligned}$$



**pion-exchange:**  $\sigma_1 \cdot \vec{q} \sigma_2 \cdot \vec{q} = \frac{q^2}{3} (S_{12} + \sigma_1 \cdot \sigma_2)$

**rho-exchange :**  $\sigma_1 \times \vec{q} \sigma_2 \times \vec{q} = \sigma_1 \cdot \sigma_2 q^2 - \sigma_1 \cdot \vec{q} \sigma_2 \cdot \vec{q}$

$$S_{12} = \frac{1}{q^2} [3\sigma_1 \cdot \vec{q} \sigma_2 \cdot \vec{q} - \sigma_1 \cdot \sigma_2 q^2]$$

# Lecture 7: Light Ion SCE Reactions and Nuclear beta-Decay

**The Game Changer:**  
**Simplicity of (p,n) and (3He,t) SCE Reactions above  $T_{\text{lab}} > 100$  AMeV**

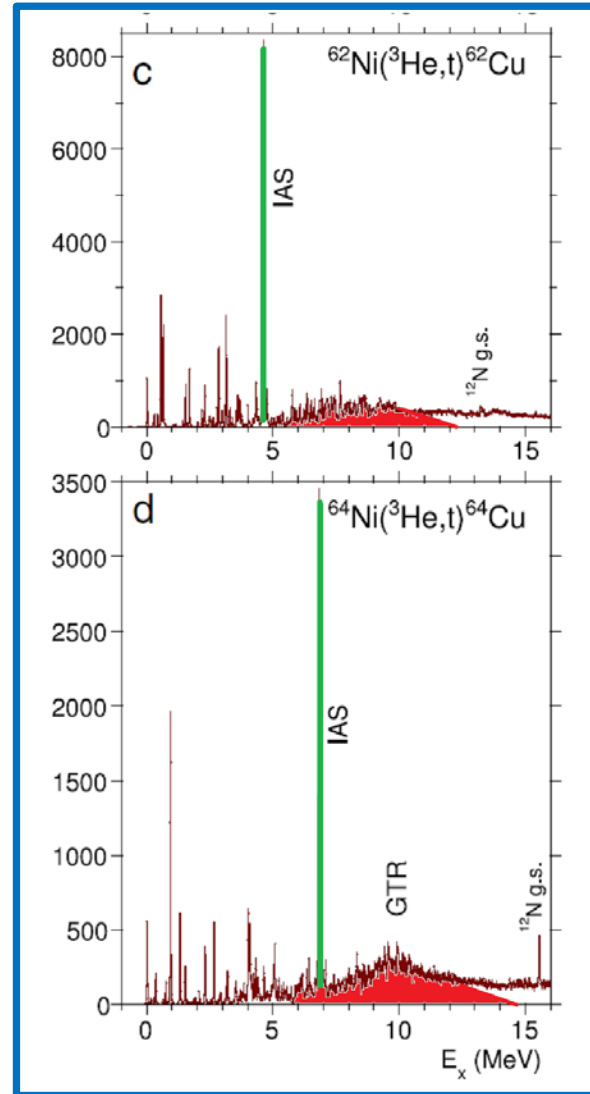
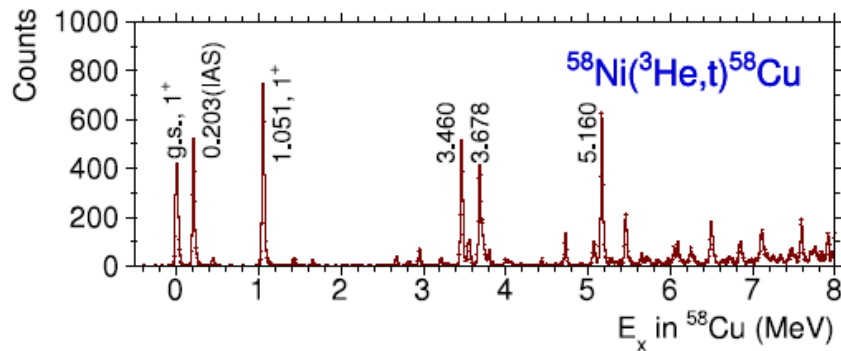
$$\begin{aligned}\frac{d\sigma_{GT}}{d\Omega}(q, \omega) &\simeq K(\omega) N_{\sigma\tau} |J_{\sigma\tau}(q)|^2 B(GT) \\ &= \hat{\sigma}_{GT}(q, \omega) B(GT),\end{aligned}$$

**SCE Cross Sections factorize into a unit cross section  $\hat{\sigma}_{GT}$  and a nuclear matrix element B(GT)!**  
(late 1970ties at IUCF)

**Spoiler:**  
**This is not always the case but depends esp. on the multipolarity!**

# Characteristics of Light Ion Single Charge Exchange Reactions on a Medium-Mass Nucleus

$\Delta E=45\text{KeV (!)}$

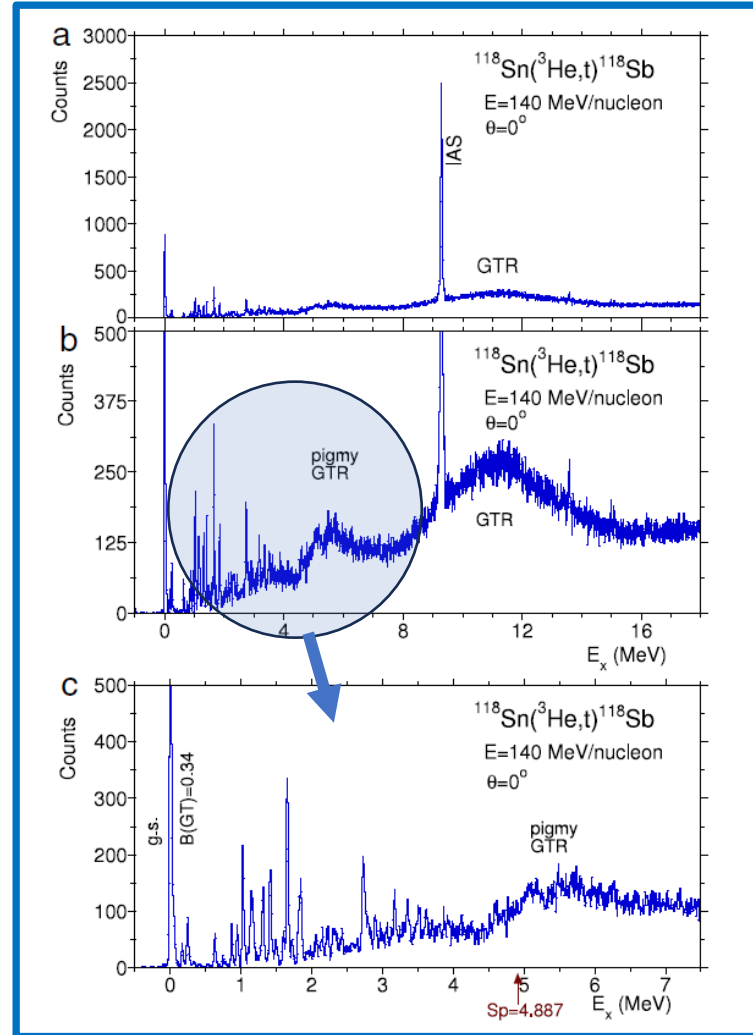


The  $(^3\text{He}, t)$  spectra on nickel target nuclei.

$T_{\text{lab}}(^3\text{He})=140 \text{ A MeV}=420 \text{ MeV}$   
 Research Center for Nuclear  
 Physics (RCNP), Osaka University

# Characteristics of Light Ion Single Charge Exchange Reactions on a Heavy Nucleus

$T_{\text{lab}}(^3\text{He})=140 \text{ A MeV}=420 \text{ MeV}$   
RCNP@Osaka



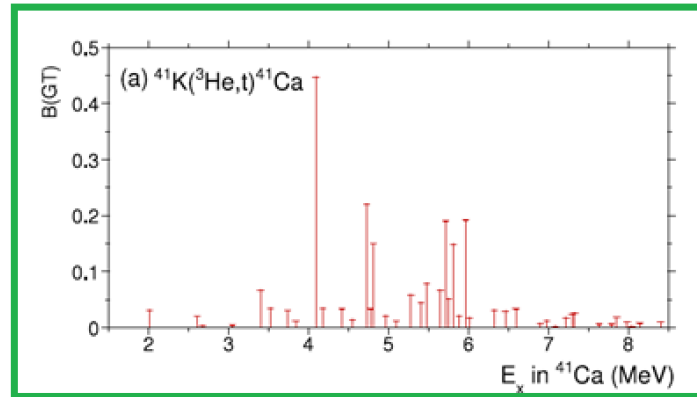
$^{118}\text{Sn}(^3\text{He}, t) ^{118}\text{Sb}$  spectrum. The discrete g.s, low-lying states, and the IAS are prominent

$^{118}\text{Sn}(^3\text{He}, t) ^{118}\text{Sb}$  spectrum with an expanded vertical scale.

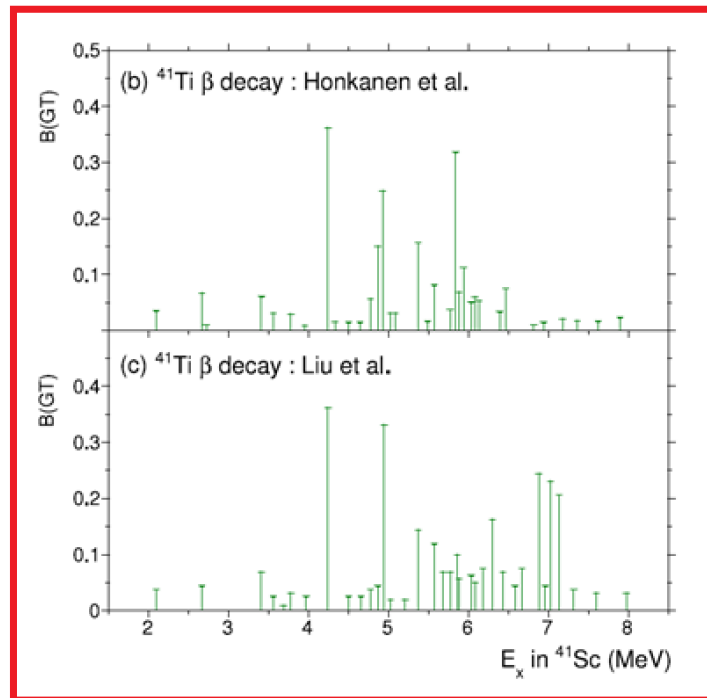
$^{118}\text{Sn}(^3\text{He}, t) ^{118}\text{Sb}$  spectrum with expanded vertical and energy scales.

**$\Delta E=45\text{KeV} (!)$**

# NME from ( $^3\text{He},t$ ) and $\beta$ -Decay

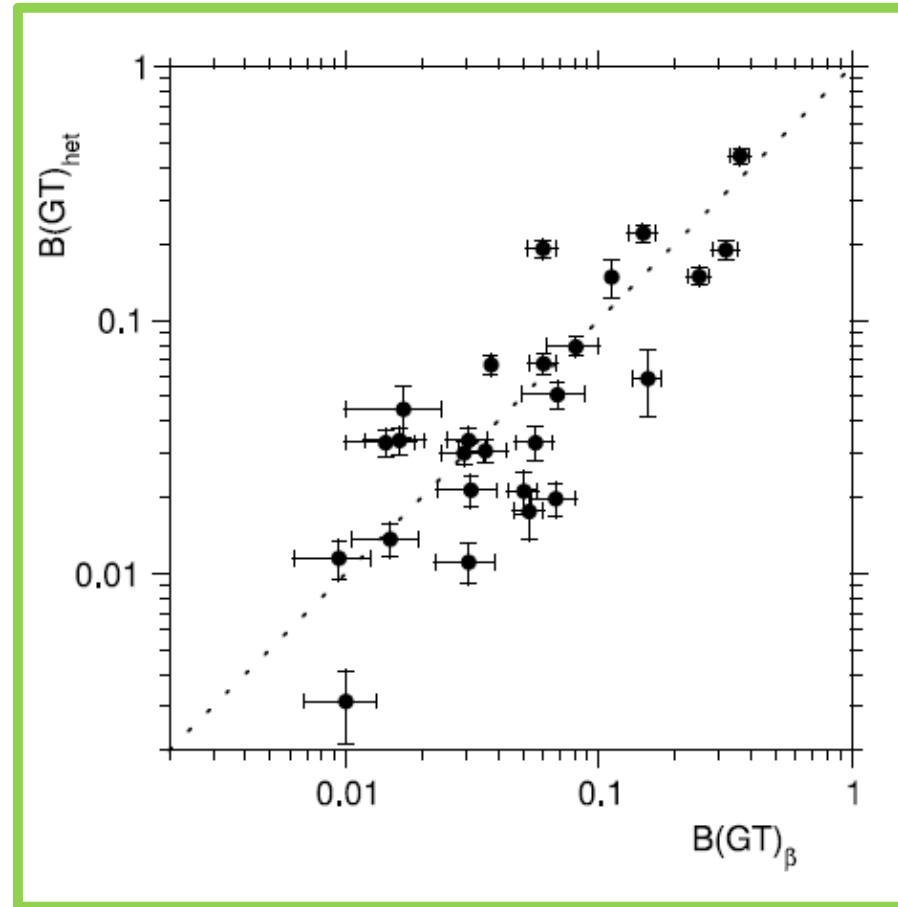


$^{41}\text{K} \rightarrow ^{41}\text{Ca}: Z \rightarrow Z+1$  „ $\beta^-$ “ transition



$^{41}\text{Ti} \rightarrow ^{41}\text{Sc}: Z \rightarrow Z-1$   $\beta^+$  transition

# Comparison of $B(\text{GT})$ from ( ${}^3\text{He}$ , ${}^3\text{H}$ ) Reactions and $\beta$ -Decay



...Deviations increase considerably for weak transitions!

Y. Fujita, B. Rubio, W. Gelletly, PPNP 66 (2011) 549

# The General Picture: Coherent Superpositions of Nuclear Multipoles

**Natural Parity ( $\pi=(-)^J$ ) „Fermi“ Transition in both Nuclei – L=J, S=0,1 :**

$$\frac{d\sigma^{FF}}{d\Omega} \sim \frac{q^{2(J_a+J_A)}}{[(2J_a+1)!!(2J_A+1)!!]^2} |\bar{N}_{\alpha\beta}|^2 \cdot \left| V_{01}^{(C)}(0) b_{J_A 0 J_A}^{(AB)} b_{J_a 0 J_a}^{(ab)} + e^{i\phi_{aA}} V_{11}^{(C)}(0) b_{J_A 1 J_A}^{(AB)} b_{J_a 1 J_a}^{(AB)} \right|^2$$

**Unnatural Parity ( $\pi=(-)^{J+1}$ ) „Gamov-Teller“-type Transition in both Nuclei – L=J±1:**

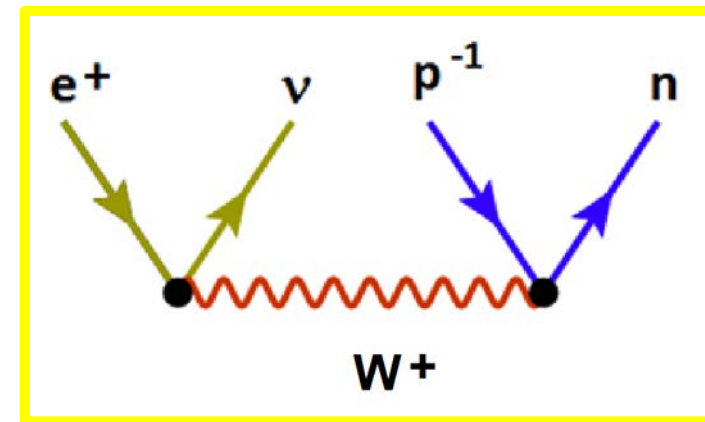
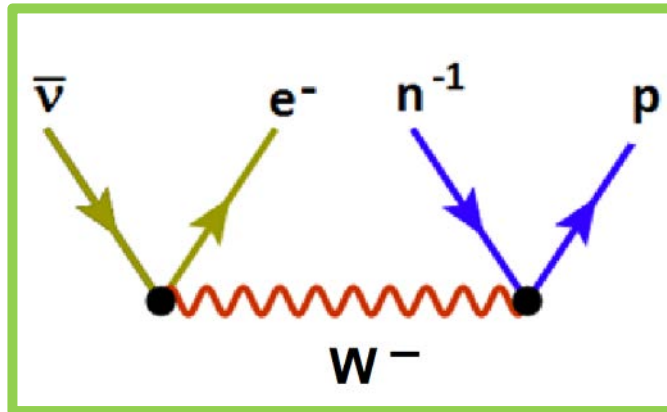
$$\frac{d\sigma^{GG}}{d\Omega} \sim \frac{q^{2(J_a+J_A-2)}}{[(2J_a-1)!!(2J_A-1)!!]^2} |V_{11}^{(C)}(0)|^2 |\bar{N}_{\alpha\beta}|^2$$

$$\times \left[ \left| b_{J_A-1 J_A}^{(AB)} + \frac{q^2}{(2J_A+1)(2J_A+3)} b_{J_A+1 J_A}^{(AB)} \right|^2 \left| b_{J_a-1 J_a}^{(ab)} + \frac{q^2}{(2J_a+1)(2J_a+3)} b_{J_a+1 J_a}^{(ab)} \right|^2 \right]$$

**...and mixed  $\sigma^{FG}$  and  $\sigma^{GF}$  , e.g.  $\sigma^{FG}$  spin-flip Fermi in  $a \rightarrow b$  and GT in  $A \rightarrow B$**

# Lecture 8: The Gamow-Teller Quenching Mystery

# Nuclear beta-Decay: Weak Charged-Current Interactions and Gamov-Teller strength

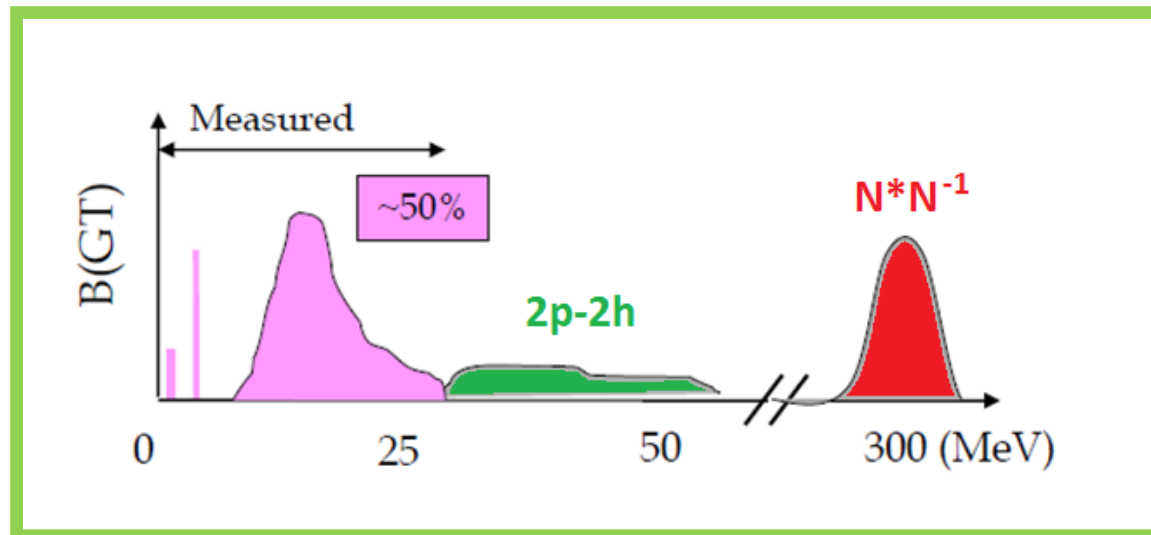
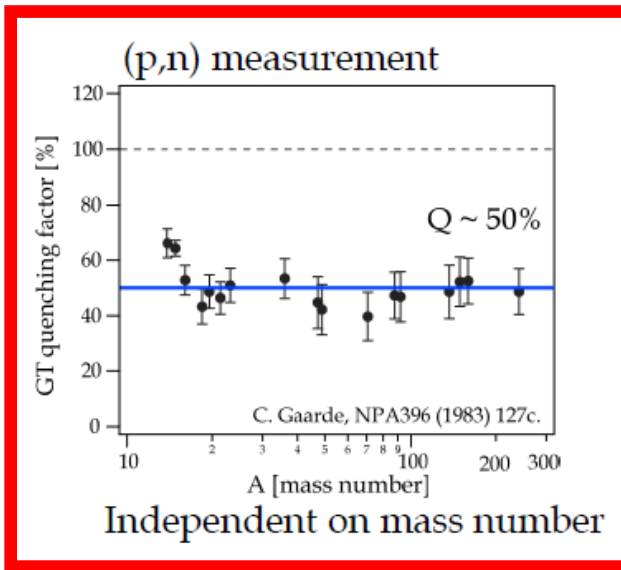


$$M(GT^\pm) \propto \left\langle f \left\| \sigma \cdot \tau_\pm \right\| i \right\rangle^2$$

GT sum rule (model independent)  
K. Ikeda PL 3, 271 (1963)

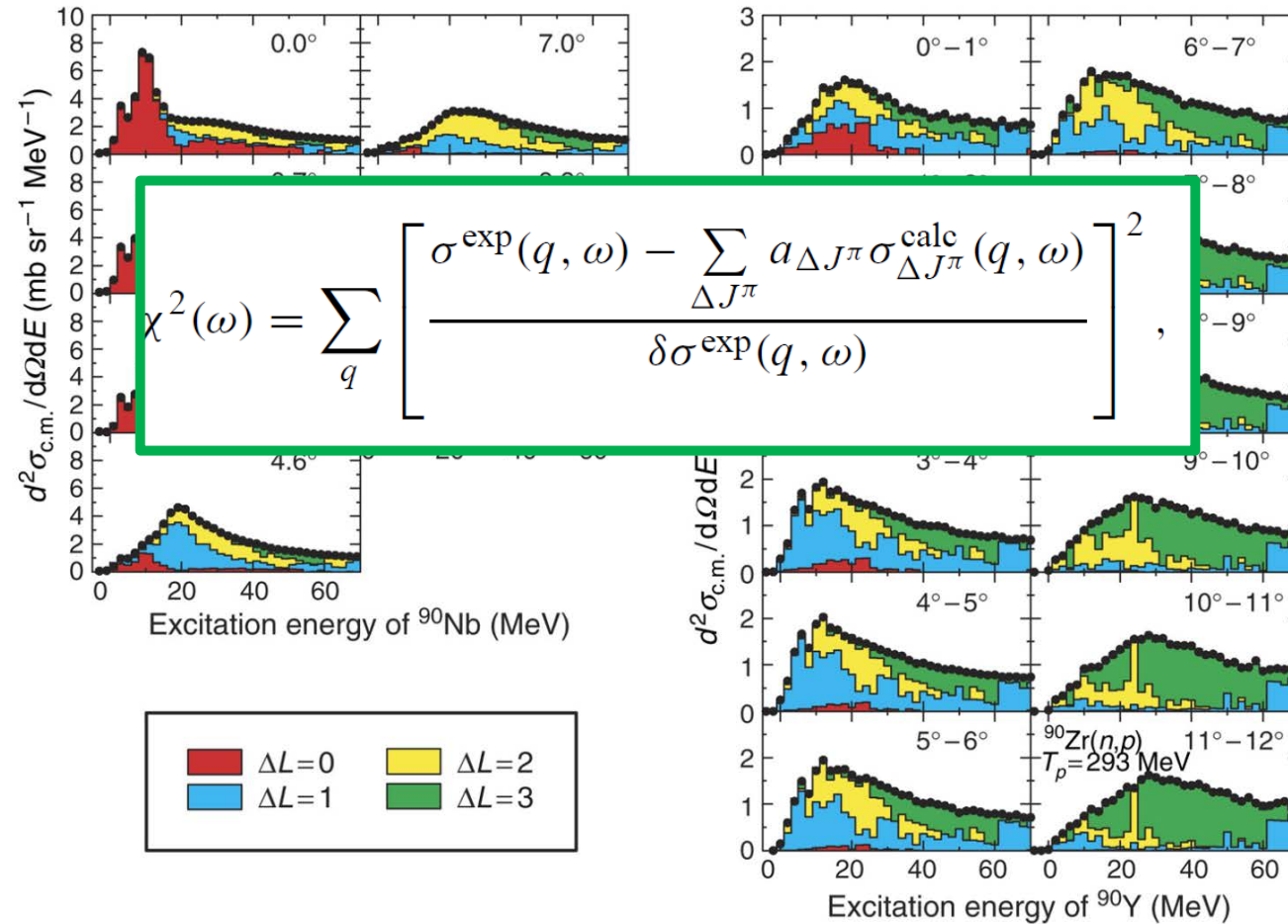
$$S_{\beta^-} - S_{\beta^+} = 3(N - Z)$$

# The GT-Quenching Mystery: ~50% of the *Ikeda Sum Rule Strength* is missing!



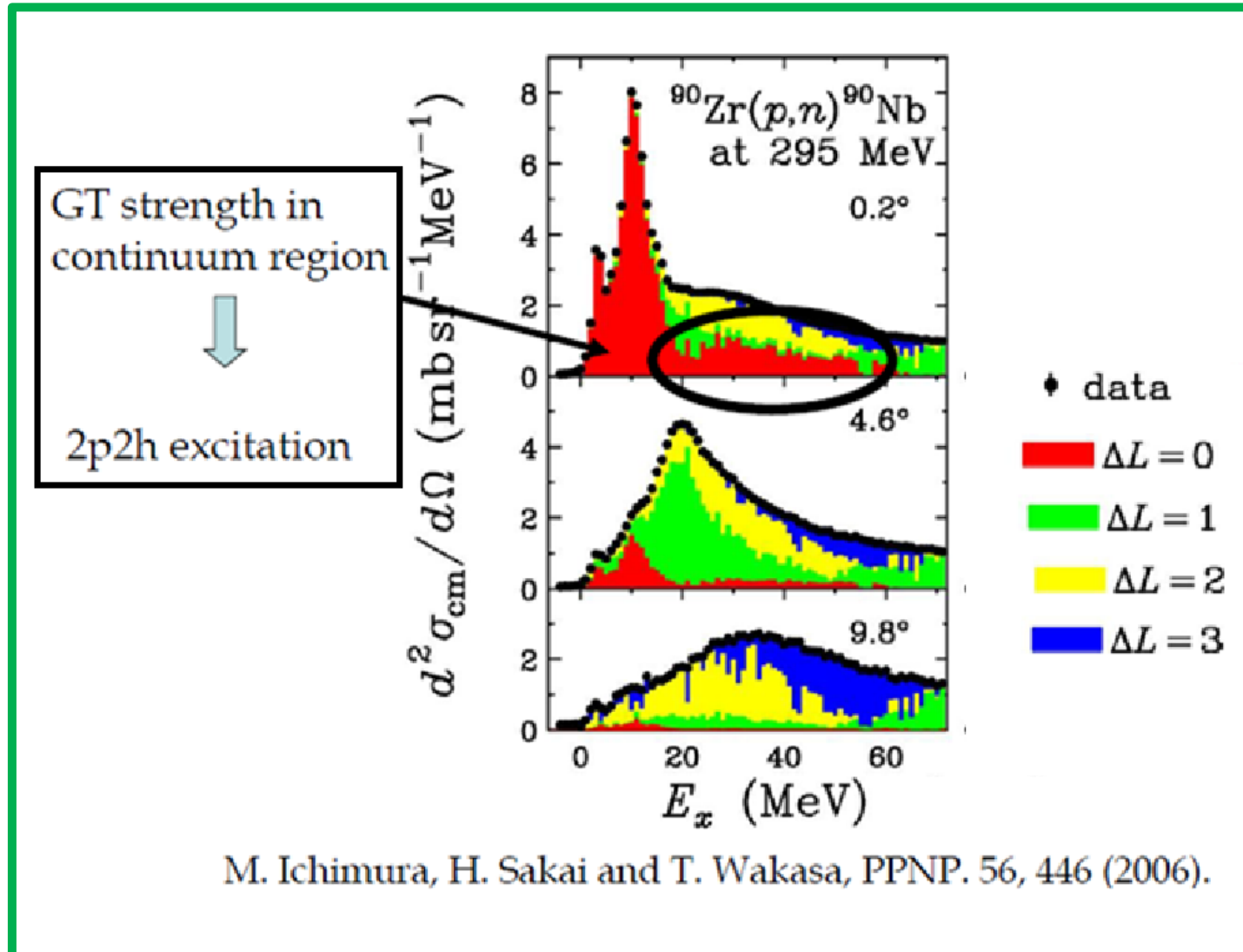
# Multipole Decomposition of (n,p) and (p,n) Reactions on $^{90}\text{Zr}$

$T_{\text{lab}} \approx 295 \text{ MeV}$



M. Ichimura et al. / Progress in Particle and Nuclear Physics 56 (2006) 446–531

# Search for Missing SCE Strength at RCNP@Osaka



# Comparison to 2p2h Nuclear Response Functions

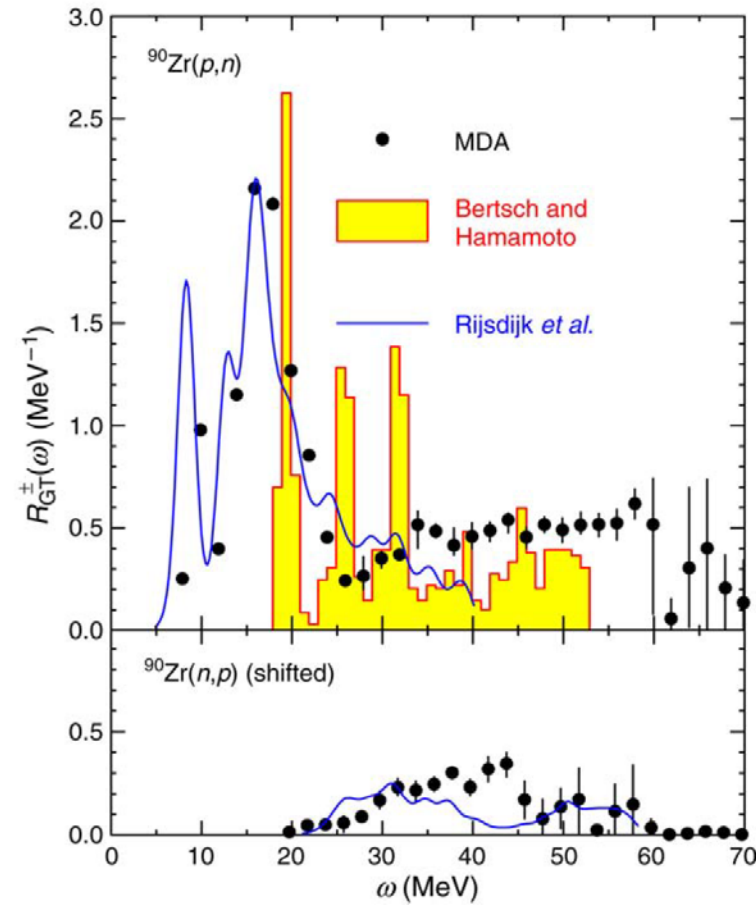
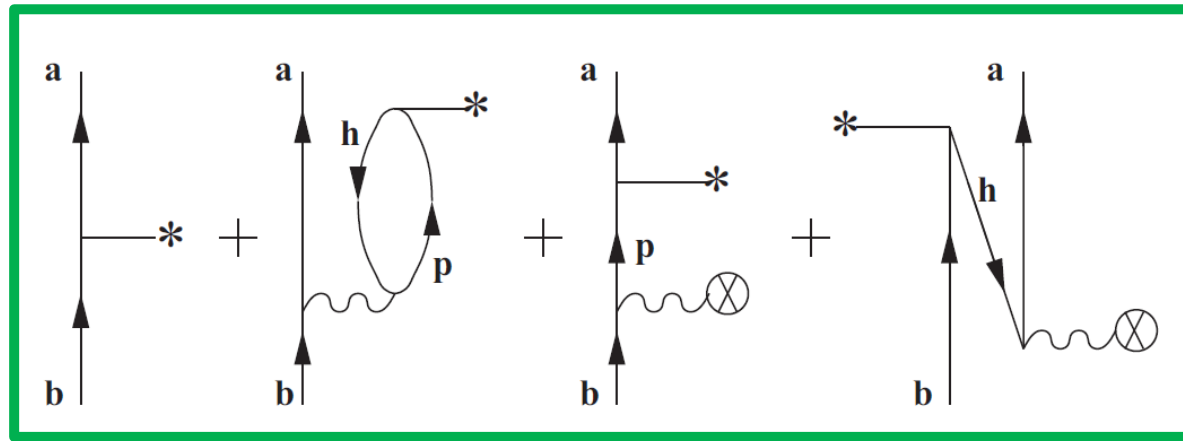


Fig. 23.  $\text{GT}^-$  (top panel) and  $\text{GT}^+$  (bottom panel) strength distributions (filled circles) obtained from the  $\Delta L = 0$  cross sections deduced from the MDA. The histogram and solid curves represent the perturbative calculation by Bertsch and Hamamoto [132] and the DRPA calculation by Rijsdijk *et al.* [134].

# Effective Operators incorporating Many-Body Dynamics

$$\hat{Q}(\epsilon) = PH_1P + PH_1Q \frac{1}{\epsilon - QHQ} QH_1P.$$

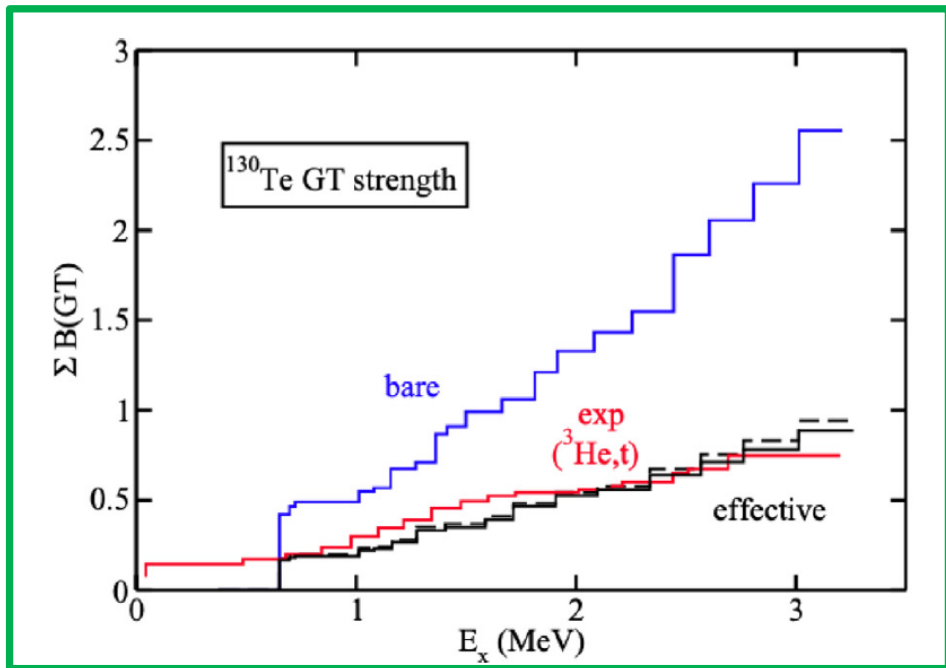
$$Q_{free}^{GT} = g_A \vec{\sigma} \vec{\tau} \rightarrow Q_{eff}^{GT}(\rho, V) \equiv g_A^*(\rho, V) \vec{\sigma} \vec{\tau}$$



$$* = Q_{free}$$

# Quenching Factors from the Many-Body Shell Model

$$q_{ab} = \frac{\langle b | O_{eff} | a \rangle}{\langle b | O_{free} | a \rangle}$$



State dependent!

$$q_{ab} \sim 0.5 \dots 0.6$$

GT<sup>-</sup> Single particle matrix elements

$n_a l_a j_a$	$n_b l_b j_c$	quenching
0g <sub>7/2</sub>	0g <sub>7/2</sub>	0.521
1d <sub>5/2</sub>	1d <sub>5/2</sub>	0.647
1d <sub>5/2</sub>	1d <sub>3/2</sub>	0.577
1d <sub>3/2</sub>	1d <sub>5/2</sub>	0.613
1d <sub>3/2</sub>	1d <sub>3/2</sub>	0.638
2s <sub>1/2</sub>	2s <sub>1/2</sub>	0.638
0h <sub>11/2</sub>	0h <sub>11/2</sub>	0.570

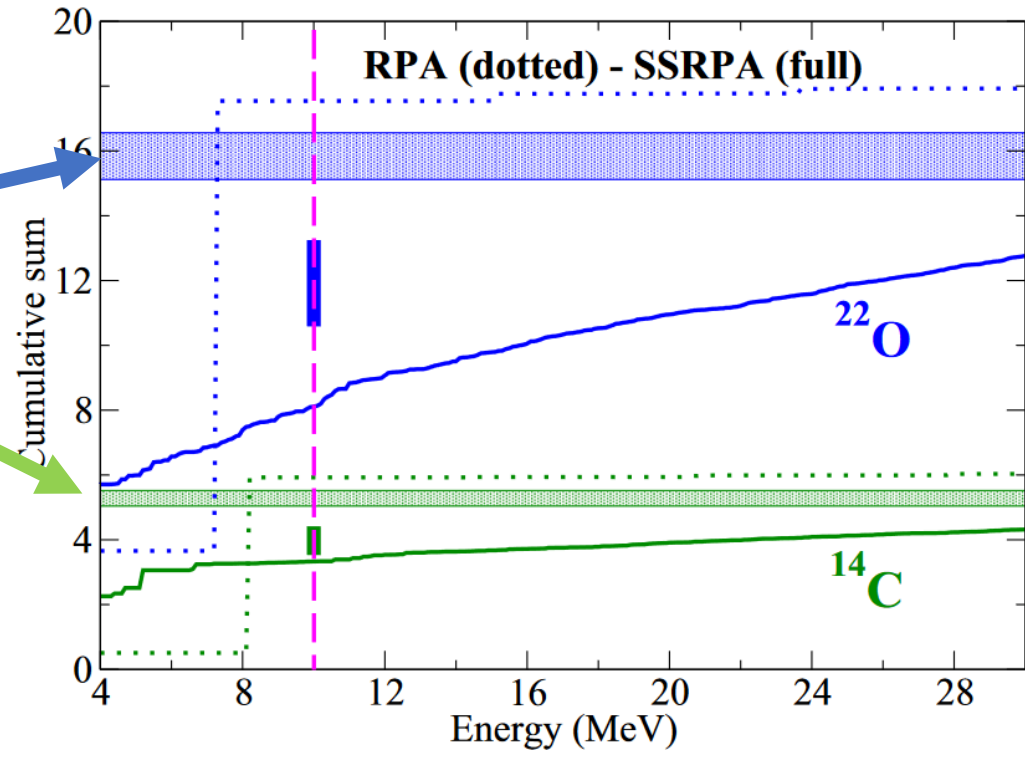
CORAGGIO et al. , PHYS. REV. C **95**, 064324 (2017)

see also: Capuzzello, H.L. et al. *Prog.Part.Nucl.Phys.* 128 (2023) 103999

# Studies of the GT-Quenching Problem by Higher Order RPA Theory

(D. Gambacurta, LNS Catania)

Ekström et al.,  
PRL 113, 262504 (2014)  
 $\chi$ EFT N<sup>2</sup>LO+2-body currents



$$S_{GT^-} - S_{GT^+}$$

**Quenching of GT Ikeda sum rules by coupling to 2p2h configurations (Skyrme EDF SGIII)**

•Phys.Rev.C 105 (2022) 1, 014321

# Lecture 9: Nuclear Matrix Elements for Astrophysics from ( $^3\text{He}$ , $^3\text{H}$ ) Reactions

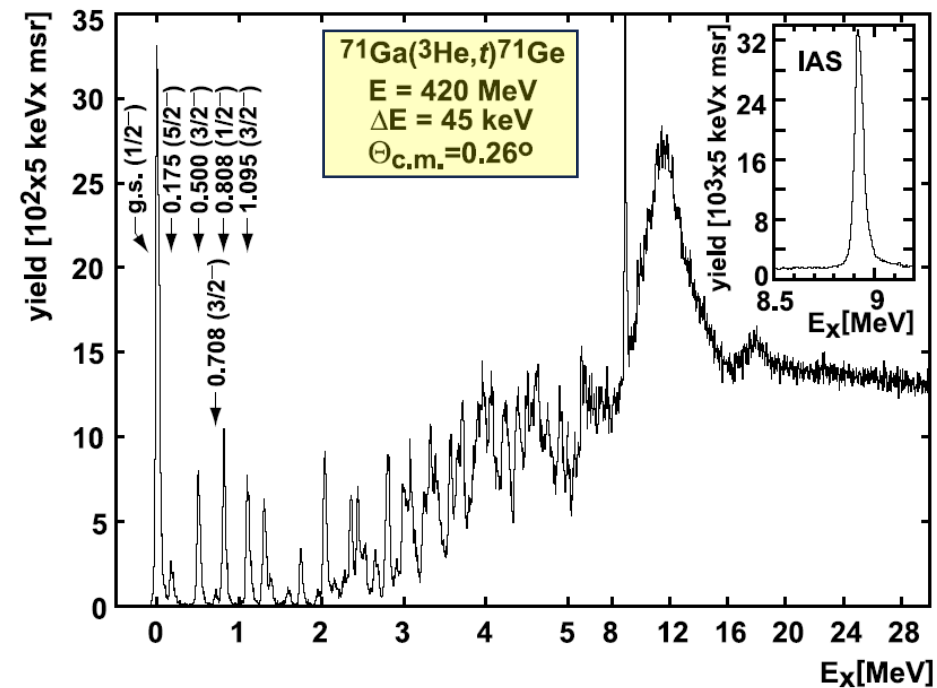


## The $^{71}\text{Ga}(^3\text{He},t)^{71}\text{Ge}$ reaction and the low-energy neutrino response

D. Frekers<sup>a,\*</sup>, H. Ejiri<sup>b</sup>, H. Akimune<sup>c</sup>, T. Adachi<sup>b</sup>, B. Bilgier<sup>d</sup>, B.A. Brown<sup>e</sup>, B.T. Cleveland<sup>f</sup>, H. Fujita<sup>g</sup>, Y. Fujita<sup>b,g</sup>, M. Fujiwara<sup>b</sup>, E. Ganioglu<sup>d</sup>, V.N. Gavrin<sup>h</sup>, E.-W. Grewe<sup>a,1</sup>, C.J. Guess<sup>e</sup>, M.N. Harakeh<sup>i,j</sup>, K. Hatanaka<sup>b</sup>, R. Hodak<sup>k</sup>, M. Holl<sup>a</sup>, C. Iwamoto<sup>c</sup>, N.T. Khai<sup>l</sup>, H.C. Kozer<sup>d</sup>, A. Lennarz<sup>a</sup>, A. Okamoto<sup>c</sup>, H. Okamura<sup>b,2</sup>, P.P. Povinec<sup>k</sup>, P. Puppe<sup>a</sup>, F. Šimkovic<sup>k</sup>, G. Susoy<sup>d</sup>, T. Suzuki<sup>b</sup>, A. Tamii<sup>b</sup>, J.H. Thies<sup>a</sup>, J. Van de Walle<sup>i</sup>, R.G.T. Zegers<sup>e</sup>

### A B S T R A C T

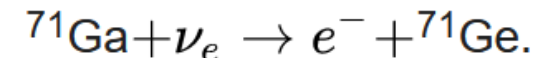
A  $^{71}\text{Ga}(^3\text{He},t)^{71}\text{Ge}$  charge-exchange experiment was performed to extract with high precision the Gamow–Teller (GT) transition strengths to the three lowest-lying states in  $^{71}\text{Ge}$ , i.e., the ground state ( $1/2^-$ ), the 175 keV ( $5/2^-$ ) and the 500 keV ( $3/2^-$ ) excited states. These are the relevant states, which are populated via a charged-current reaction induced by neutrinos from reactor-produced  $^{51}\text{Cr}$  and  $^{37}\text{Ar}$  sources. A precise measurement of the GT transition strengths is an important input into the calibration of the SAGE and GALLEX solar neutrino detectors and addresses a long-standing discrepancy between the measured and evaluated capture rates from the  $^{51}\text{Cr}$  and  $^{37}\text{Ar}$  neutrino calibration sources, which has recently spawned new ideas about unconventional neutrino properties.



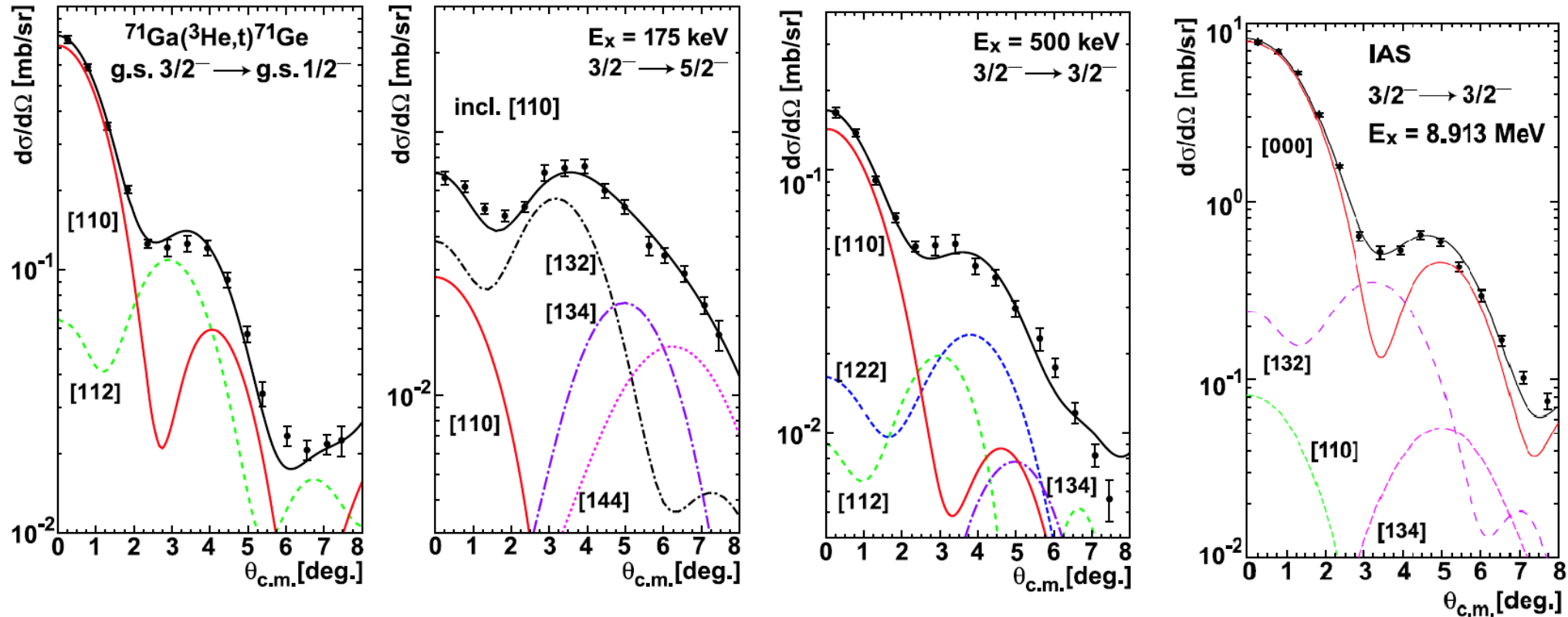
**Exp.: RCNP@Osaka and  
Grand Raiden Spectrometer**

**Purpose:**

**Provide data for the  
calibration of the  
GALLEX/GNO and SAGE  
underground neutrino  
detectors using**



# DWBA Analysis and Search for the lowest $J^\pi = 1^+$ GT-Transitions and the $J^\pi = 0^+$ IAS



## Angular Momentum Transfers

$$[ABC] = [J_{\text{proj}} J_{\text{targ}} J_{\text{tot}}]$$

$$\text{GT-strength} \leftrightarrow J_{\text{targ}} = 1$$

*D. Frekers et al. / Physics Letters B 706 (2011) 134*

## B(GT) and B(F) derived from the DWBA Analysis

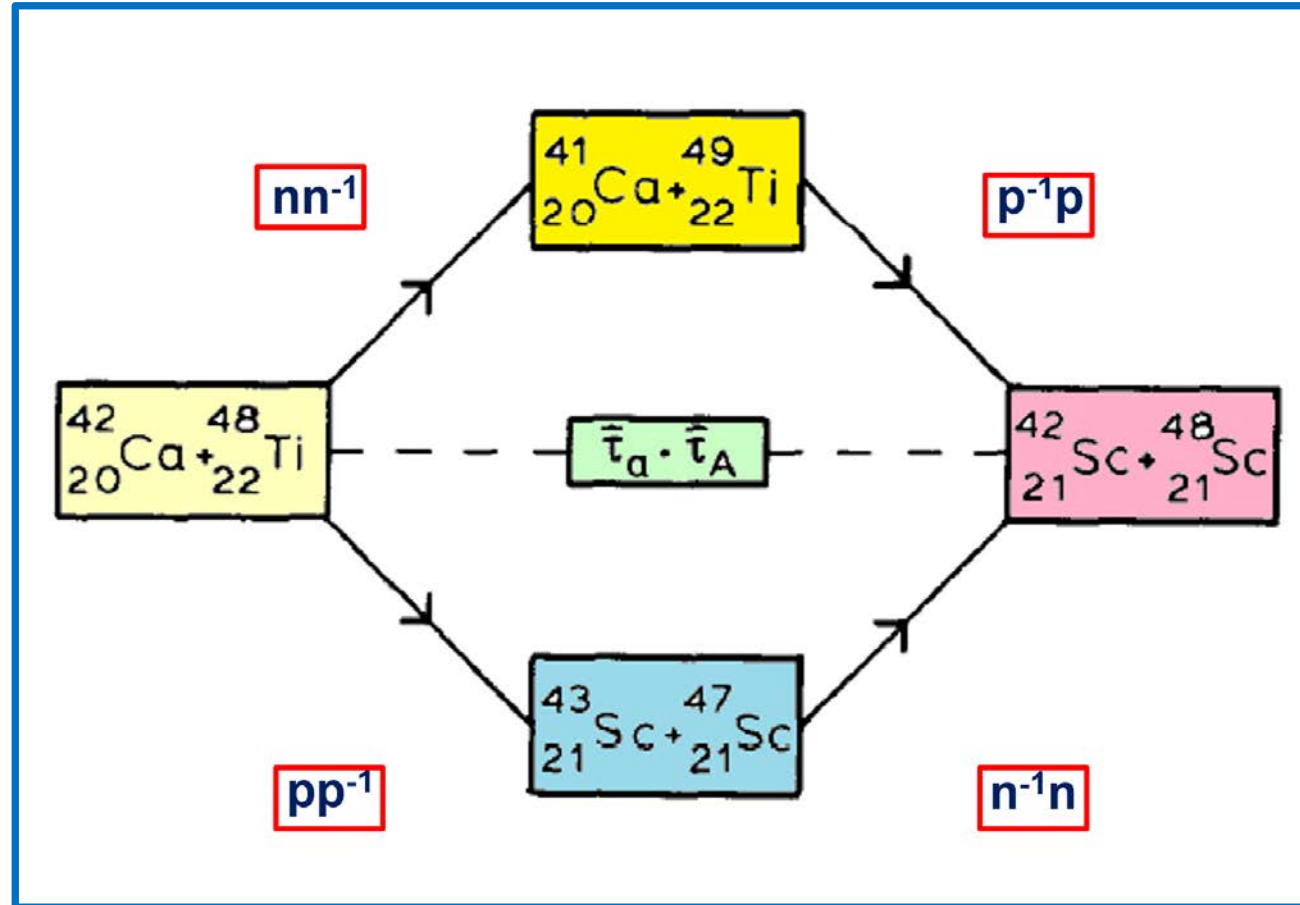
**Table 3**

Various low-energy cross sections and  $B(\text{GT})$  values for the  ${}^{71}\text{Ga}({}^3\text{He}, t){}^{71}\text{Ge}$  reaction. The values for the Fermi transition to the IAS have been included. The errors are statistical errors only, whereby we conservatively added 50% of the non-GT, resp. non-F component of the calculated  $q = 0$  cross section into the error calculations for the  $B(\text{GT})$ , resp.  $B(\text{F})$  values. The g.s.  $B(\text{GT})$  value and the  $B(\text{F})$  value are, however, reference values, whose error numbers (given in curly brackets) enter into the evaluation of the effective interaction volume integrals (see text).

${}^{71}\text{Ge}$ $E_x$ [keV]	$J^\pi$ of level	Data point $\theta = 0.26^\circ$ [mb/sr]	$d\sigma/d\Omega$ $(\theta = 0^\circ)$ [mb/sr]	$d\sigma/d\Omega$ $(q = 0)$ [mb/sr]	% GT	$B(\text{GT})$ $(\times 10^{-2})$
g.s.	$1/2^-$	0.746(23)	0.777(9)	0.786(9)	92%	8.52{40}
175	$5/2^-$	0.067(5)	0.070(4)	0.071(4)	40%	0.34(26)
500	$3/2^-$	0.165(9)	0.169(4)	0.171(4)	87%	1.76(14)
8913	IAS	7.89(40)	8.35(11)	9.04(12)	% F	$B(\text{F})$
$\Gamma \approx 50$					96%	9.00{22}

# Lecture 10: Heavy Ion SCE Reactions

# Scheme of a Heavy Ion SCE Reaction

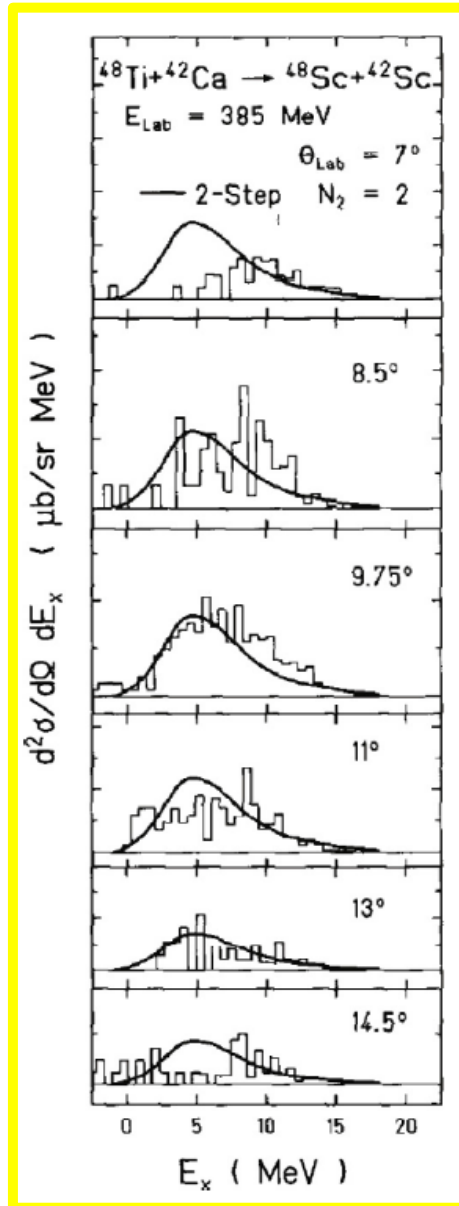


# Heavy ion Single Charge Exchange Reaction at the Coulomb-Barrier

## Pioneering work

- The first measurement of SCE reactions with heavy target and heavy ion beam
- The first fully microscopic description including 2-step transfer and 1-step mesonic SCE

C. Brendel, H.L. et al., Nucl. Phys. A 477 (1988) 162



H. Lenske, MAYORANA 2023

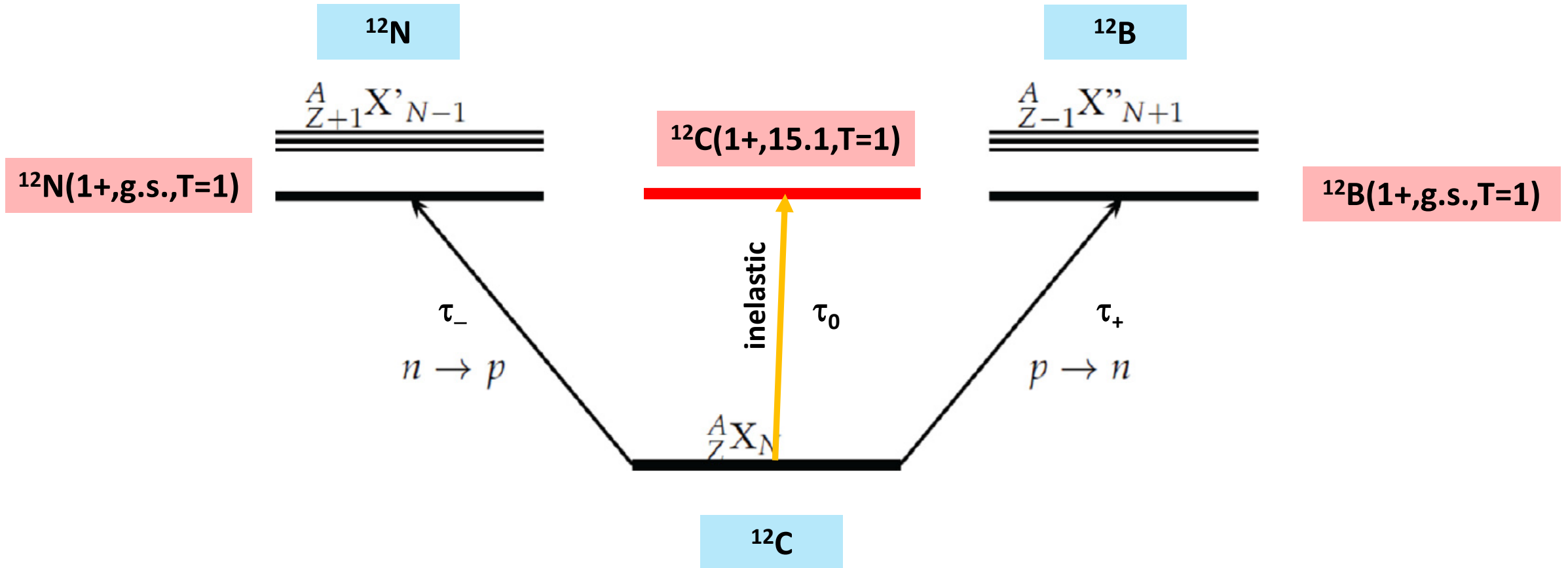


- Dominance of 2-Step Transfer-SCE

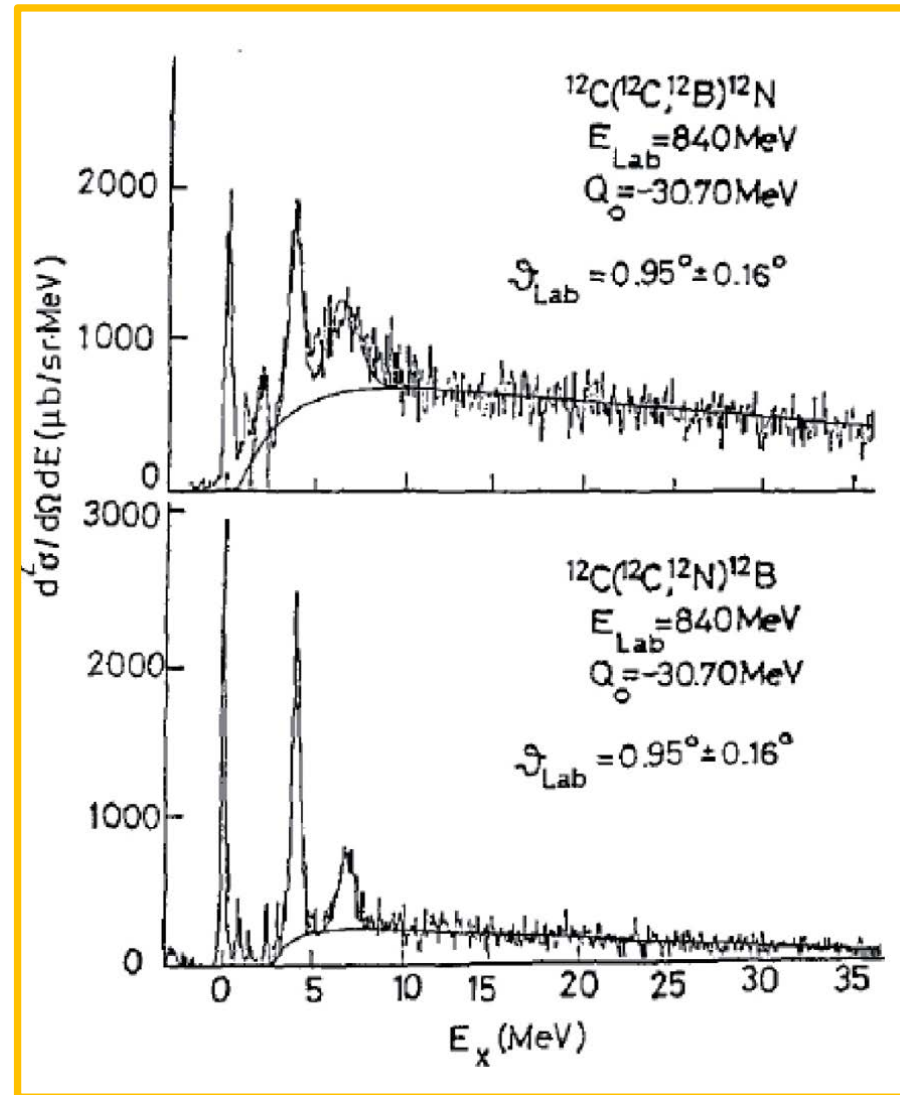
- Supression of 1-Step Mesonic SCE

# Versatility of Heavy Ion Reactions

A=12 T=1 Isotriplet – Proof of Isospin Symmetry in Nuclei



# $\tau_{\pm}$ Spectral Distributions of the reaction $^{12}\text{C}+^{12}\text{C} \rightarrow ^{12}\text{B}+^{12}\text{N}$ at 70 A MeV



$^{12}\text{C}+^{12}\text{C} \rightarrow ^{12}\text{B}(1+\text{g.s.})+^{12}\text{N}(J\pi, \text{Ex})$

$^{12}\text{C}+^{12}\text{C} \rightarrow ^{12}\text{N}(1+\text{g.s.})+^{12}\text{B}(J\pi, \text{Ex})$

W. von Oertzen, Nuclear Phys. A482 (1988) 357

# Reaction Mechanism of a Heavy Ions SCE Reaction

## Heavy Ion SCE Reaction Dynamics

- Transfer SCE (TSCE) is a mean-field 2-step process
- Best results if donor and acceptor nuclei are of similar shell-structure
- Symmetric systems like  $^{12}\text{C} + ^{12}\text{C}$  are most favorable for TSCE
- High angular momentum states favor TSCE
- $A_p \approx A_T$  and low incident energies ( $T_{lab} < 30\text{A MeV}$ ) favor TSCE

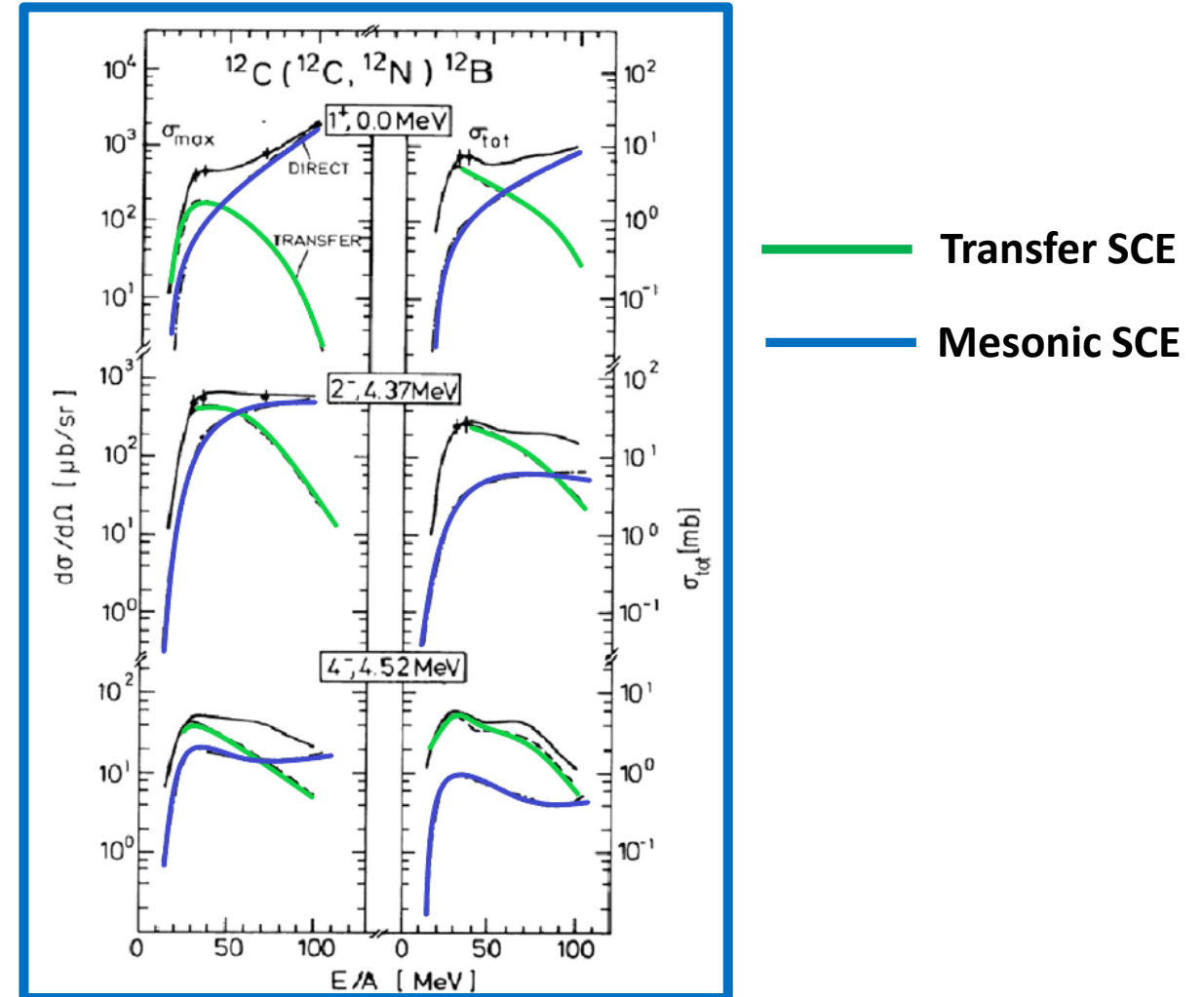
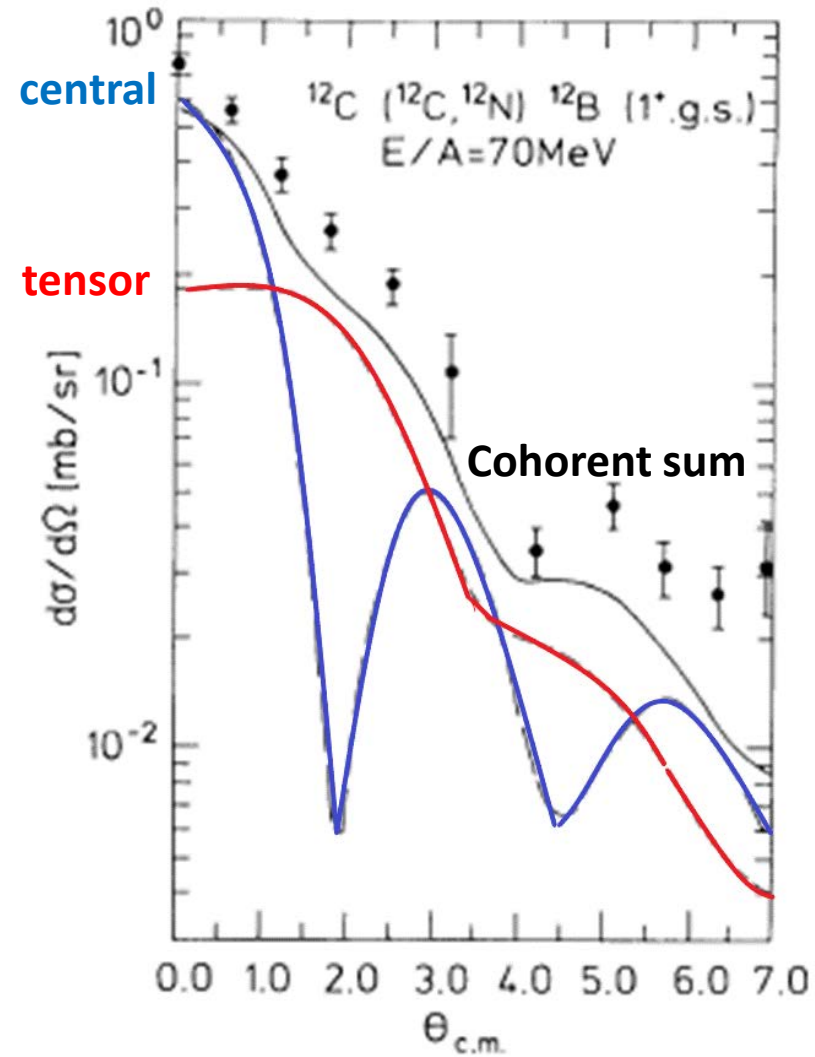


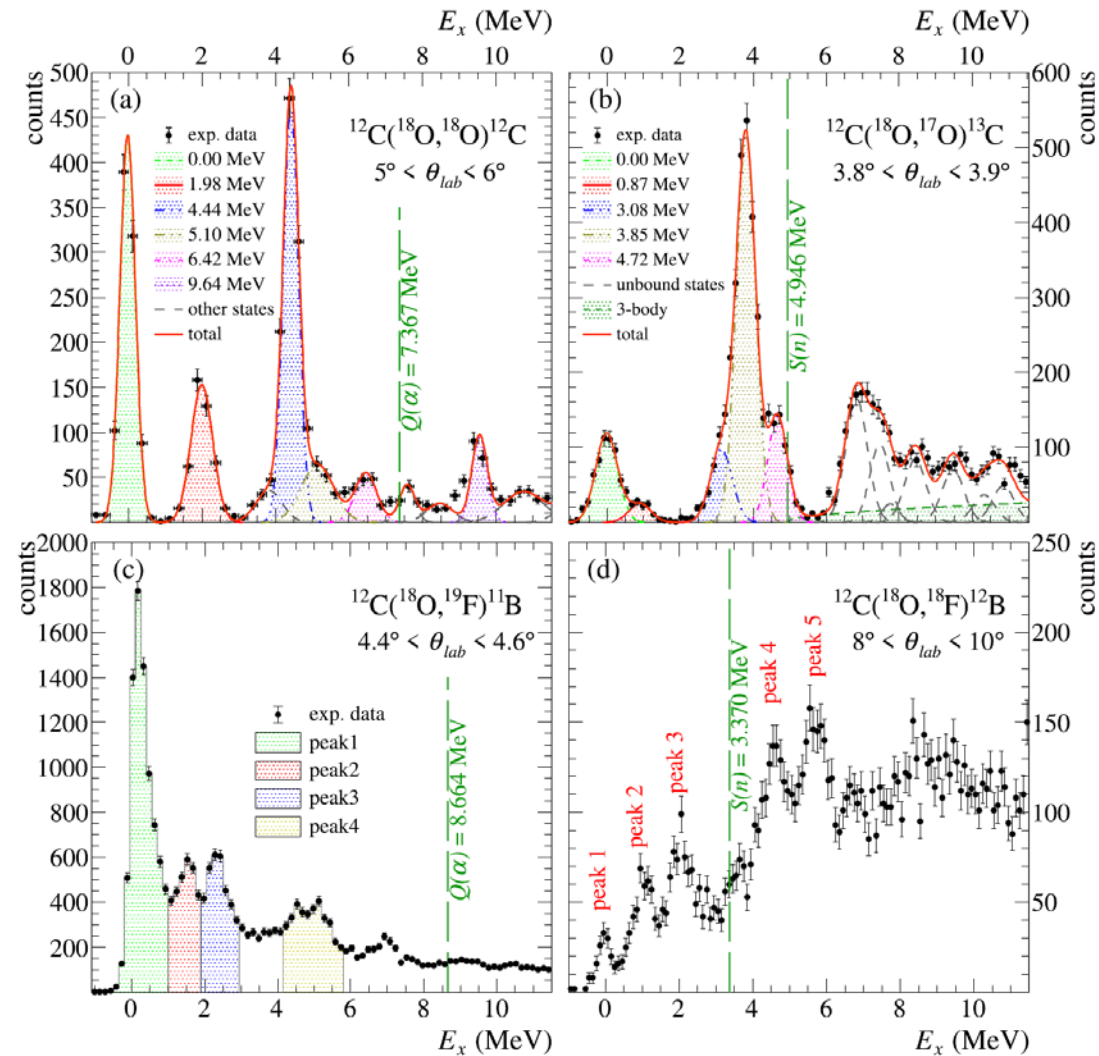
**Fig. 3.10.** Angular distributions for the reaction  $^{12}\text{C} + ^{12}\text{C} \rightarrow ^{12}\text{B}(1^+, \text{g.s.}) + ^{12}\text{N}(1^+, \text{g.s.})$  (left) and the energy dependence of the peak cross sections for several final states in  $^{12}\text{N}(J^\pi, E_x)$  and the angle integrated total cross section (right). Theoretical results for the direct (dashed-dotted lines) and transfer (dashed lines) charge-exchange contributions and also of the coherent sum of both (full lines) are shown and compared to data (circles) at  $E/A = 30$  and  $70$  MeV. Note in the left panel the change in abscissa for  $E/A = 70$  MeV and  $E/A = 100$  MeV.

# Heavy Ion SCE Reactions: Central and Tensor Interaction



H. Lenske et al.,  
Phys. Rev. Lett. 62, 1457 (1989)

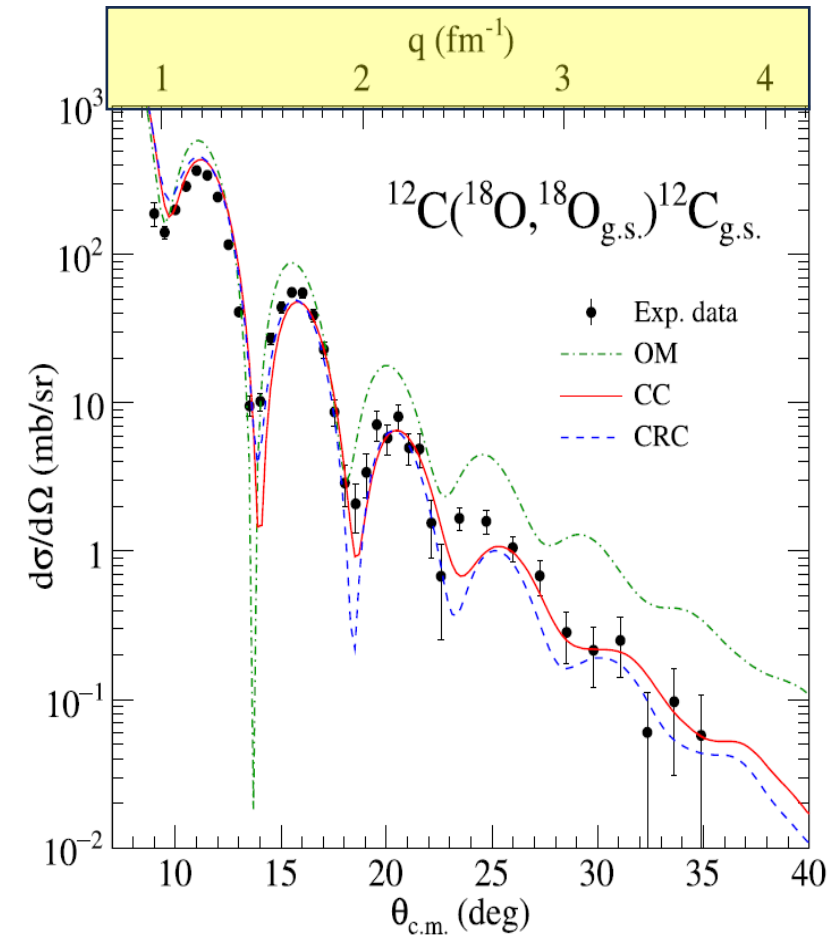
# Recent Inelastic and Transfer Studies on $^{12}\text{C}$ -Targets at LNS Catania



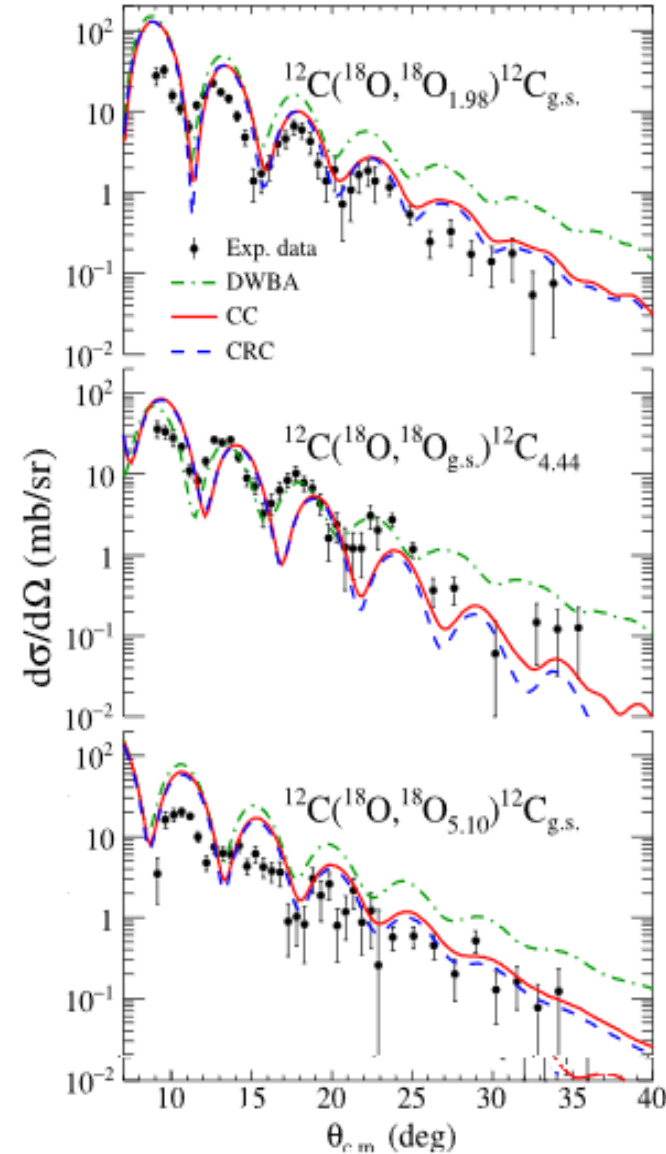
# Heavy Ion Elastic and Inelastic Scattering Reactions

## DWBA and CC Description

Heavy Ion Scattering  
 $\equiv$   
 Nuclear Physics at Large  
 Momentum Transfer  
 (here:  $q \leq 800$  MeV/c (!))



Experimental angular distribution of  $^{12}\text{C}(^{18}\text{O}, ^{18}\text{O}_{\text{g.s.}})^{12}\text{C}_{\text{g.s.}}$  elastic scattering at 275 MeV incident energy. Results of OM, CC, and CRC approaches are shown

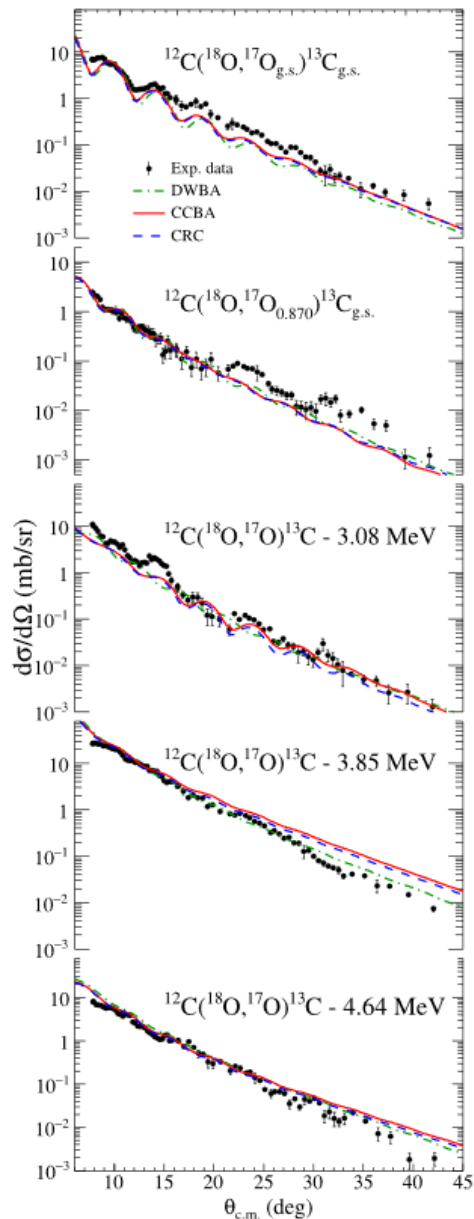


Experimental angular distribution of the  $^{12}\text{C}(^{18}\text{O}, ^{18}\text{O})^{12}\text{C}$  inelastic scattering at 275 MeV incident energy associated with the peaks at 1.98, 4.44, and 5.10 MeV. Theoretical calculations for the inelastic transitions in DWBA, CC, and CRC approaches are shown

A. SPATAFORA *et al.* PHYS. REV. C 107, 024605 (2023)

# $^{18}\text{O}+^{12}\text{C}$ @ $T_{\text{lab}}=275$ MeV Single Nucleon Transfer Reactions

Microscopic Description by  
DWBA and CC Methods



Projectile Neutron  
**Stripping** Reactions



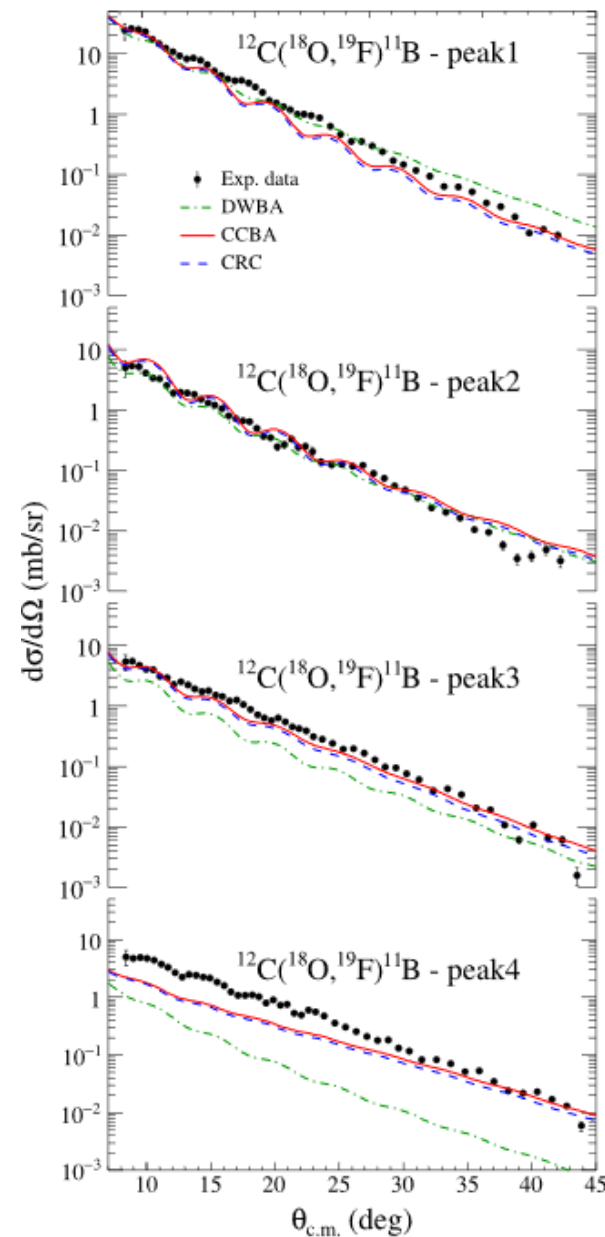
Target Neutron  
**Pickup** Reactions



Projectile proton  
**Pickup** Reactions



Target Proton  
**Stripping** Reaction



# Remarks on Nuclear Response Functions for beta-Decay and Charge Exchange Reactions

$$E(N,Z)/A = -16\text{MeV} + E_{\text{surf}}/A^{1/3} + E_{\text{pair}} + E_{\text{shell}} + E_{\text{coul}} \\ + [(N-Z)/A]^2(a_4 + C_{\text{sym}}/A^{1/3})$$

Function(al) of neutron (N) and proton (Z) numbers

→ Generalize to a functional of neutron ( $q=n$ ) and proton ( $q=p$ ) densities

$$E(\tau_q, \rho_q, \kappa_q \dots) = T(\tau_q) + \frac{1}{2} E_{\text{int}}(\rho_q, \kappa_q \dots)$$

Nuclear Energy Density Functional (EDF)

# Elements of Density Functional Theory

$$E(\rho, \kappa) \approx E(\rho_0, \kappa_0) + \sum_{q=p,n} \left( (T_q + U_q(\rho_0)) \delta\rho_q + \Delta_q \delta\kappa_q \right) + \sum_{q,q'=p,n} f_{qq'}(\rho_0) \delta\rho_q \delta\rho_{q'} + \dots$$

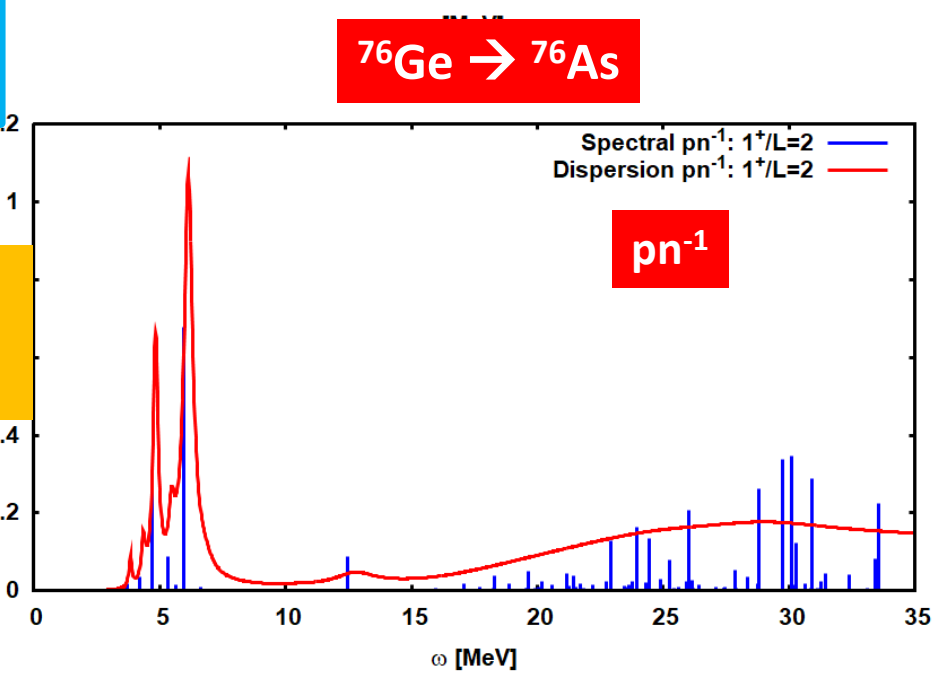
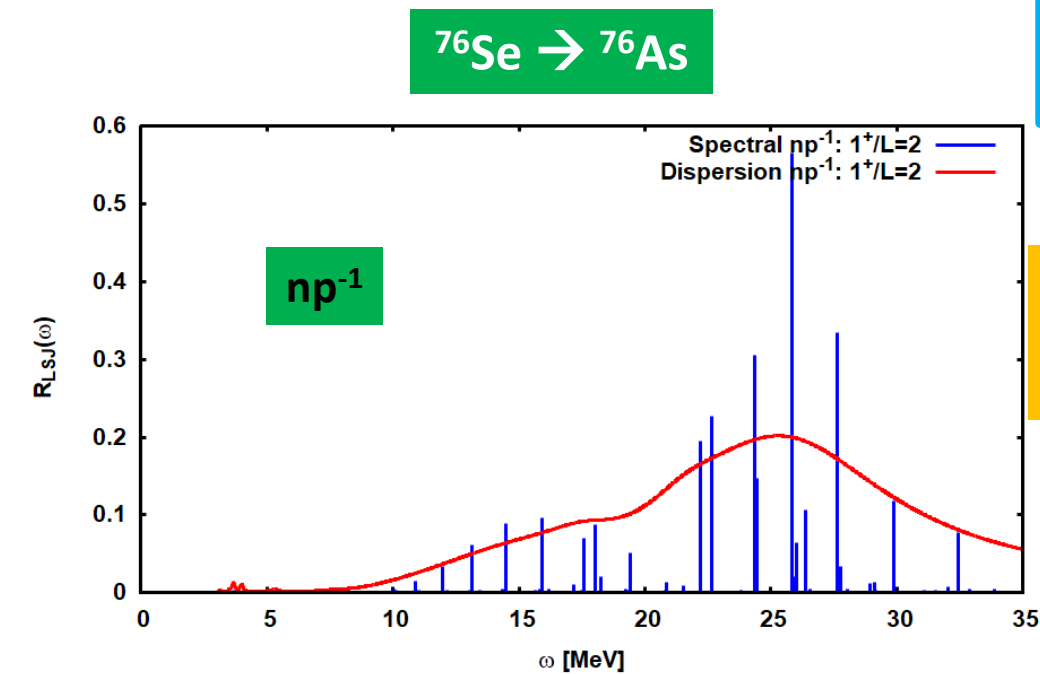
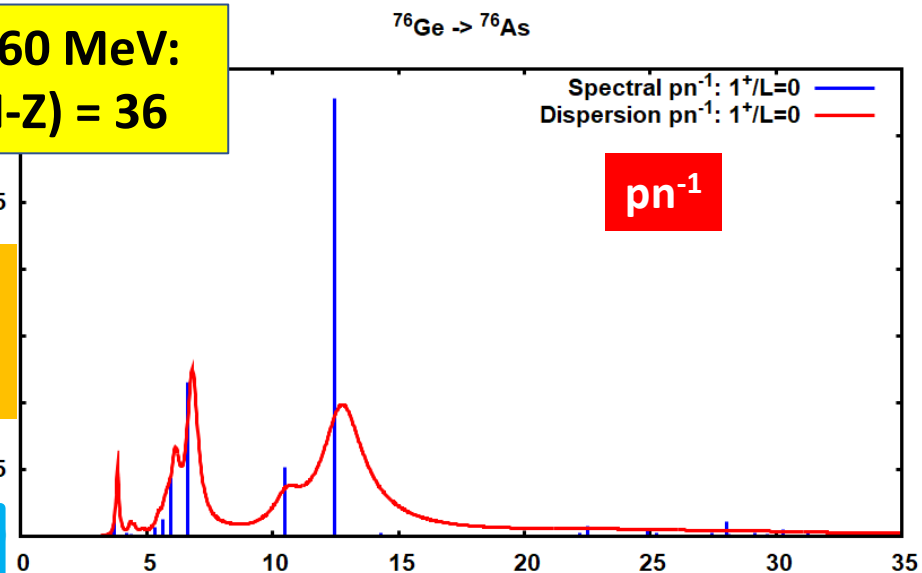
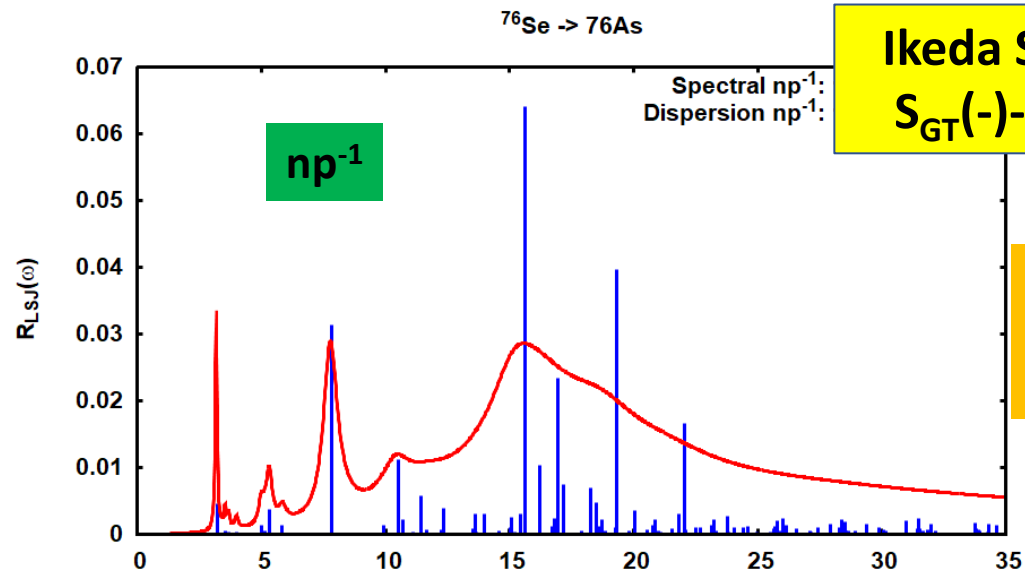
$$\delta\rho_q \sim \varphi_k^\dagger \varphi_n \sim a_k^\dagger a_k ; \delta\kappa_q \sim \varphi_k^\dagger \varphi_n^\dagger \sim a_k^\dagger a_k^\dagger \text{ \& h.c.}$$

**Single Particle Self-Energy:**

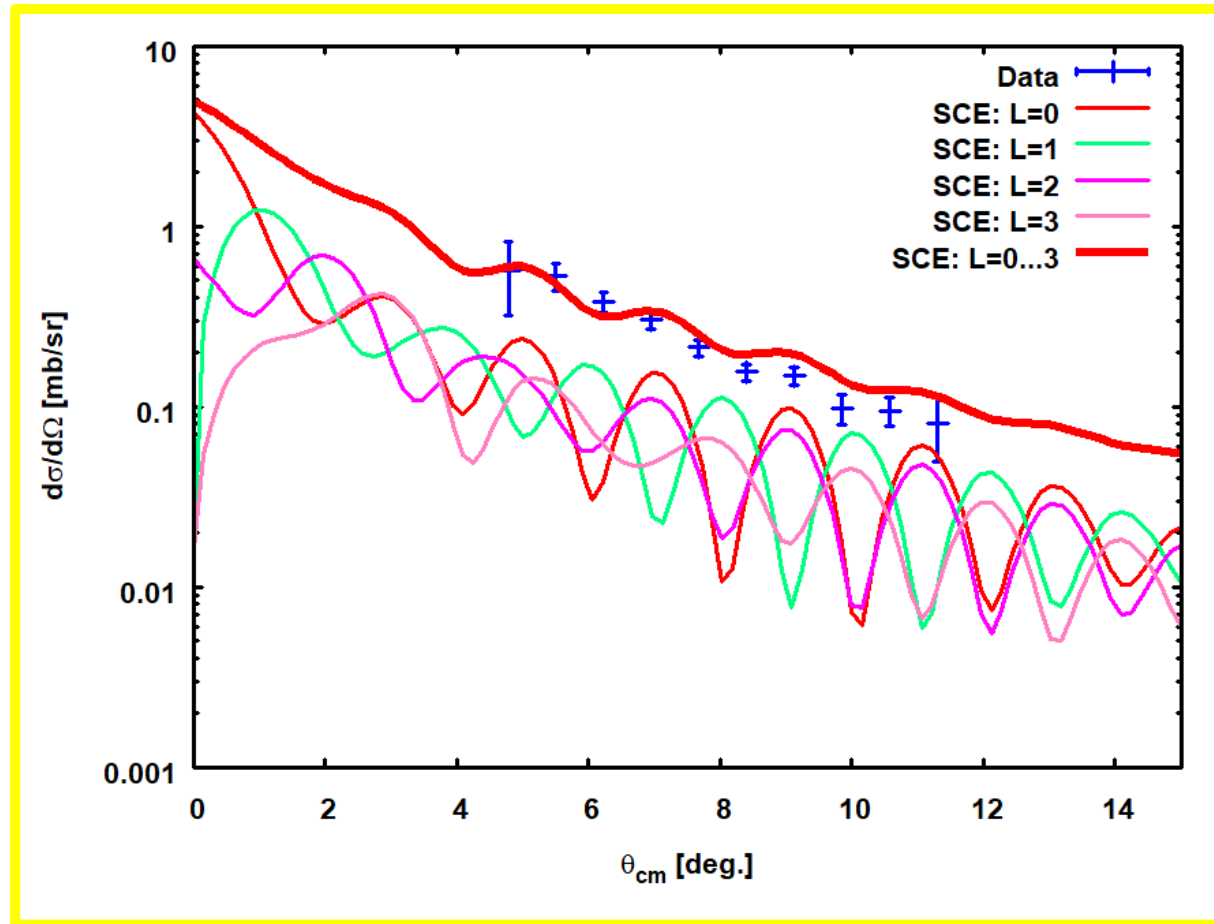
$$U_q = \frac{\delta}{\delta\rho_q} \frac{1}{2} \langle V \rangle = \sum_{q'} V_{qq'}(\rho) \rho_{q'} + \frac{1}{2} \sum_{q'q''} \rho_{q'} \rho_{q''} \frac{\delta}{\delta\rho_q} V_{q'q''}(\rho)$$

**Self-consistent Residual Interaction :**

$$f_{qq'} = V_{qq'}(\rho) + 2 \sum_{q''} \rho_{q''} \frac{\delta}{\delta\rho_q} V_{q'q''}(\rho) + \frac{1}{2} \sum_{k'k''} \rho_{k'} \rho_{k''} \frac{\delta^2}{\delta\rho_q \delta\rho_{q'}} V_{k'k''}(\rho)$$

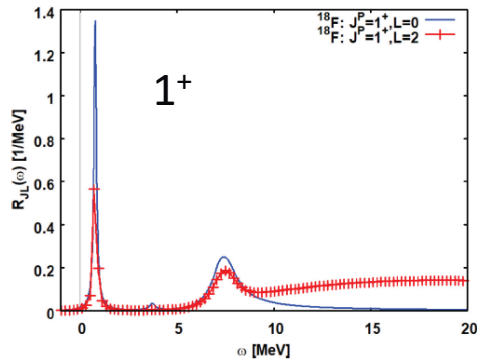
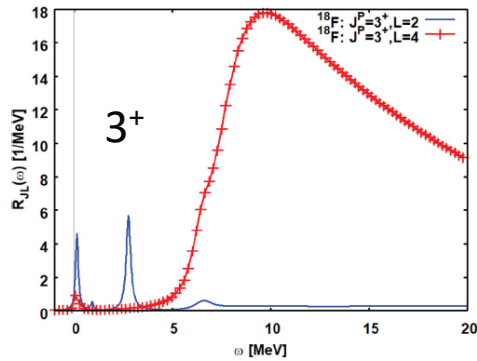
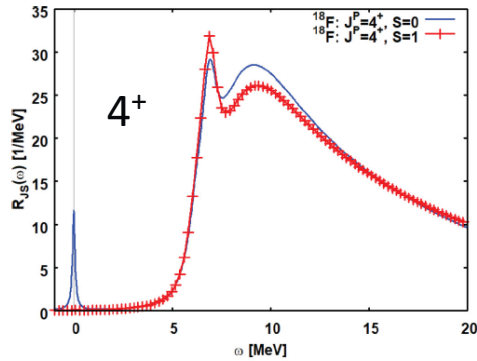


**GiEDF+HFB+QRPA**  
e.g. *Eur.Phys.J.A* 57  
(2021) 3, 89



F. Cappuzzello et al., PPNP (108) (2023)

$^{18}\text{O} \rightarrow ^{18}\text{F}$



# SCE Spectroscopy: ccQRPA Response Functions

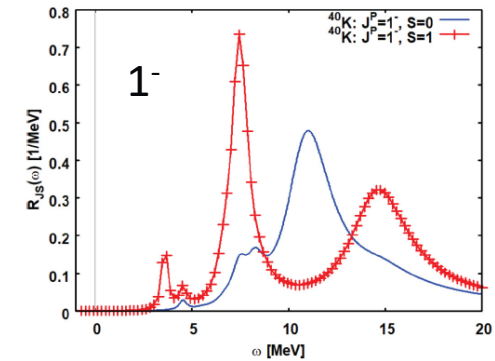
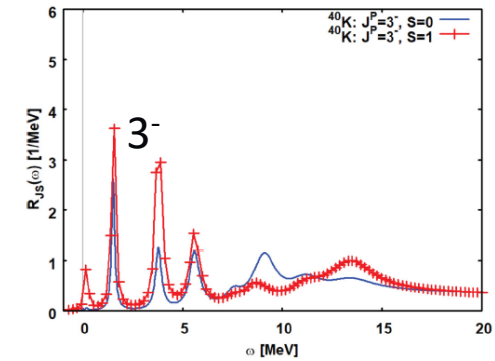
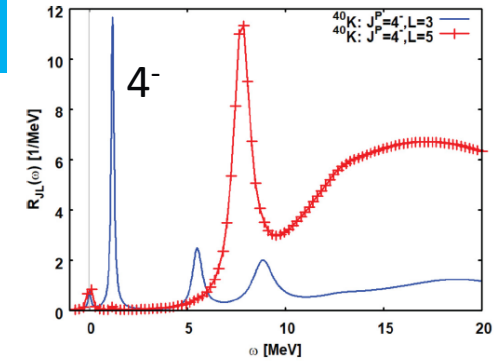
PHYSICAL REVIEW C 98, 044620 (2018)

Fermi (S=0) and Gamow-Teller (S=1)  
Transition Operators:

$$T_{LSJM} = \left( \frac{r}{R_d} \right)^L [\sigma^S \otimes Y_L]_{JM} \tau_{\pm}$$

...including DCP self-energies  
and continuum effects

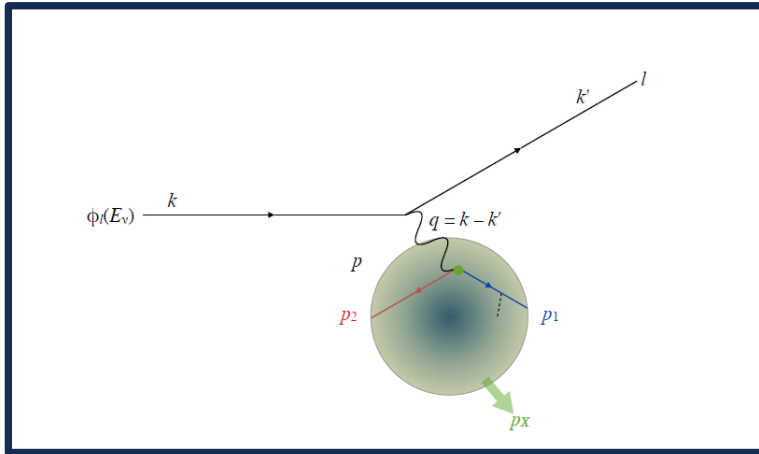
$^{40}\text{Ca} \rightarrow ^{40}\text{K}$



# **Lecture 11:**

# **Heavy Ion SCE Reactions at Relativistic Energies**

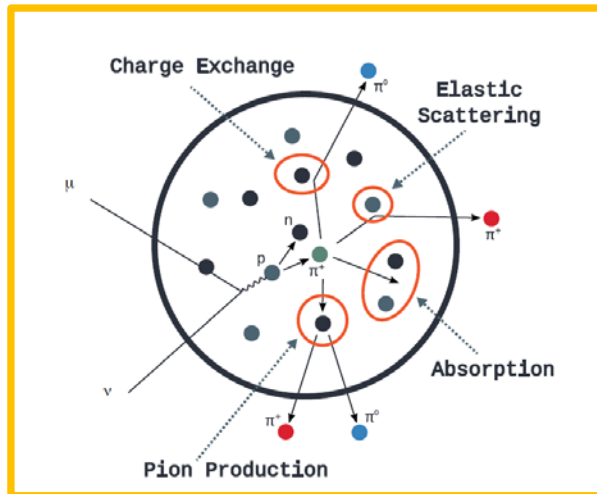
# Motivation 1: Neutrino Oscillation and Neutrino-Matter Interactions



## NuSTEC<sup>a</sup> White Paper: Status and Challenges of Neutrino-Nucleus Scattering

L. Alvarez-Ruso,<sup>1</sup> M. Sajjad Athar,<sup>2</sup> M. B. Barbaro,<sup>3</sup> D. Cherdack,<sup>4</sup> M. E. Christy,<sup>5</sup> P. Coloma,<sup>6</sup> T. W. Donnelly,<sup>7</sup> S. Dytman,<sup>8</sup> A. de Gouvêa,<sup>9</sup> R. J. Hill,<sup>10,6</sup> P. Huber,<sup>11</sup> N. Jachowicz,<sup>12</sup> T. Katori,<sup>13</sup> A. S. Kronfeld,<sup>6</sup> K. Mahn,<sup>14</sup> M. Martini,<sup>15</sup> J. G. Morfín,<sup>6</sup> J. Nieves,<sup>1</sup> G. Perdue,<sup>6</sup> R. Petti,<sup>16</sup> D. G. Richards,<sup>17</sup> F. Sánchez,<sup>18</sup> T. Sato,<sup>19,20</sup> J. T. Sobczyk,<sup>21</sup> and G. P. Zeller<sup>6</sup>

NuSTEC = Neutrino Scattering Theory Experiment Collaboration  
(PPNP 106 (2018) 1-68)



## F. Challenges: The Resonance Region (Section VII)

The resonance region is characterized by transfers of energy larger than in QE peak region corresponding to larger hadronic invariant mass. The most important contribution is from the  $\Delta(1232)$  resonance:

$$\nu_\mu p \rightarrow \mu^- \Delta^{++}, \quad \Delta^{++} \rightarrow p\pi^+$$

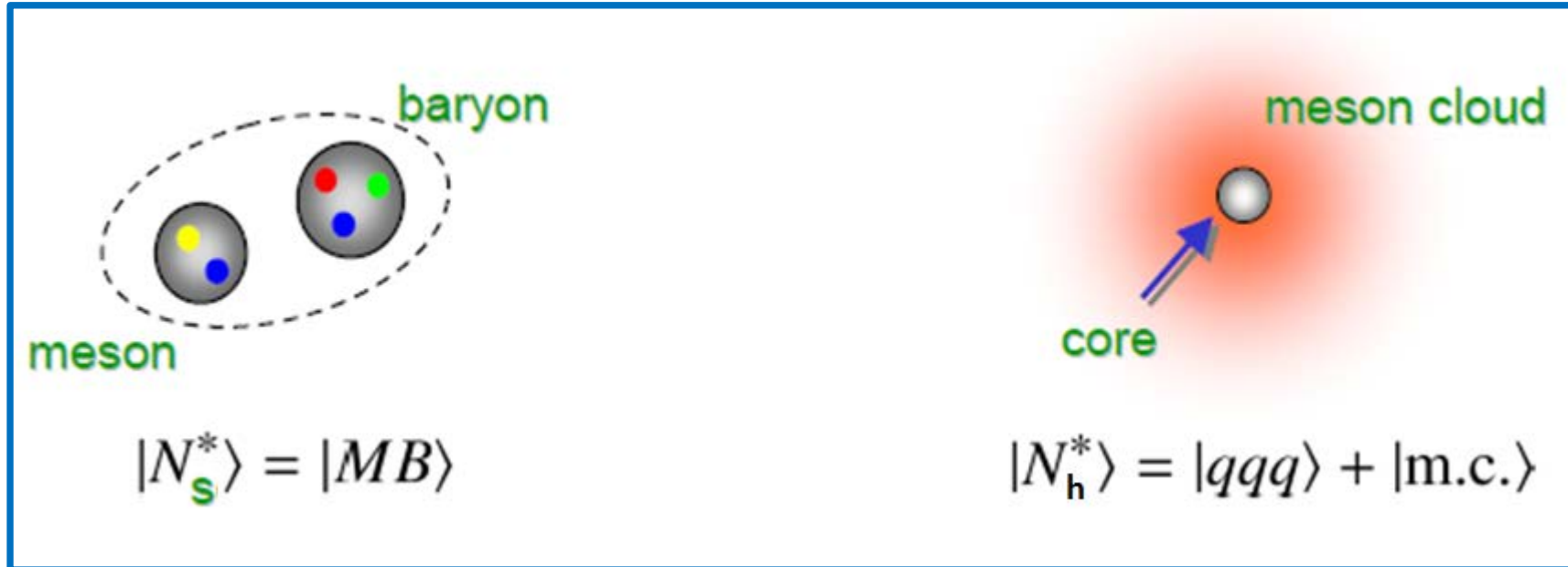
and

$$\bar{\nu}_\mu n \rightarrow \mu^+ \Delta^-, \quad \Delta^- \rightarrow n\pi^-,$$

## Motivation 2: QCD Aspects of Resonances

- hadronic (*soft scale*) molecular-type components  $|N_s\rangle$
- QCD (*hard scale*) confined components  $|N_h\rangle$
- $N^*$  in compact stellar objects  $\rightarrow$  neutron stars

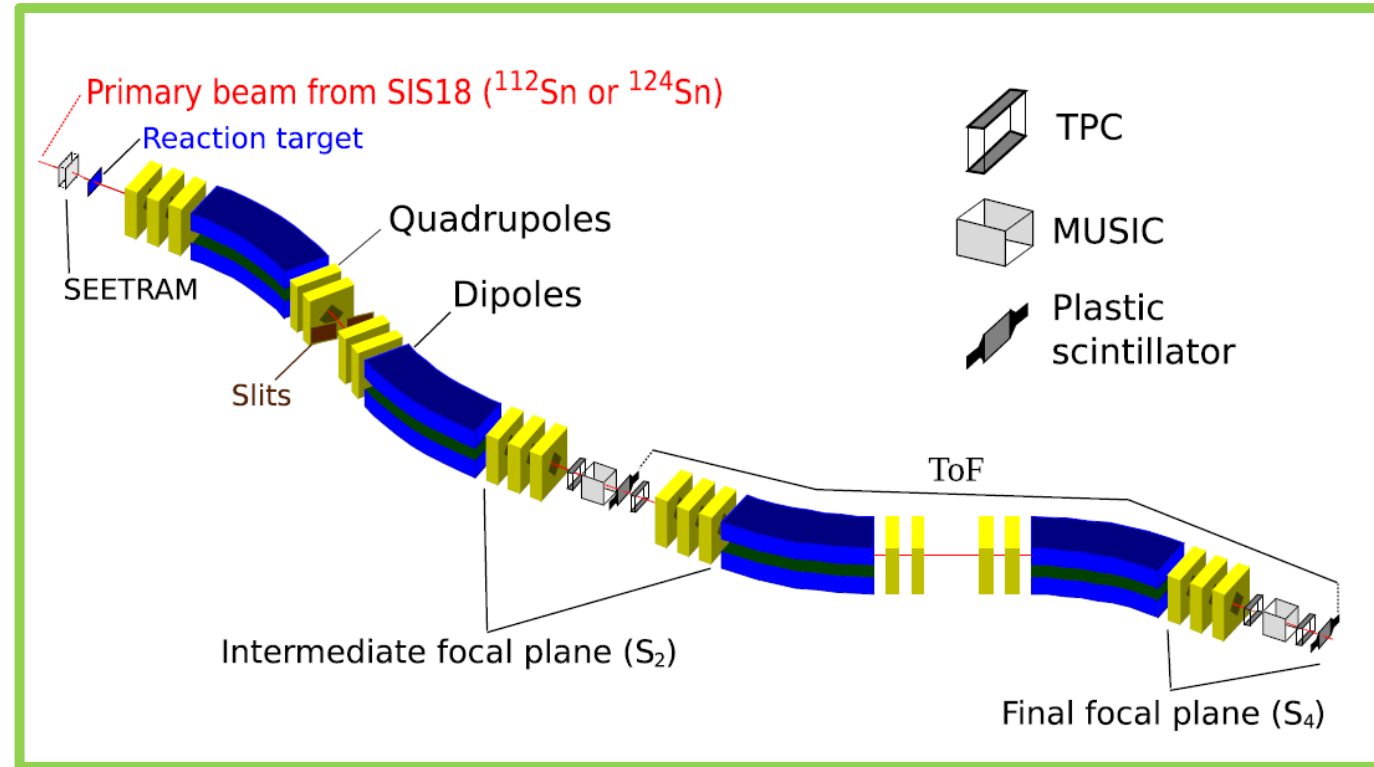
$$|N^*\rangle = |N_s^*\rangle + |N_h^*\rangle = x_1 |mB\rangle + x_2 |qqq\rangle + x_3 |qqq\rangle \otimes |q\bar{q}\rangle + \dots$$



Strong Medium Dependence

Weak Medium Dependence

# Relativistic Heavy Ion Reactions at the FRS@GSI



H.L. et al, PPNP 98 (2018)

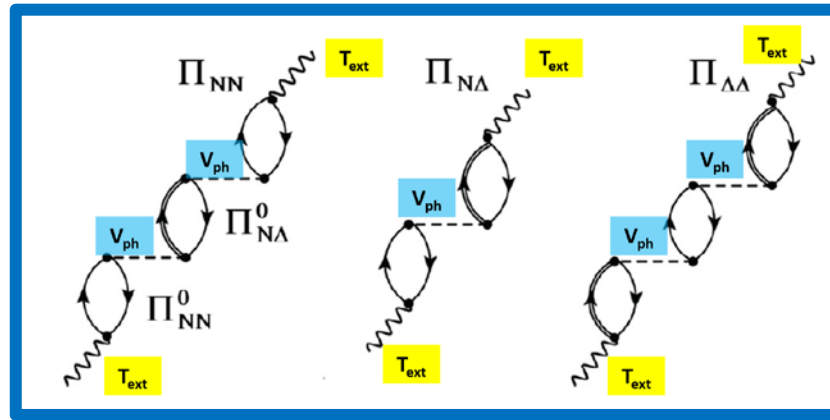
J. L. Rodríguez-Sánchez, H.L., et al., PHYS. REV. C 106, 014618 (2022)

# Substitutional $N^*N^{-1}$ Excitations in Nuclei - „N\*RPA“

$$\Pi = \Pi^0 + \Pi^0 \hat{V} \Pi$$

$$\begin{pmatrix} \Pi_{NN} & \Pi_{N\Delta} \\ \Pi_{\Delta N} & \Pi_{\Delta\Delta} \end{pmatrix} = \begin{pmatrix} \Pi_{NN}^0 & 0 \\ 0 & \Pi_{\Delta\Delta}^0 \end{pmatrix} + \begin{pmatrix} \Pi_{NN}^0 & 0 \\ 0 & \Pi_{\Delta\Delta}^0 \end{pmatrix} \begin{pmatrix} V_{NN} & V_{N\Delta} \\ V_{\Delta N} & V_{\Delta\Delta} \end{pmatrix} \begin{pmatrix} \Pi_{NN} & \Pi_{N\Delta} \\ \Pi_{\Delta N} & \Pi_{\Delta\Delta} \end{pmatrix}$$

Coupled  $N^*N^{-1} \leftrightarrow \Delta N^{-1}$  Dyson Equation including N and  $N^*$  self-energies



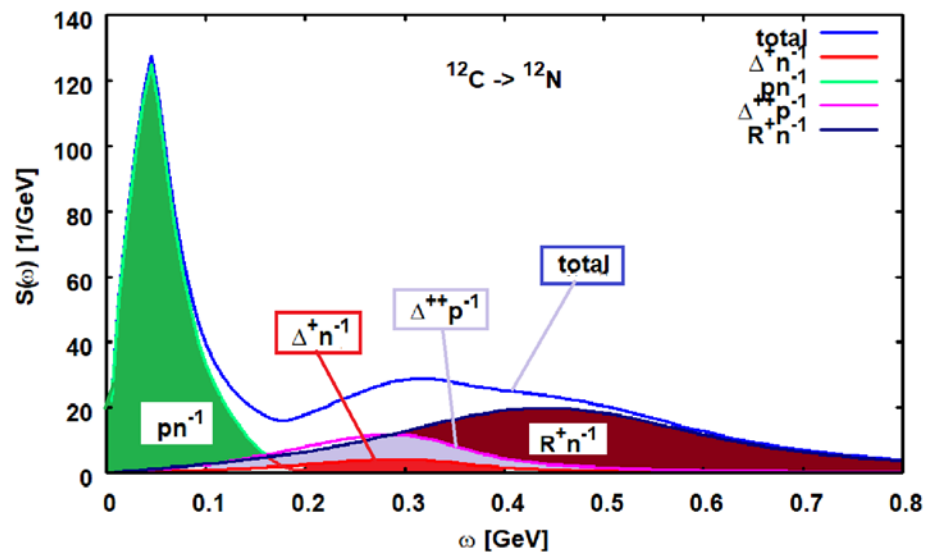
$V_{ph}$  by pion, rho, delta/ $a_0$  - meson exchange and „short range“  $g'$

Polarization Tensor and Nuclear Response (H=N, $\Delta$ ...)

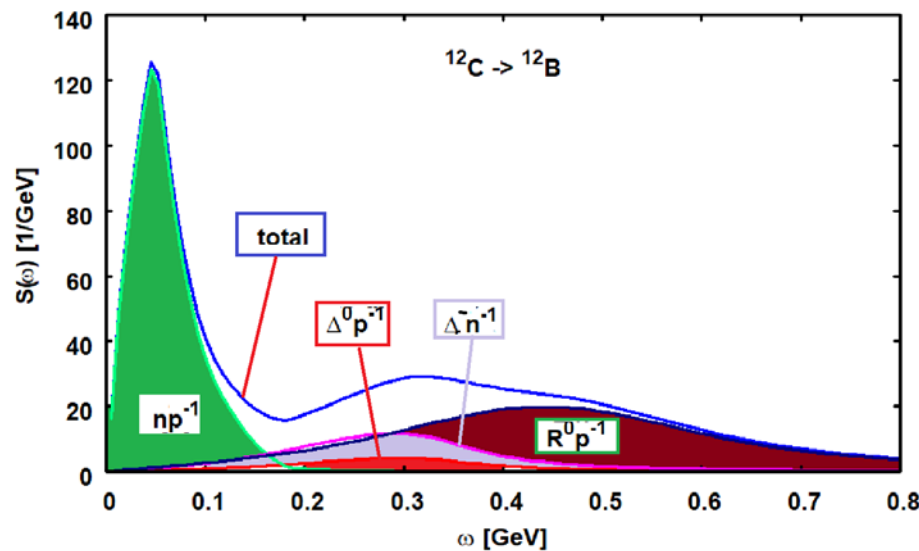
$$R_H^{(X)\mu\nu}(\omega, \vec{q}) = -\frac{1}{\pi} \text{Im} \left( \Pi_{HH}^{(X)\mu\nu}(\omega, \vec{q}) \right) = -\frac{1}{\pi} \text{Im} \left( \langle X | T_{ext}^{\dagger\mu}(\vec{q}) G_{HH}(\omega) T_{ext}^\nu(\vec{q}) | X \rangle \right)$$

# N\*N<sup>-1</sup> Spectral Distributions for <sup>12</sup>C – P<sub>33</sub>(1232) and P<sub>11</sub>(1440) Longitudinal Response@q=300 MeV/c

$\tau_+$  operator :  $pn^{-1}$  – type  
external probe:  $\vec{\sigma} \bullet \vec{p}$

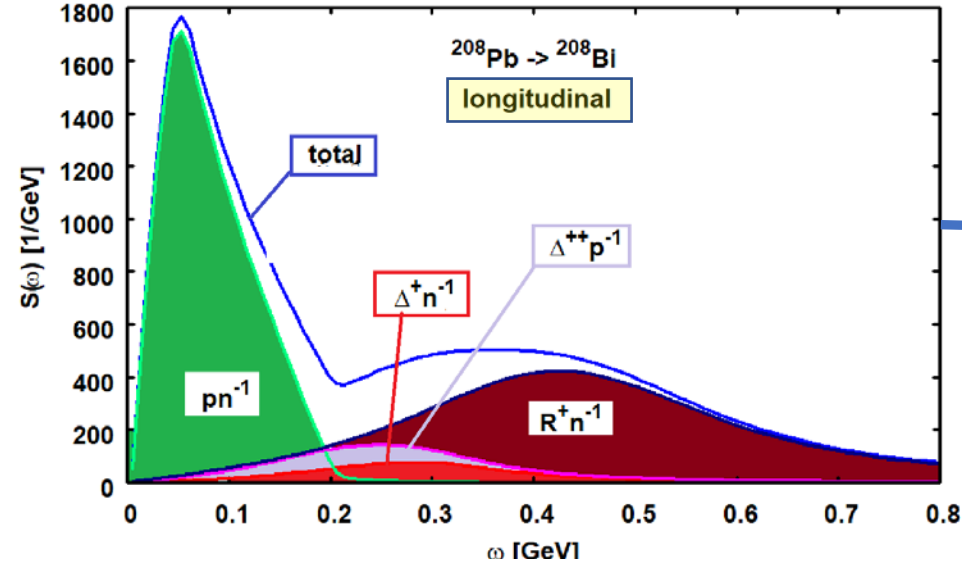


$\tau_-$  modes :  $np^{-1}$  – type  
external probe:  $\vec{\sigma} \bullet \vec{p}$



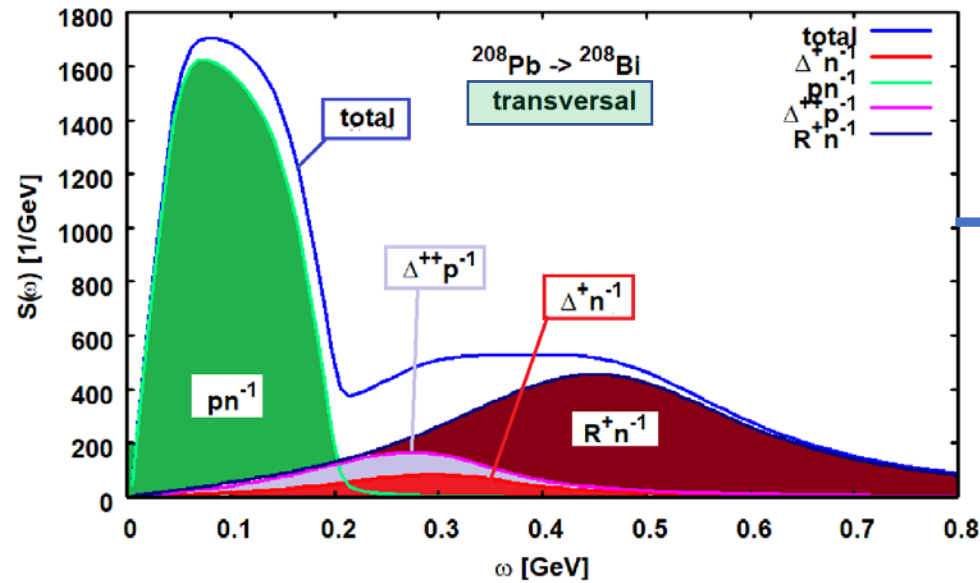
# $N^*N^{-1}$ Spectral Distributions for $^{208}\text{Pb} \rightarrow ^{208}\text{Bi}$

## Longitudinal and Transversal Response @ $q=300 \text{ MeV}/c$

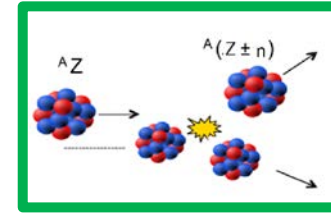


Operator:

$\sigma \cdot q$  ( $\pi$ -meson)



$\sigma \times q$  ( $\rho$ -meson)



# Comparison to the FRS@GSI Data

# Theoretical Results for $^{112}\text{Sn}$ on Pb, Cu, $^{12}\text{C}$ , and Proton Targets

Rodriguez et al., PHYSICAL REVIEW C 106, 014618 (2022)

$^{112}\text{Sn}(0^+) \rightarrow ^{112}\text{Sb}(3^+)$

$S(p) = 2.948 \text{ MeV}$

States  $E_x < S(p)$ :

$1^+ \leq J^\pi \leq 12^-$

$[p_p n_p^{-1}]$

$Z_p \rightarrow Z_p + 1$

$\leftrightarrow$

$Z_T \rightarrow Z_T - 1$

$[n_T p_T^{-1}]$

$^{112}\text{Sn}(0^+) \rightarrow ^{112}\text{In}(1^+)$

$S(p) = 6.027 \text{ MeV}$

States  $E_x < S(p)$ :

$0^+ \leq J^\pi \leq 18^\pm$

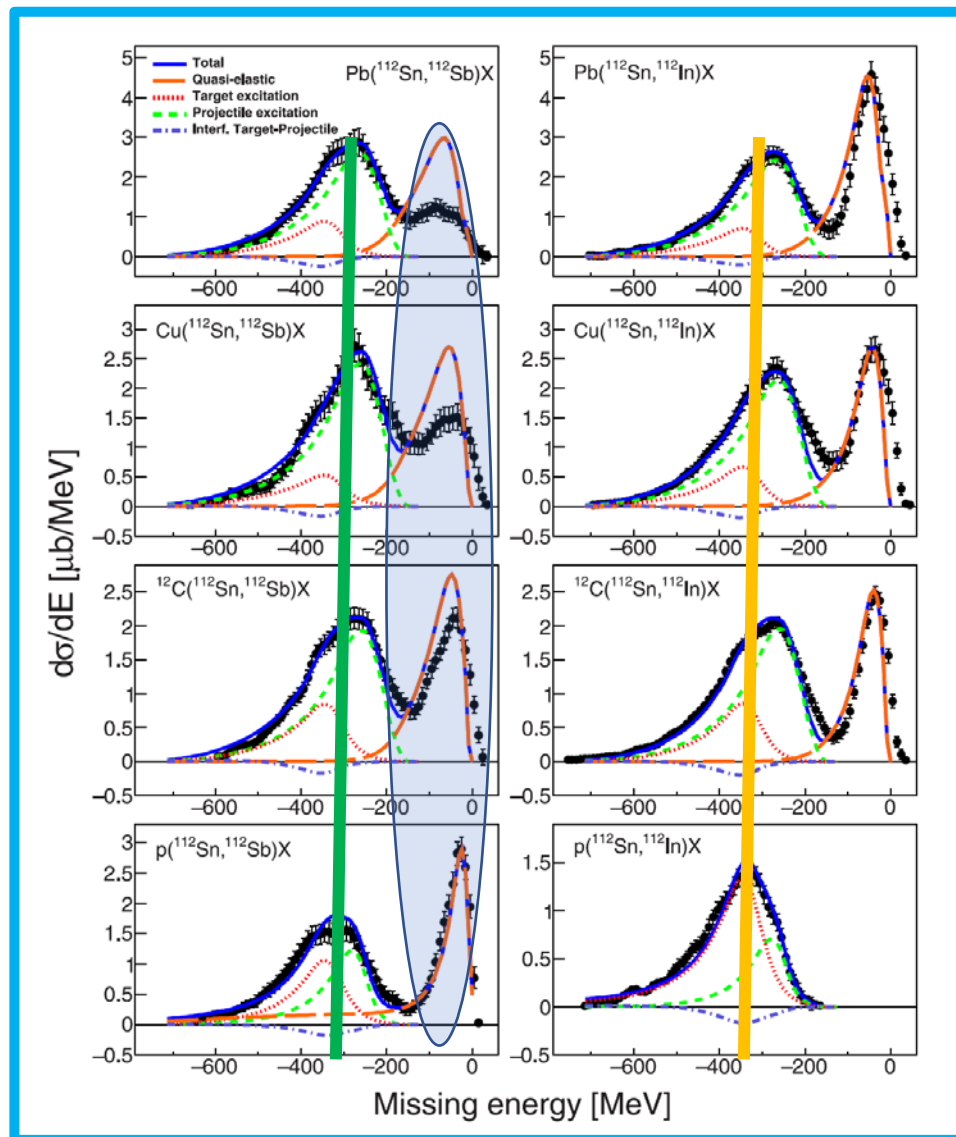
$[n_p p_p^{-1}]$

$Z_p \rightarrow Z_p - 1$

$\leftrightarrow$

$Z_T \rightarrow Z_T + 1$

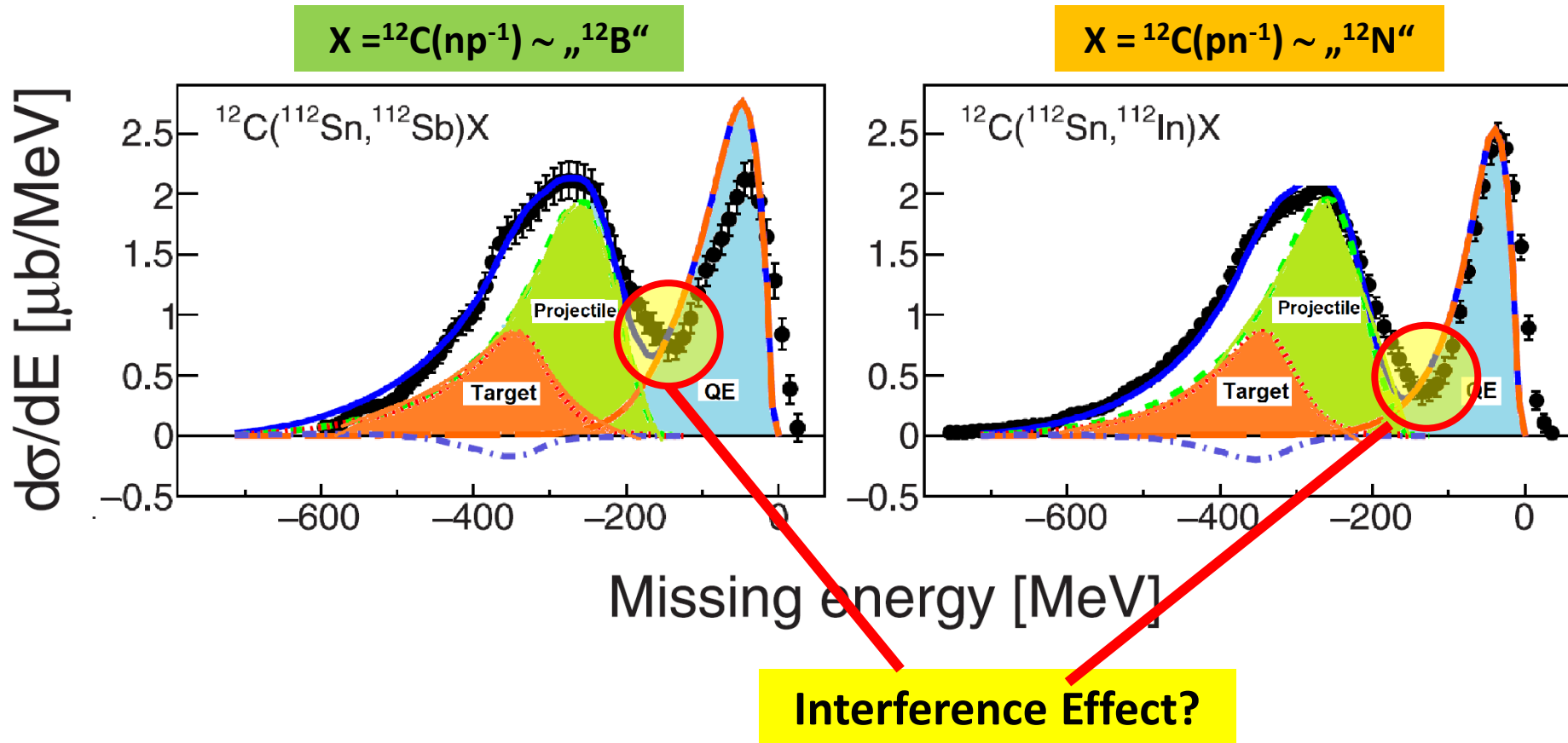
$[p_T n_T^{-1}]$



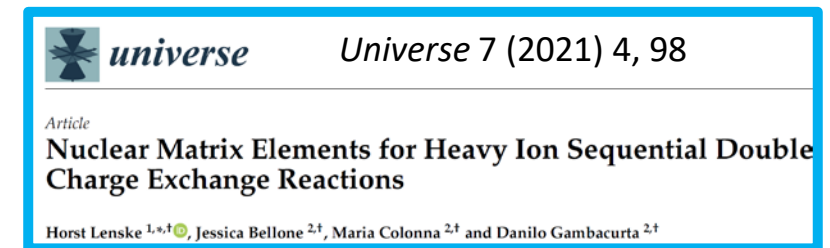
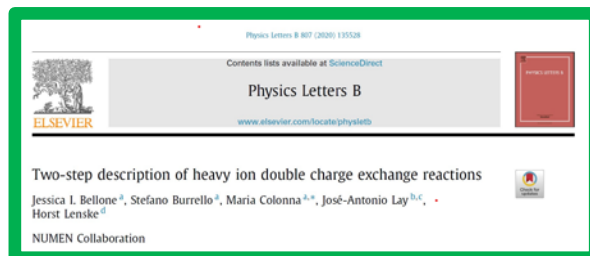
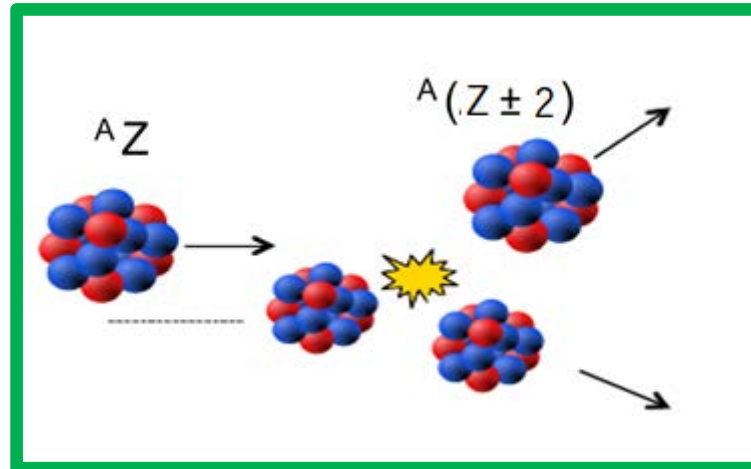
H. Lenske, MAYORANA 2023

# $^{112}\text{Sn}@1\text{GeV}$ on $^{12}\text{C}$

## Quasi-elastic, Projectile, and Target Excitations



# Lecture 12: Double Charge Exchange Reactions



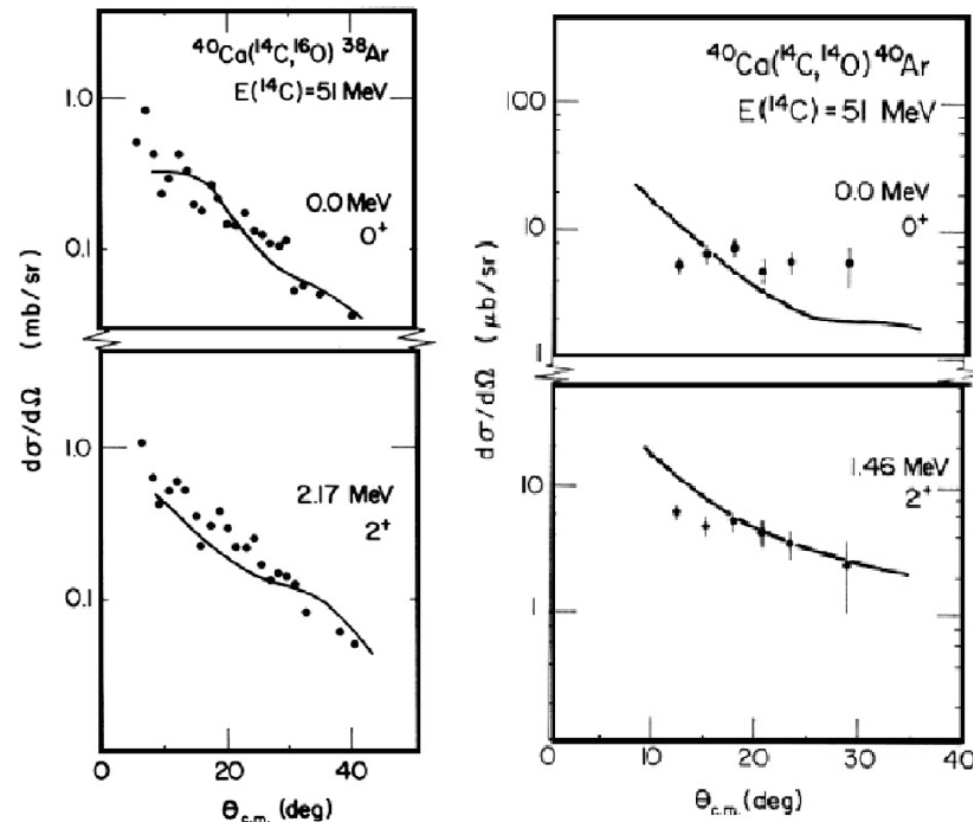
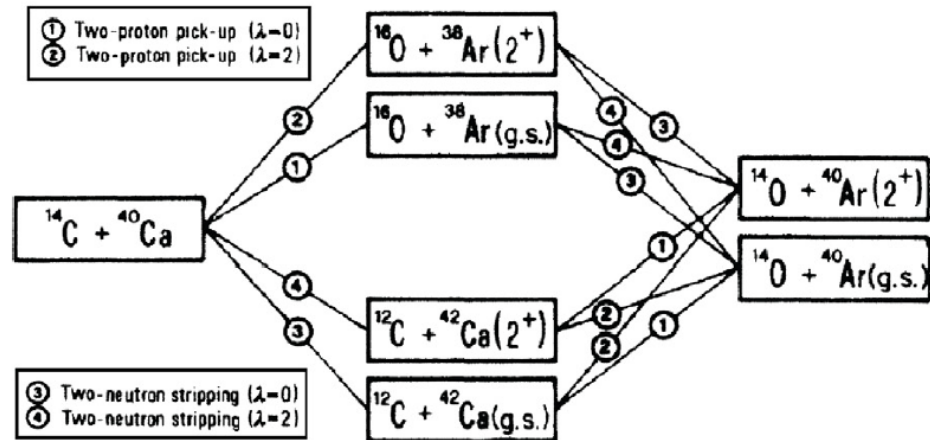
**Status of the GERDA experiment for the  $0\nu 2\beta$  decay of  $^{76}\text{Ge}$ :  
(2011-2019 campaign)**

$$T_{1/2}^{0\nu\beta\beta} > 1.8 \cdot 10^{26} \text{ yr at 90\% C.L.}$$

**...bad news for theory: no experimental check visible for DBD-NME**

# Early Double Charge Exchange (DCE) Reaction Studies at Barrier Energies

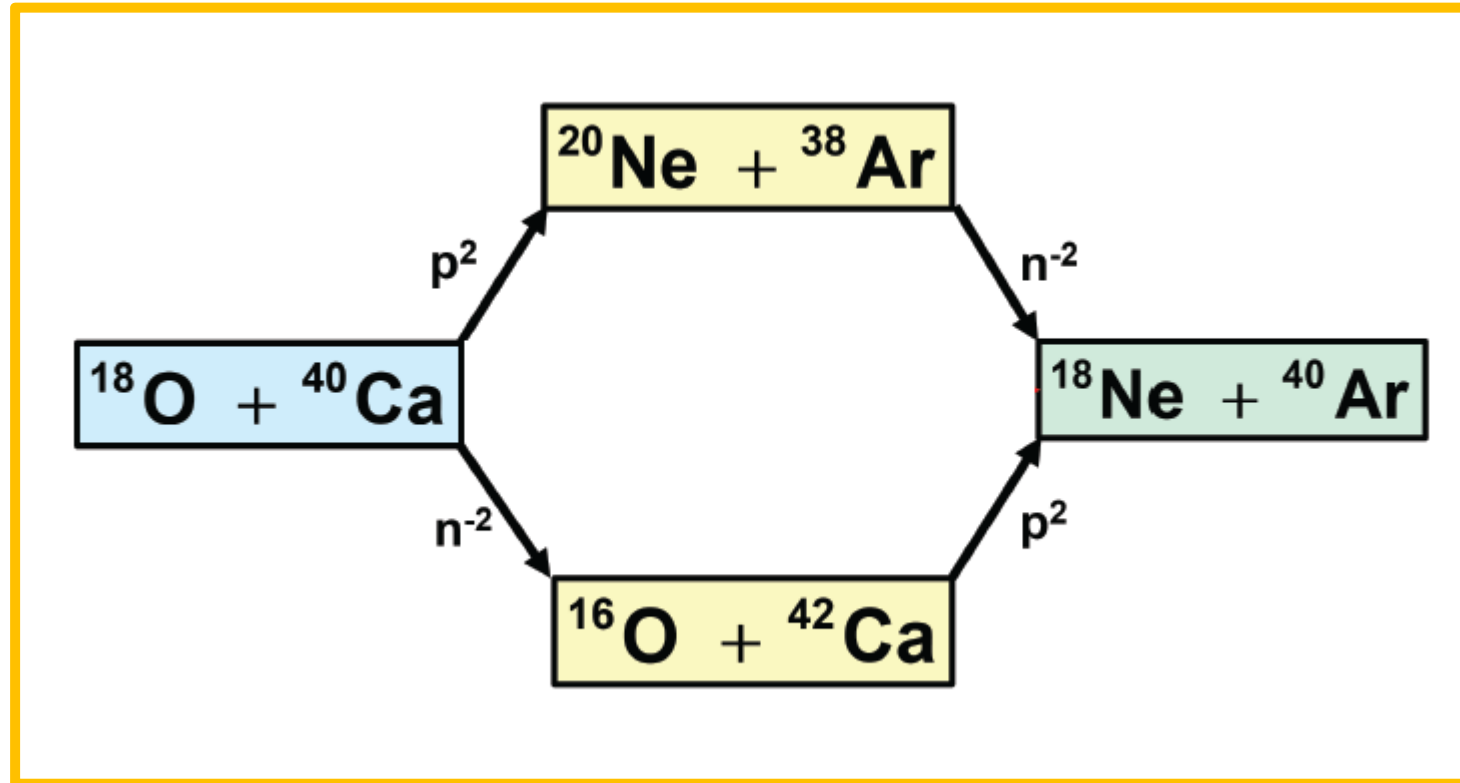
## Sequential Two-Particle Transfer



The proton and neutron pair transfer scheme used in the Dasso–Pollarolo–Vitturi approach to the DCE reaction  $^{40}\text{Ca}(^{14}\text{C}, ^{14}\text{O})^{40}\text{Ar}$ .

# Heavy Ion DCE Reaction Mechanism

## New Mechanism: Mesonic DCE!



### Transfer DCE (TDCE):

- Dasso-Pollarolo-Vitturi (1980+): sequential Collective Pair Transfer, PRC 34:743 (1986)
- Microscopic TDCE: D. Carbone, H.L., et al. , DOI: [10.1103/PhysRevC.102.044606](https://doi.org/10.1103/PhysRevC.102.044606)

# Mult-Methods Reaction Network for DCE Reactions



F. Cappuzzello, H. Lenske, M. Cavallaro et al.

Progress in Particle and Nuclear Physics xxx (xxxx) xxx

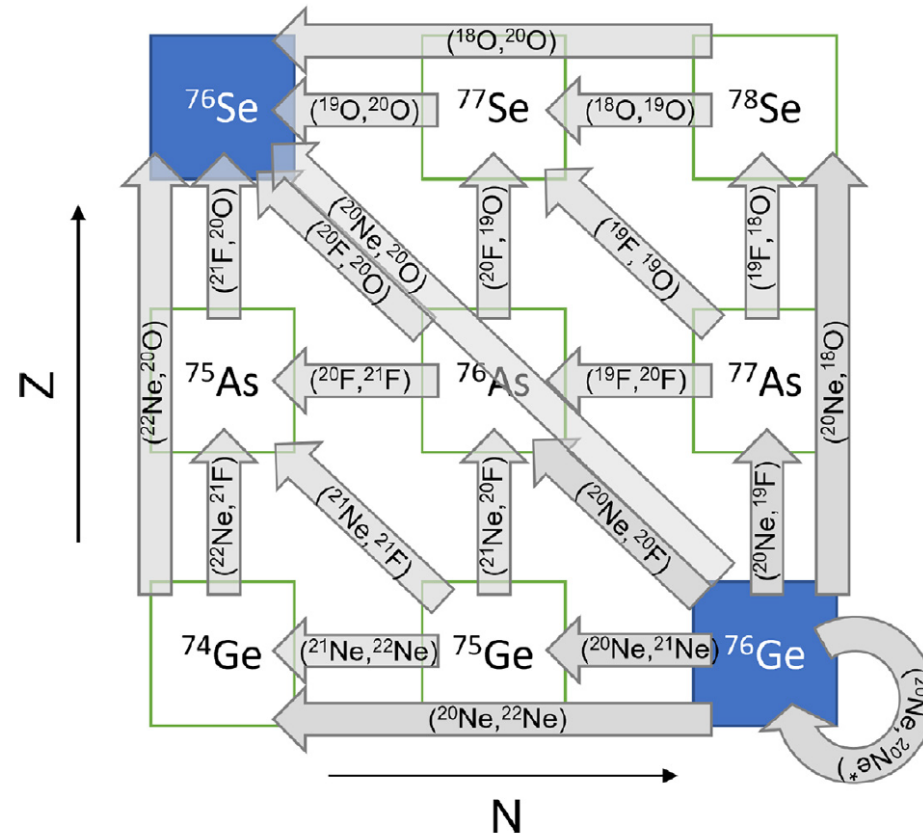
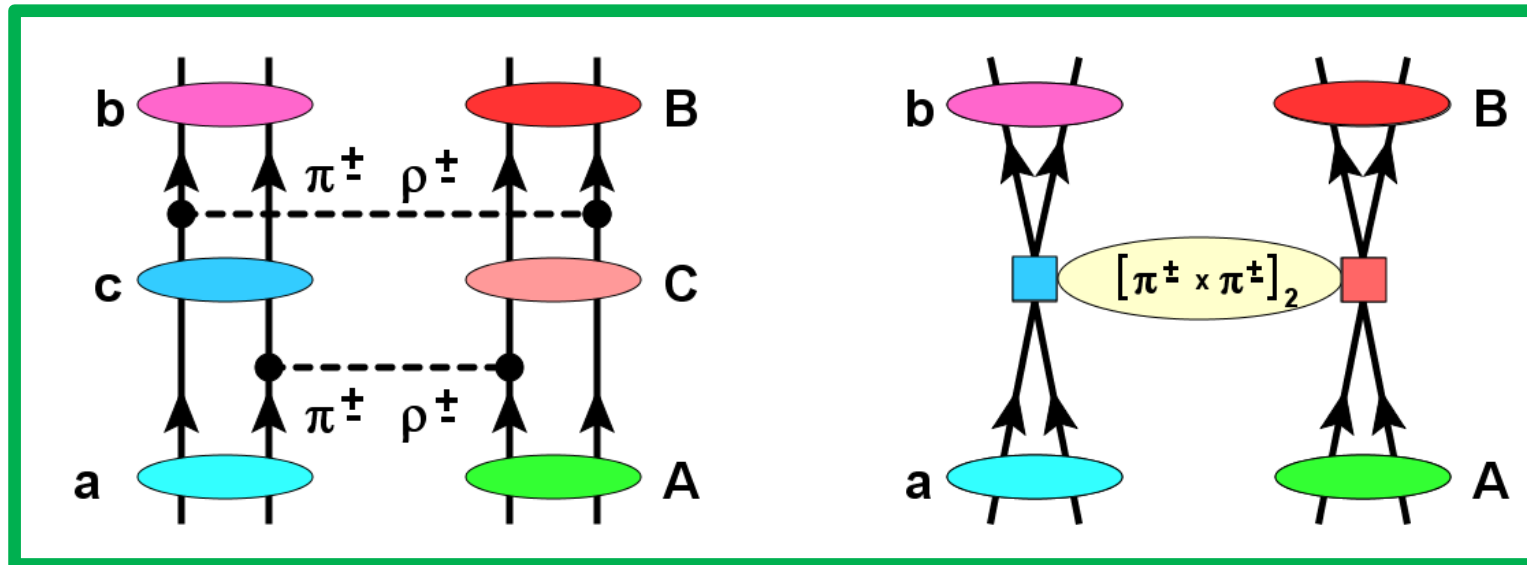


**Fig. 2.1.** Network of possible reaction routes connecting initial and final states in the  ${}^{76}\text{Ge}({}^{20}\text{Ne}, {}^{20}\text{O}){}^{76}\text{Se}$  DCE reaction. The scheme is limited to the 4th order in the single nucleon transfer process. The projectile–ejectile pairs are indicated inside the arrows.

# Mesonic Nuclear Double Charge Exchange (DCE) Reactions

Sequential „two-step“ SCE

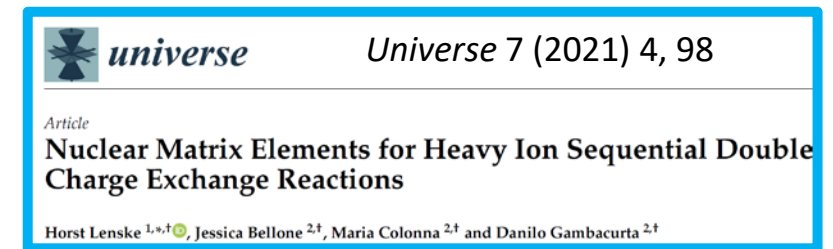
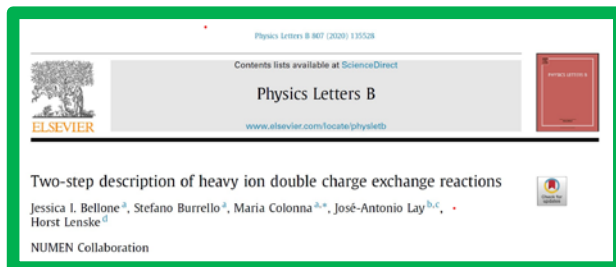


DSCE

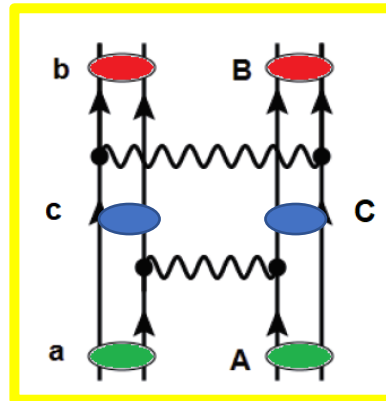
$\rightarrow 2\nu 2\beta$

MDCE

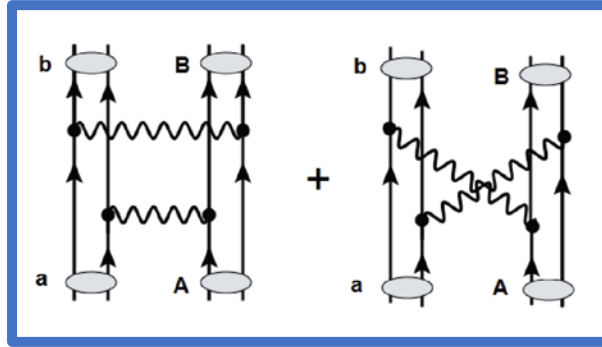
$\rightarrow 0\nu 2\beta$



# The DSCE Reaction Mechanism



# The DSCE Reaction Amplitude



$$\mathcal{M}_{\alpha\beta}^{(DSCE)}(\mathbf{k}_\alpha, \mathbf{k}_\beta) = \langle \chi_\beta^{(-)}, bB | \mathcal{T}_{NN} \mathcal{G}_{aA}^{(+)}(\omega_\alpha) \mathcal{T}_{NN} | aA, \chi_\alpha^{(+)} \rangle.$$

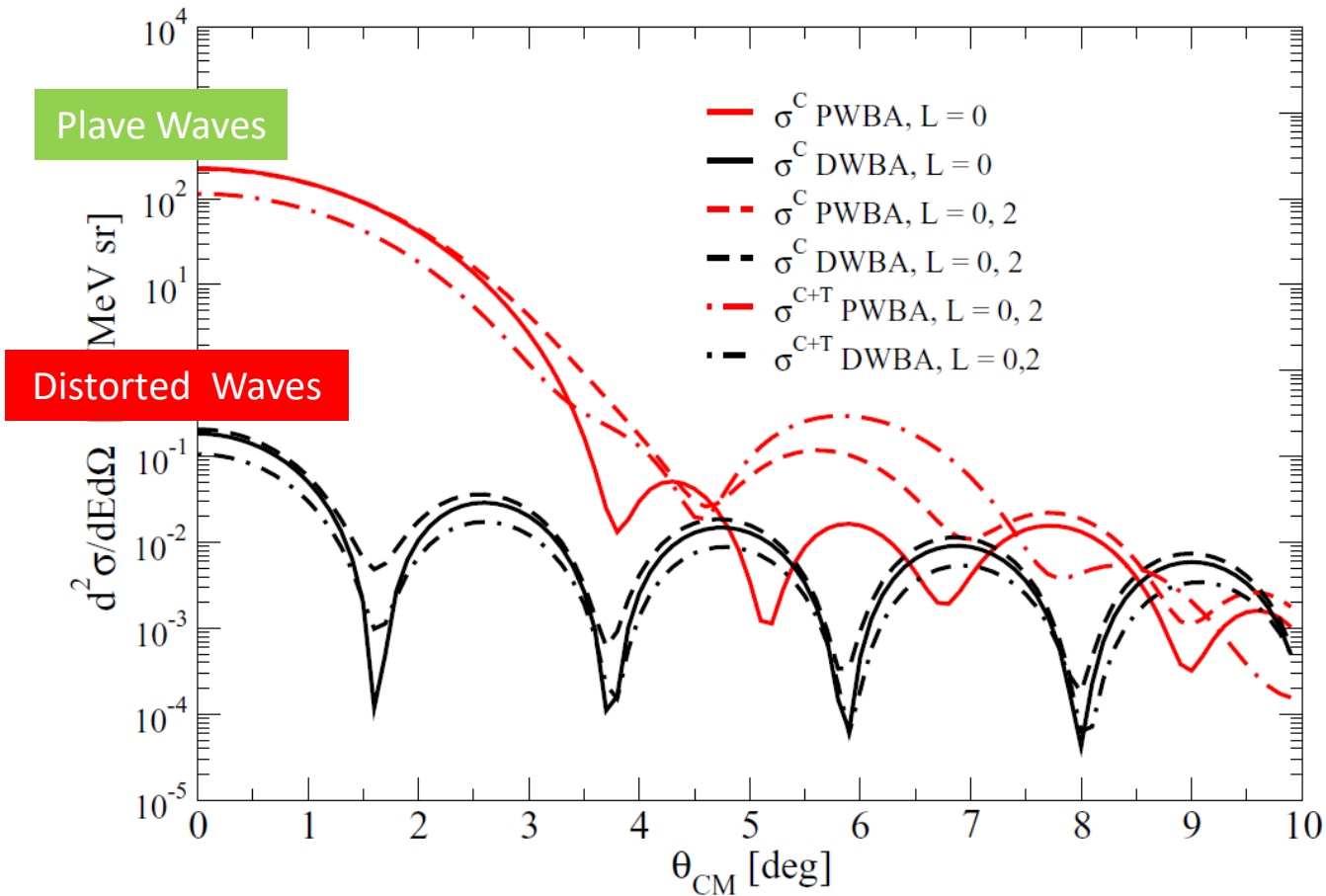
2nd order DSCE ME  $\leftrightarrow$  Folding of two (half off-shell) 1st order SCE amplitudes

$$\mathcal{M}_{\alpha\beta}^{(2)}(\mathbf{k}_\alpha, \mathbf{k}_\beta) = \sum_{\gamma=\{c,C\}} \int \frac{d^3k_\gamma}{(2\pi)^3} M_{\gamma\beta}^{(1)}(\mathbf{k}_\gamma, \mathbf{k}_\beta) \frac{\tilde{S}_\gamma^+}{\omega_\alpha - E_c - E_C - T_\gamma + i\eta} M_{\alpha\gamma}^{(1)}(\mathbf{k}_\alpha, \mathbf{k}_\gamma).$$

J. Bellone, M. Colonna, J.-A. Lay, H.L., PLB 807 (2020); H.L. et al. *Universe* 7 (2021) 4, 98

# Ion-Ion Interaction Effects in Differential Cross sections

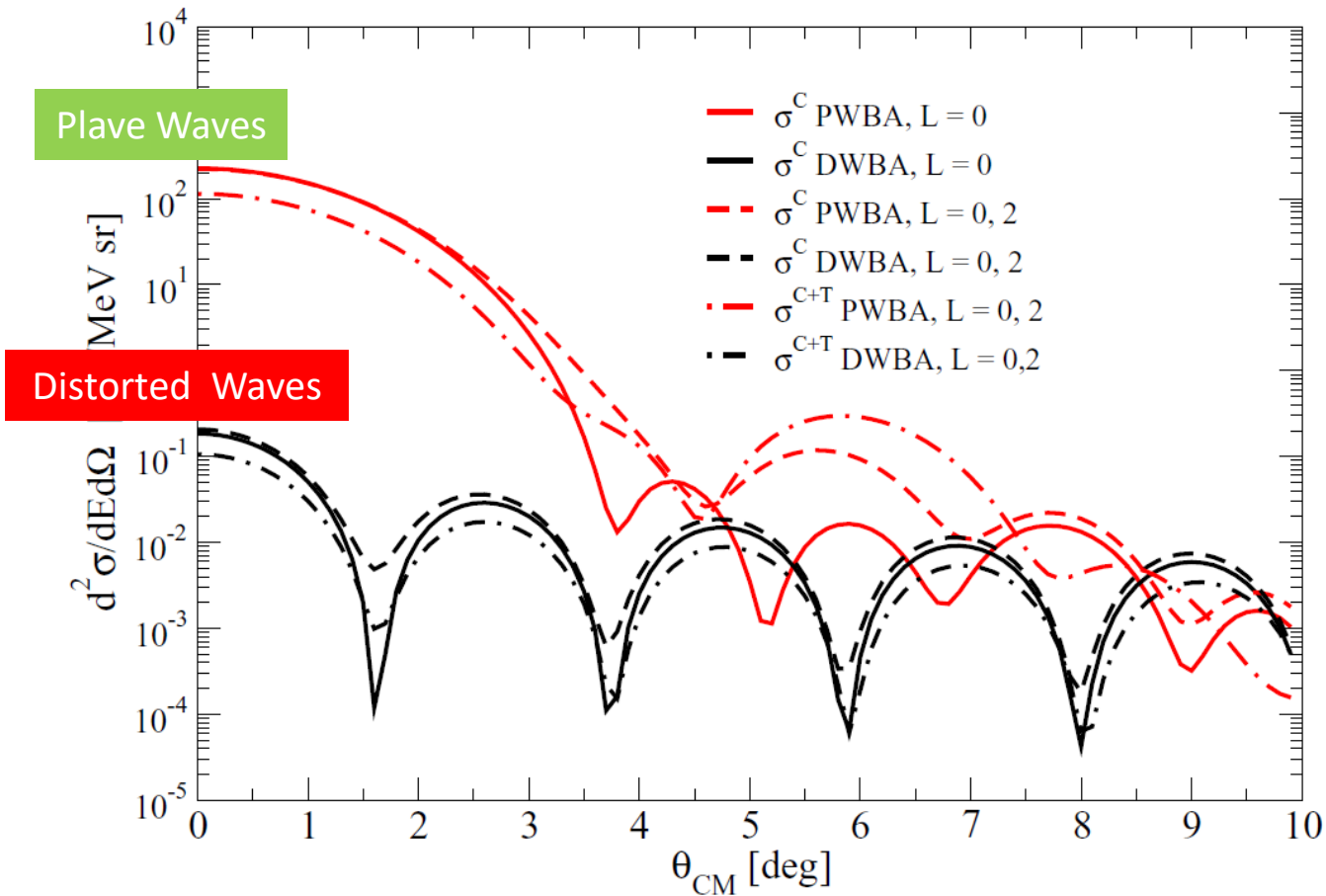
## $^{18}\text{O}+^{40}\text{Ca}@15\text{AMeV}$



Strong Absorption  $\rightarrow$  scaling of the cross section by  $N_{\alpha\beta} \sim e^{-\alpha\sigma(\text{react})}$

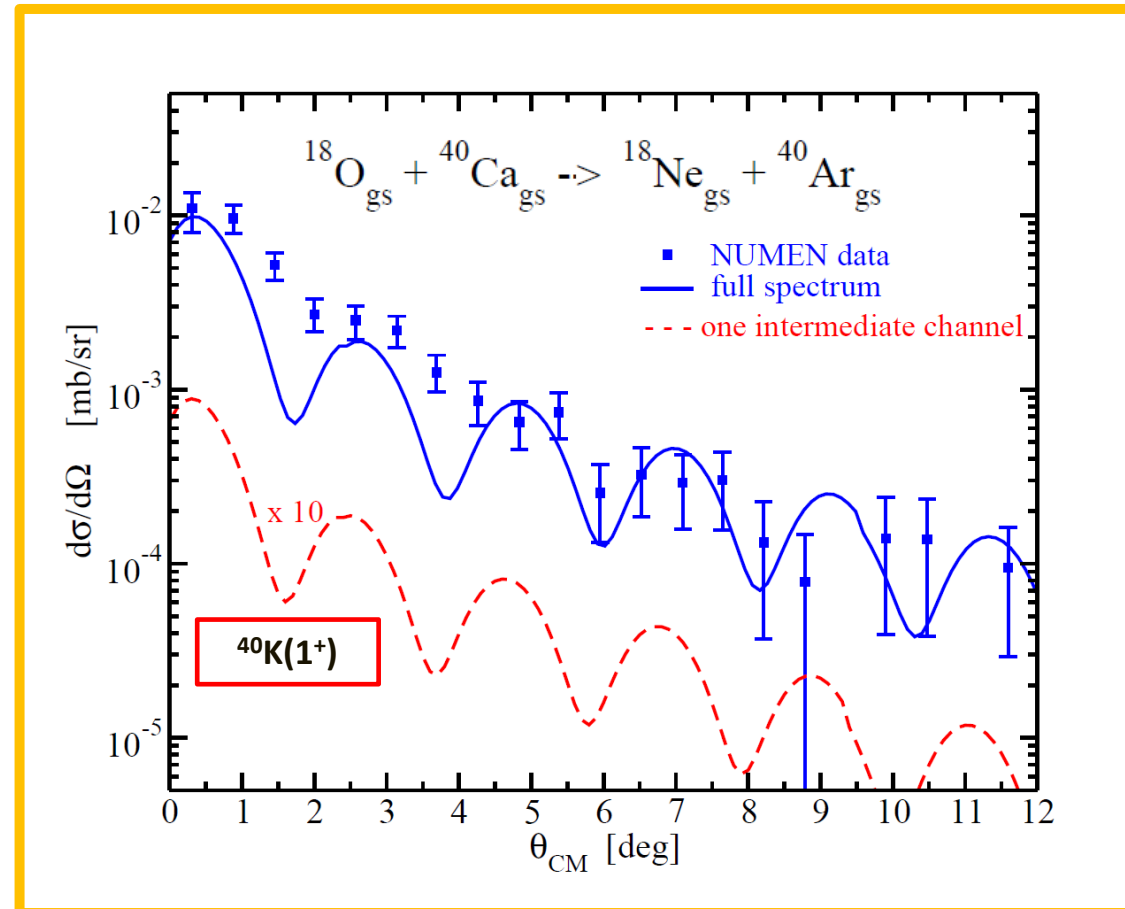
# Ion-Ion Interaction Effects in Differential Cross sections

## $^{18}\text{O}+^{40}\text{Ca}@15\text{AMeV}$



Strong Absorption  $\rightarrow$  scaling of the cross section by  $N_{\alpha\beta} \sim e^{-\alpha\sigma(\text{react})}$

# Microscopic DSCE Theory: 2nd Order DWA and QRPA Nuclear Spectroscopy

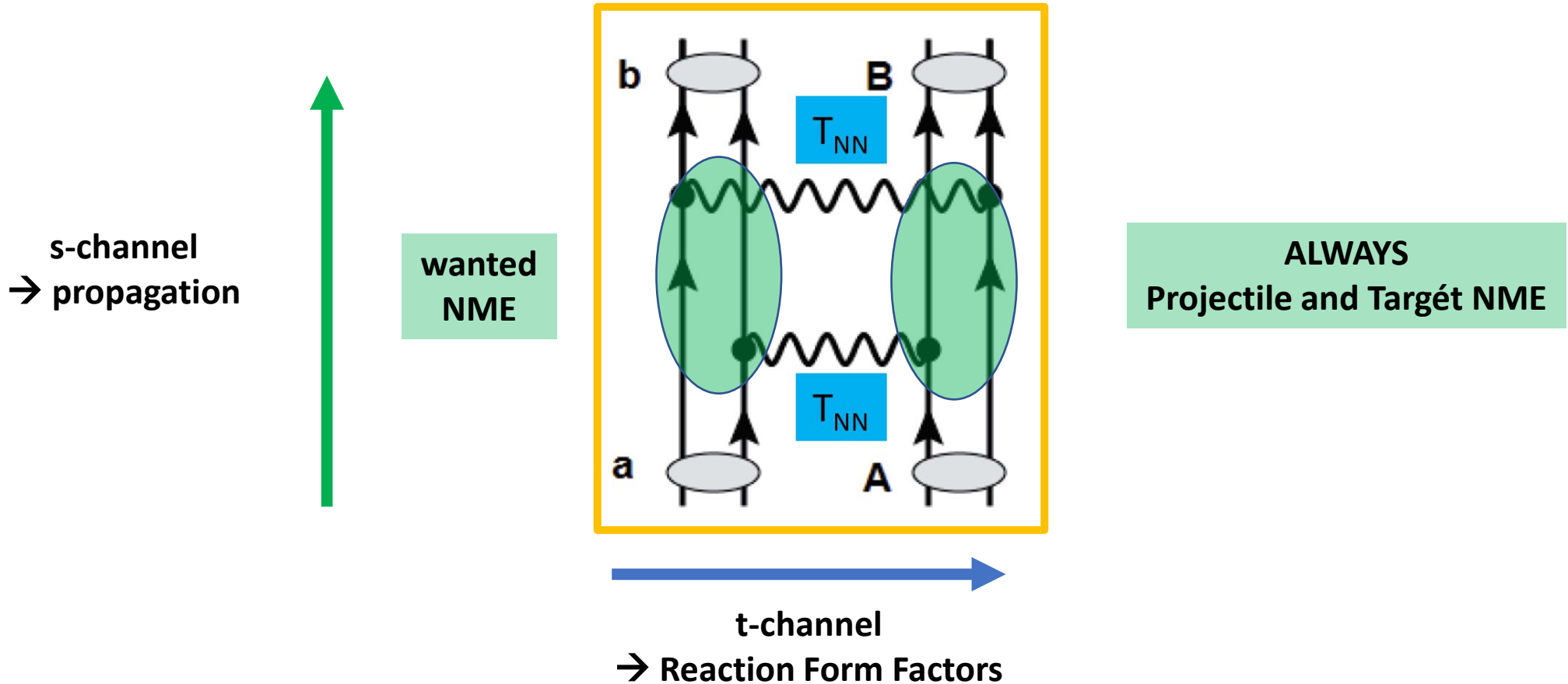


- **Optical potentials:**  
HFB g.s. densities and NN T-matrix
- **Nuclear Response:**  
QRPA Theory:  $J^\pi \leq 5^\pm$
- **Cross section reproduced**  
In magnitude

Theory: **Jessica Bellone** et al., PLB 807 (2020), Data: F. Cappuzzello et al., EPJ A51 (2015)

# DSCE Reaction and 2v2β—type Nuclear Matrix Elements

$$\mathcal{M}_{\alpha\beta}^{(2)}(\mathbf{k}_\alpha, \mathbf{k}_\beta) = \sum_{\gamma=\{c,C\}} \int \frac{d^3k_\gamma}{(2\pi)^3} M_{\gamma\beta}^{(1)}(\mathbf{k}_\gamma, \mathbf{k}_\beta) \frac{\tilde{S}_\gamma^+}{\omega_\alpha - E_c - E_C - T_\gamma + i\eta} M_{\alpha\gamma}^{(1)}(\mathbf{k}_\alpha, \mathbf{k}_\gamma)$$



H.L. et al. *Universe* 7 (2021) 4, 98

# The Merits of Contour Integration and Orthogonal Transformations: From Reaction Amplitudes to $2\nu 2\beta$ -type NME's

$$M_{\beta\alpha}^{(2)}(\mathbf{k}_\beta, \mathbf{k}_\alpha) = \int d^3p_1 d^3p_2 \oint_{C_+} \frac{d\nu}{2i\pi} \sum_{S_1, S_2} \Pi_{\alpha\beta}^{(S_2 S_1)}(\mathbf{p}_2, \mathbf{p}_1; \nu) I_{S_1 S_2}^{(DSC E)}(\mathbf{p}_2, \mathbf{p}_1; \nu \omega_\alpha)$$

$$\Pi_{\alpha\beta}^{S_1 S_2}(\mathbf{p}_2, \mathbf{p}_1; \nu) = \sum_{SM_S} (-)^{S_1+S_2-S} \oint_{C_+} \frac{d\omega}{2i\pi} (-)^{M_S} \Pi_{(S_1 S_2) SM_S}^{(AB)}(\mathbf{p}_2, \mathbf{p}_1; \omega) \cdot \Pi_{(S_1 S_2) S-M_S}^{(ab)}(\mathbf{p}_2, \mathbf{p}_1; \nu - \omega)$$

**Nuclear polarization tensors**

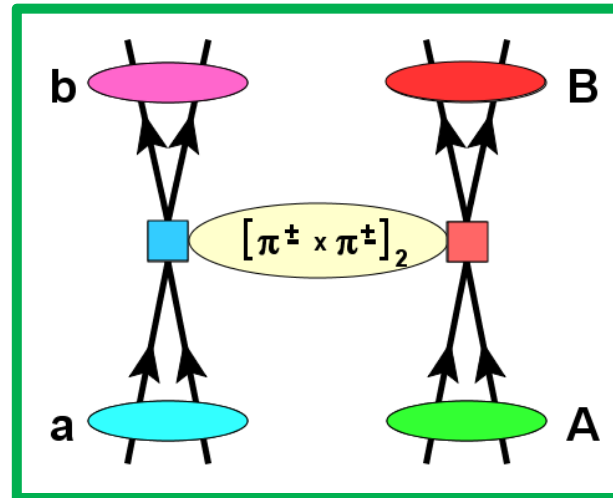
$$\Pi_{(S_1 S_2) SM}^{(AB)}(\mathbf{p}_2, \mathbf{p}_1; \omega) = \sum_C \frac{\left[ F_{S_2 T}^{(BC)}(\mathbf{p}_2) \otimes F_{S_1 T}^{(CA)}(\mathbf{p}_1) \right]_{SM}}{\omega - (E_A - E_C)}$$

**$2\nu 2\beta$ -type NME for  $\mathbf{p} \rightarrow 0$  and  $\omega \rightarrow E_{2e}$**

$$F_{ST}^{(DE)}(\mathbf{p}) = \langle J_E M_E | e^{i\mathbf{p}\cdot\mathbf{r}} \boldsymbol{\sigma}^S \tau_{\pm} | J_D M_D \rangle$$

H.L. et al. *Universe* 7 (2021) 4, 98

# Mesonic Majorana DCE (MDCE) Scenario

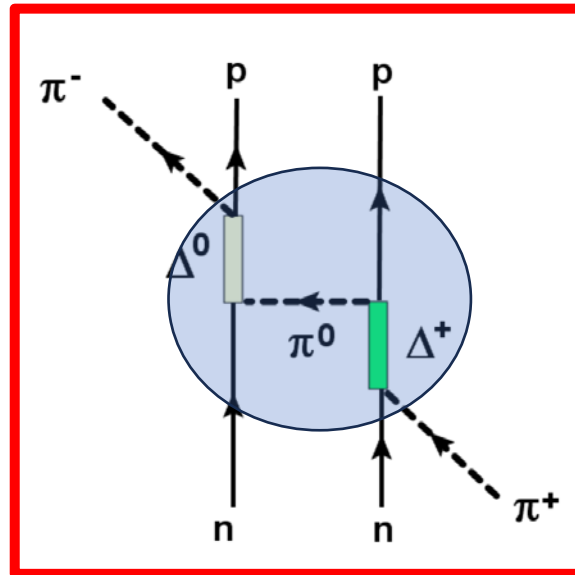


Quest for an Isotensor interaction  $\sim [\tau_1 \times \tau_2]_2$ :  
Conversion of **two units of charge** in a **single step**?

# Effective Rank-2 Isotensor Interaction

Searches for elementary Isotensor  $I=2$  mesons were unsuccessful

Dynamically generated Isotensor Interactions!



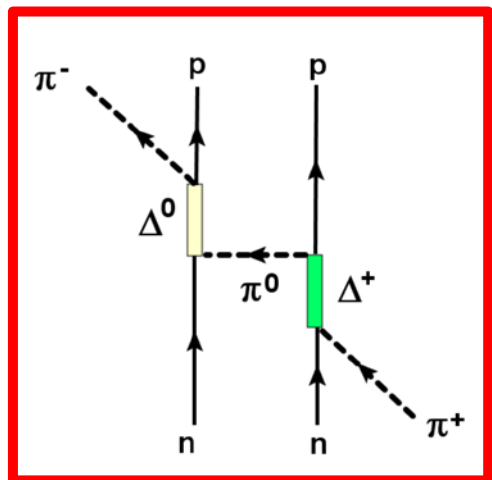
$(\pi^+, \pi^-)$  DCE reactions

$$V_{\pi^\pm N, \pi^\mp N'}^{(I=2)} \sim T_{\pi^\pm N \pi^0 N''} G_{\pi^0 N''} T_{\pi^0 N'' \pi^\mp N'}$$

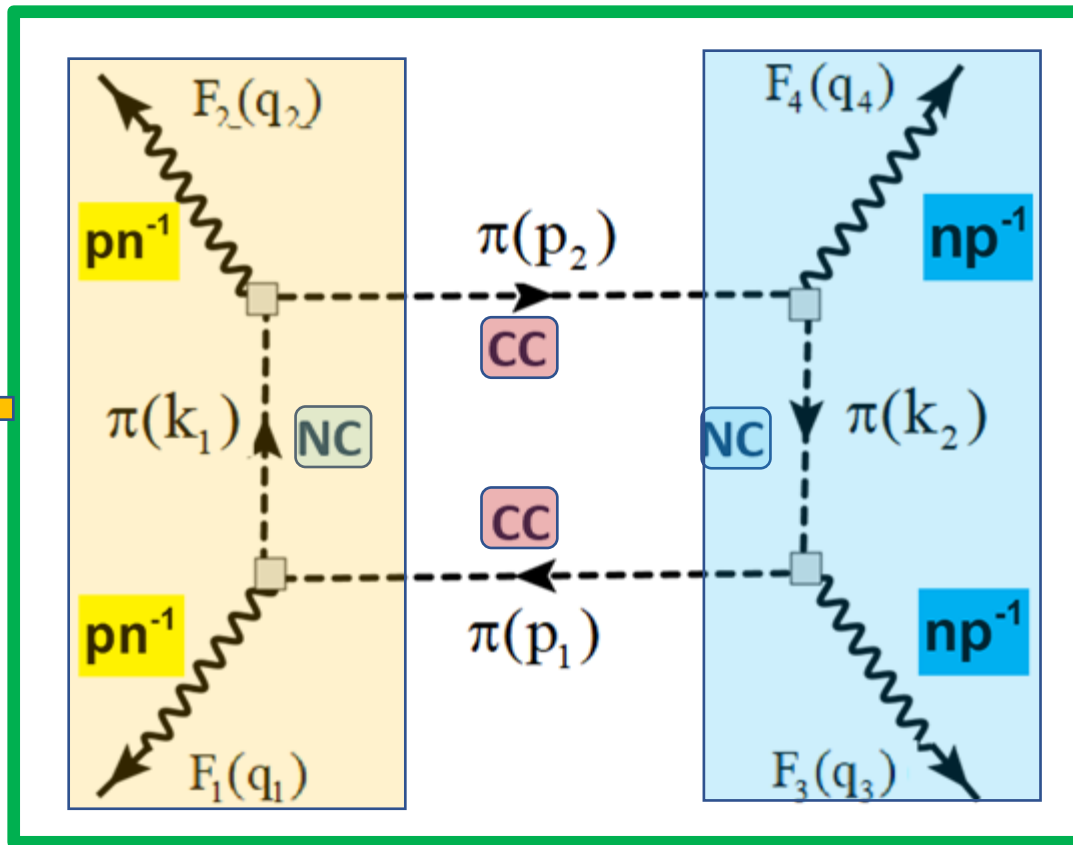
H.L. et al., PPNP 98 (2019) 103716

# DCE by Double Meson Exchange

\*\*\* Cooperation of Charged (CC) and Neutral (NC) Hadronic Currents \*\*\*



On-shell counterpart:  
( $\pi^+, \pi^-$ ) reaction

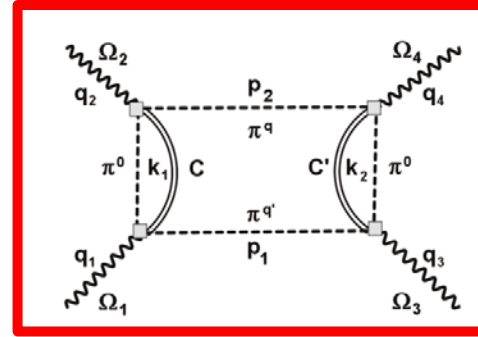


MDCE  
Box Diagrams

(  $\square$  =  $T_{\pi N}$  )

Virtual rank-2 Isotensor Interaction by Correlated Meson Exchange

# MDCE **Isotensor** Transition Kernel



$$\mathcal{U}_{\alpha\beta}(\mathbf{p}_1, \mathbf{p}_2) = \mathcal{W}_{12}(\mathbf{p}_1, \mathbf{p}_2) D_{\pi^q \pi^{q'}}(\mathbf{p}_1, \mathbf{p}_2) \mathcal{W}_{34}(\mathbf{p}_2, \mathbf{p}_1),$$

$$\mathcal{W}_{ij}(\mathbf{p}, \mathbf{p}') = \sum_n \int \frac{d^3k}{(2\pi)^3} F_{jn}(\mathbf{p}', \mathbf{k}) D_{\pi^0}(k^2, \omega_n) F_{ni}(\mathbf{p}, \mathbf{k}).$$

$$F_{dc}(\mathbf{p}, \mathbf{k}) = \langle d | e^{\pm i\mathbf{q}_d \cdot \mathbf{r}} \tilde{T}_{\pi N}(\mathbf{p}, \mathbf{k}) | c \rangle \quad (\mathbf{q}_d = \mathbf{p} \pm \mathbf{k})$$

MDCE-NME in projectile and target: two SCE-vertices connected by  $\pi^0$  exchange  
**2-Nucleon Mechanism fostered by 2-body correlations**

## MDCE Vertices in Closure Approximation

$$D_{\pi^0 C}(k^2) \sim -\frac{1}{k^2 + m_{\pi^0}^2} \left( 1 + \frac{(\omega_A - \omega_C)^2}{m_{\pi^0}^2} + \dots \right)$$

Pion Mass  $\rightarrow$  NATURAL SEPARATION SCALE!  $\rightarrow$  keep the 1st term only  $\rightarrow$  Closure

## MDCE Transition Potential in Closure Approximation „MDCE Pion Potential“

$$\mathcal{U}_\pi(\mathbf{x}) = \int \frac{d^3 k}{(2\pi)^3} T_{\pi N}(\mathbf{p}_2, \mathbf{k}) \frac{e^{i\mathbf{k}\cdot\mathbf{x}}}{k^2 + m_{\pi^0}^2} T_{\pi N}(\mathbf{p}_1, \mathbf{k}).$$

# The MDCE Nuclear Transition Amplitude in Closure Approximation

$$\mathcal{W}_{AB}(\mathbf{p}_1, \mathbf{p}_2) = -\langle B | e^{-i\mathbf{p}_2 \cdot \mathbf{r}_2} \mathcal{U}_\pi(\mathbf{x}) e^{i\mathbf{p}_1 \cdot \mathbf{r}_1} \mathcal{T}_{2\pm 2} | A \rangle,$$

Rank-2 Isotensor Operator

$$\mathcal{T}_{2\pm 2} = [\boldsymbol{\tau}_1 \otimes \boldsymbol{\tau}_2]_{2\pm 2}$$

Pion-Potential

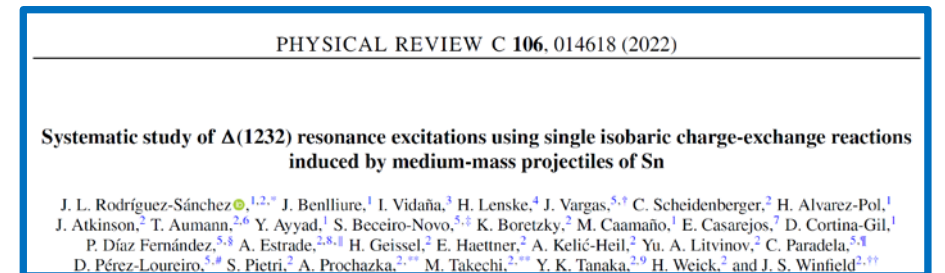
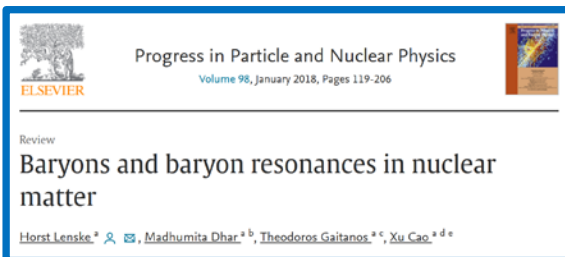
$$\mathcal{U}_\pi(\mathbf{x}) = \int \frac{d^3k}{(2\pi)^3} T_{\pi N}(\mathbf{p}_2, \mathbf{k}) \frac{e^{i\mathbf{k} \cdot \mathbf{x}}}{k^2 + m_{\pi^0}^2} T_{\pi N}(\mathbf{p}_1, \mathbf{k}).$$

$$T_{\pi N}(\mathbf{p}_j, \mathbf{k}) = T_0(w) + \frac{1}{m_\pi^2} \left( T_1(w) \mathbf{p}_j \cdot \mathbf{k} + iT_2(w) \boldsymbol{\sigma}_j \cdot (\mathbf{p}_j \times \mathbf{k}) \right)$$

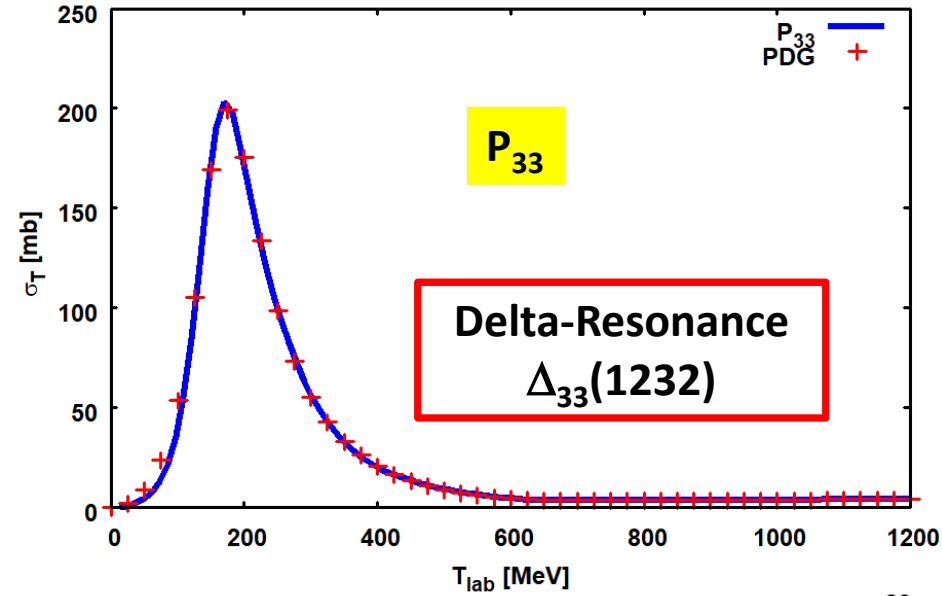
→ 6 potentials:  $U_{00}(\mathbf{x})$ ,  $U_{11}(\mathbf{x})$ ,  $U_{22}(\mathbf{x})$ ,  $U_{01}(\mathbf{x})$ ,  $U_{02}(\mathbf{x})$  and  $U_{12}(\mathbf{x})$

# Pion-Nucleon Interactions

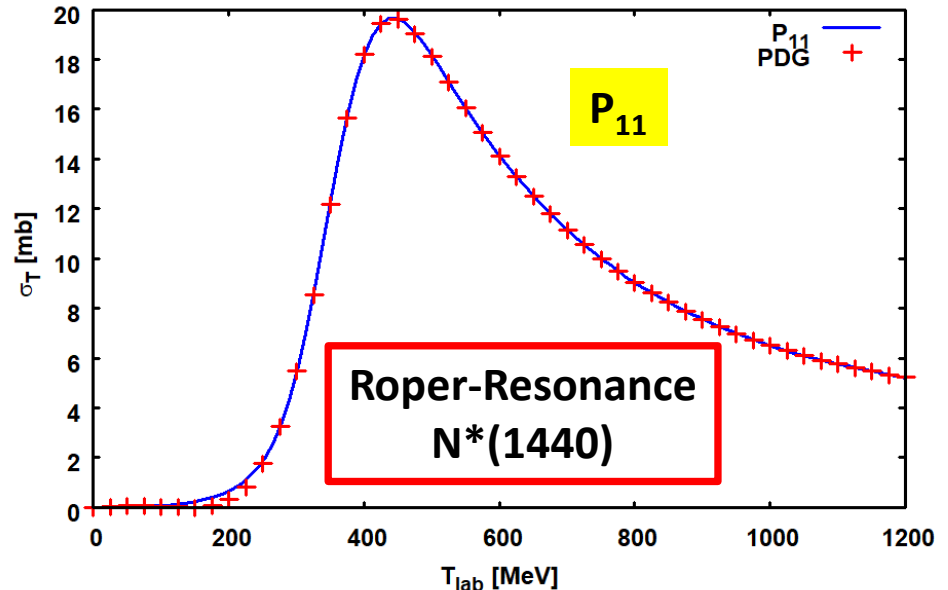
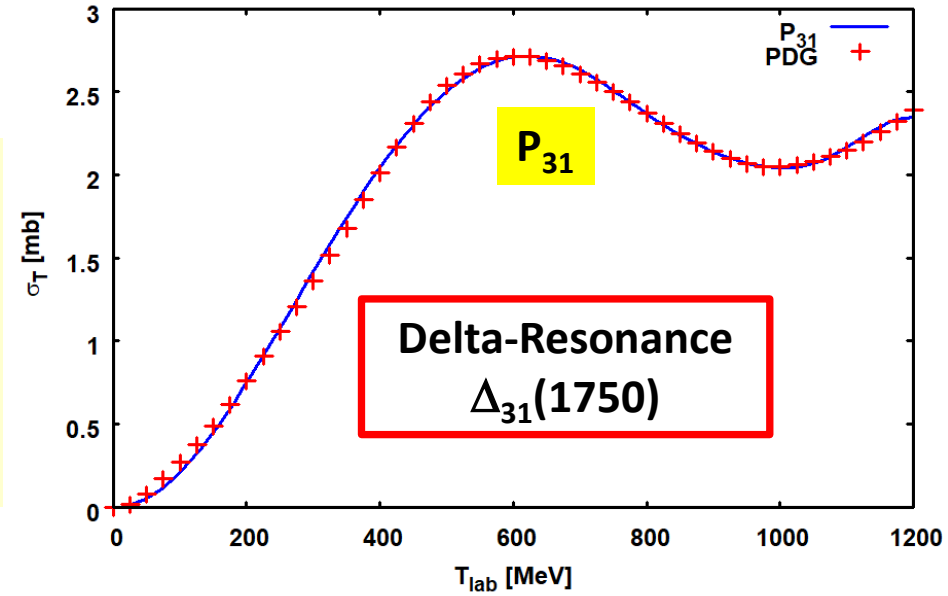
$$T_{\pi N}(p_j, k) = T_0(w) + \frac{1}{m_\pi^2} \left( T_1(w) p_j \cdot k + iT_2(w) \sigma_j \cdot (p_j \times k) \right)$$



# $\pi$ -N total Cross Sections

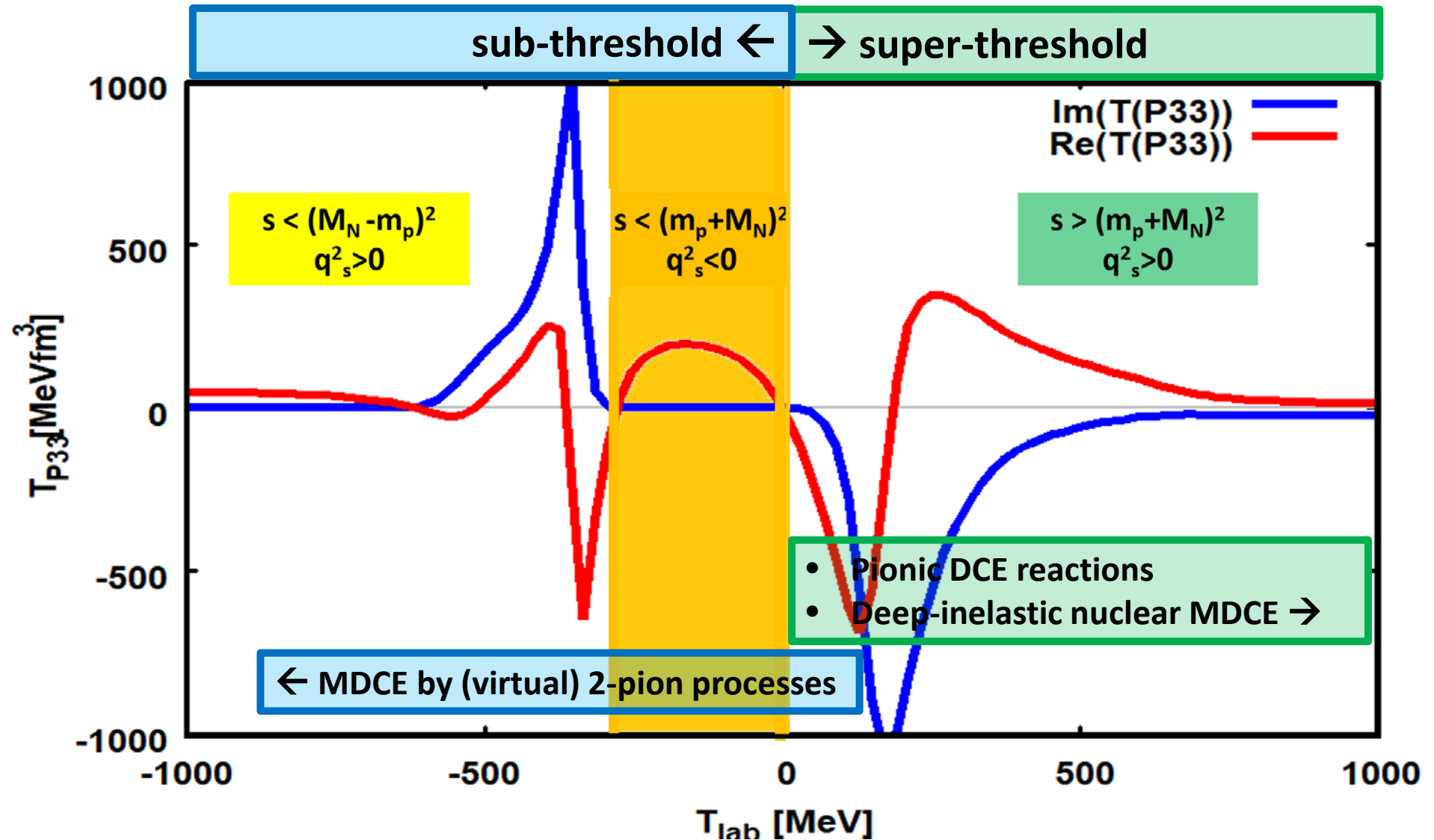


Relevant partial waves:  
 $P_{33}, P_{11}, P_{31}, S_{11}, S_{31}$   
 (Notation:  $L_{212J}$ )  
 $T_0 \sim \{S_{11}, S_{31}\}$   
 $T_{1,2} \sim \{P_{11}, P_{31}, P_{31}\}$

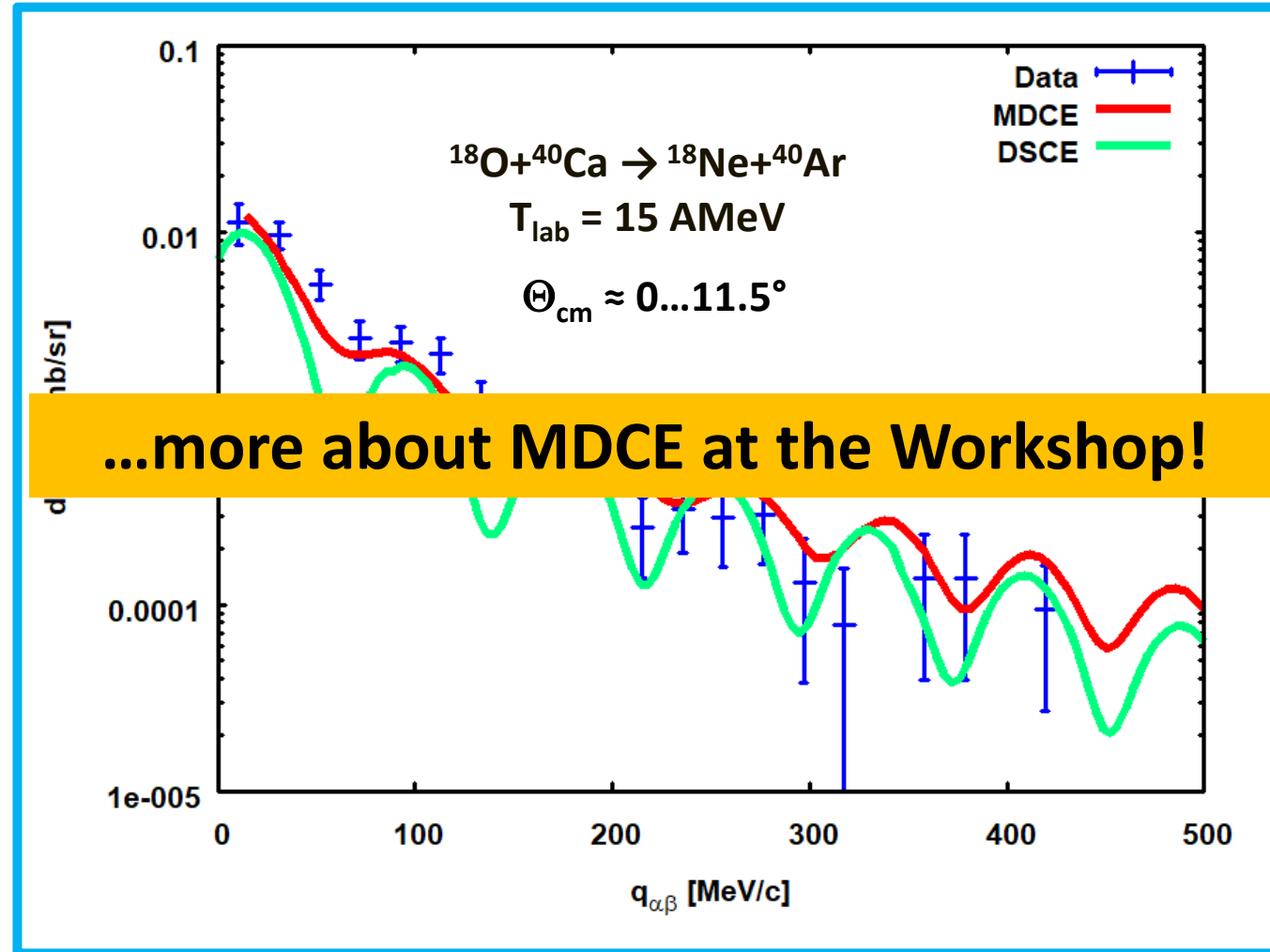


Review on the Giessen  $\pi$ +N  
 CC approach:  
 H.L. et al., PPNP 98 (2018) 119

# Kinematical Regions of Importance for Hadronic DCE Reactions



# DCE Reactions: Probing Nuclear Physics @ High Momentum Transfer



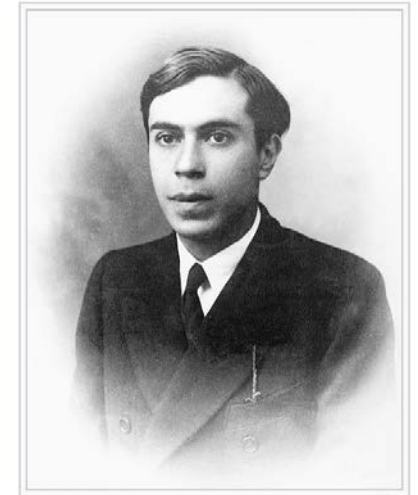
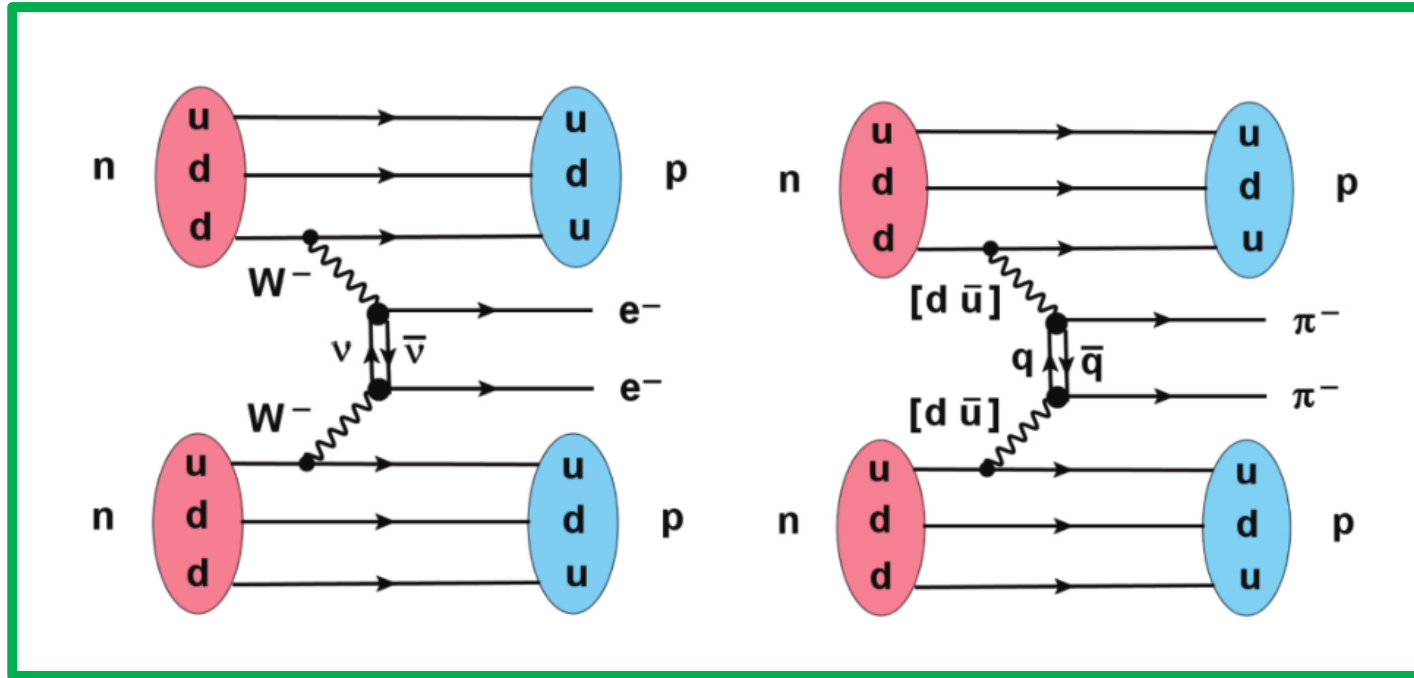
**MDCE Preliminary!**

2-step DSCE: intermediate states with  $J^\pi \leq 5^\pm$   
 1-step MDCE:  $^{40}\text{Ca}(0^+) \rightarrow ^{40}\text{Ar}([n^{-2}p^2]0^+)$  :  $J=0^+$  with  $L=S=0$  &  $[L=2 \times S=2]_{0^+}$

Data: F. Cappuzzello et al., EPJ A51 (2015)

# MDCE and $0\nu 2\beta$ Double Beta-Decay

## The Majorana Aspect



Ettore Majorana  
 \*Aug., 5, 1906, at Catania  
 disappeared, Mar, 1938  
 + 1959 in Venezuela?  
 + in a Sicilian monastery?

- Topological Correspondence of MDCE on the Diagrammatic Level
- MDCE as a Surrogate Reaction for  $0\nu 2\beta$ -NME

# That's what we learnt

**Lecture 1:** Basic Concepts of Quantum-Mechanical Scattering Theory

**Lecture 2:** Nuclear Reaction Theory in a Nutshell

**Lecture 3:** Theory of Nuclear Direct Reactions

**Lecture 4:** Optical Potentials and Elastic Scattering

**Lecture 5:** Perturbative Approach to Non-Elastic Reactions

**Lecture 6:** Single Charge Exchange (SCE) Reactions

**Lecture 7:** Light Ion SCE Reactions and beta-Decay

**Lecture 8:** The Gamow-Teller Quenching Mystery

**Lecture 9:** Nuclear Matrix Elements for Astrophysics

**Lecture 10:** Heavy Ion SCE Reactions

**Lecture 11:** Heavy Ion SCE Reactions at Relativistic Energies

**Lecture 12:** Double Charge Exchange (DCE) Reactions